

Supplementary Information for

Lewis Acid-Driven Self-Assembly of Diiridium Macrocyclic Catalysts Imparts Substrate Selectivity and Glutathione Tolerance

Hieu D. Nguyen, Rahul D. Jana, Dylan T. Campbell, Thi V. Tran, Loi H. Do*

*Department of Chemistry, University of Houston, 4800 Calhoun Rd.,
Houston, Texas, 77204, United States*

**Email: loido@uh.edu*

<u>TABLE OF CONTENTS</u>	<u>Page(s)</u>
General Procedures	S5
Physical Methods	S5
Synthesis and Characterization	S6-S15
Scheme S1 Synthesis of complexes Ir1' and Ir2	S6
Experimental Details	S7-S14
Table S1 Screening conditions for amide coupling using model substrates	S15
Transfer Hydrogenation Studies	S16-S25
Procedure for Transfer Hydrogenation Studies	S16
Table S2 Biocompatibility evaluation of Ir2	S17
Figure S1 Substrate scope studies of Ir1 and Ir2	S18
Figure S2 Substrate scope studies of Ir1 and Ir2 (continued)	S19
Table S3 Comparing the activity of Ir catalysts	S20
Figure S3 Representative GC plots of products obtained from the transfer hydrogenation of 4-benzyloxybenzaldehyde and HCOONa using Ir1 (a) and Ir2 (b)	S21
Figure S4 ¹ H NMR spectra of Ir1 + crotonaldehyde	S22
Figure S5 ¹ H NMR spectra of Ir1 + hydrocortisone	S23
Figure S6 ¹ H NMR spectra of Ir2 + crotonaldehyde	S24
Figure S7 ¹ H NMR spectra of Ir2 + hydrocortisone	S25
Glutathione Tolerance Studies	S26-S37
Procedure for Glutathione Tolerance Studies	S26
Determination of H ₂ O ₂ Concentration by Quantofix® Peroxides Test Strips	S26
Figure S8 ¹ H NMR spectra of GSH + benzaldehyde	S27
Table S4 GSH tolerance of complexes Ir1/Ir2 in H ₂ O/DMSO	S28
Figure S9 Representative GC plots for the transfer hydrogenation between HCOONa and benzaldehyde, using Ir1/Ir2 catalysts in the presence of GSH	S29
Figure S10 GSH tolerance of complexes Ir1/Ir2 in PBS/DMSO	S30
Figure S11 Maximum tolerance of Ir2 to GSH in H ₂ O/DMSO	S31
Figure S12 Tolerance of Ir2 to various biological S-containing nucleophiles	S32

Figure S13	Calibration curve to determine H ₂ O ₂ concentration	S33
Figure S14	Peroxide color-strips obtained from solutions containing Ir1/Ir2 in the presence of benzaldehyde after various times.	S34
Figure S15	Peroxide color-strips obtained from solutions containing Ir1/Ir2 in the absence of benzaldehyde after various times.	S35
Table S5	Effect of GSH on Ir1/Ir2 in the presence of H ₂ O ₂ scavengers	S36
Table S6	Effect of GSH on Ir1/Ir2 in the presence of GSH scavengers	S37
Cation Effect Studies		S38-S51
Procedure for Cation Effect Studies		S38
Table S7	Reactions of Ir1/Ir2 in the presence of different formate salts	S39
Figure S16	¹ H NMR spectra of Ir2 with different salts in D ₂ O: DMSO- <i>d</i> ₆ (9:1)	S40
Procedure for Titration Studies by UV-vis Absorption Spectroscopy		S41
Figure S17	UV-vis absorbance spectra of Ir1 (0.1 mM) in DMSO: H ₂ O (1:9) before and after the addition of 4.0 mM of NaCl at 37 °C	S41
Figure S18	UV-vis absorbance spectra of Ir1 (0.1 mM) in DMSO: H ₂ O (1:9) before and after the addition of up to 16 equiv. of NaCl at 37 °C	S42
Figure S19	UV-vis absorbance spectra of Ir2 (0.1 mM) in DMSO/H ₂ O (1:9, v/v) before and after the addition of 20 - 40 equiv. of NaCl at 37 °C	S43
Figure S20	UV-vis absorbance spectra of Ir2 (0.1 mM) in DMSO/H ₂ O (1:9, v/v) before and after the addition of up to 40 equiv. of NaPF ₆ at 37 °C	S44
Figure S21	UV-vis absorbance spectra of NaCl (4.0 mM, left) and NaPF ₆ (4.0 mM, right) in DMSO/H ₂ O (1:9, v/v) at 37 °C.	S45
Figure S22	UV-vis absorbance spectra of Ir1 (red trace, 0.1 mM) and Ir2 (blue trace, 0.1 mM) in DMSO: PBS (1:9) at 37 °C	S46
Figure S23	Images of cuvettes containing Ir1 (left) and Ir2 (right) in DMSO/PBS (1:9, v/v) at 37 °C.	S46
Figure S24	UV-vis absorbance spectra of Ir2 (0.1 mM) in DMSO/H ₂ O (1:9, v/v) before (black trace) and after the addition of up to 40 equiv. of tetramethylammonium chloride (red trace) at 37 °C.	S47
Particle Size Measurement Using Dynamic Light Scattering (DLS)		S48
Figure S25	Size distribution vs. intensity data obtained from DLS analysis of Ir2 in the presence of NaCl in DMSO:H ₂ O (1:9).	S49
Table S8	Relative size of particles formed from Ir2 + NaCl in Figure S25	S49
Figure S26	Size distribution of Ir2 in PBS/DMSO (9:1)	S50
Figure S27	Size distribution of Ir2 in modified DMEM/DMSO (9:1)	S50
Figure S28	Size distribution of Ir2 in DMEM/DMSO (9:1)	S51
Control Experiments		S52-S58
Table S9	Oxidation of benzaldehyde by H ₂ O ₂ after 24 h	S52
Table S10	Oxidation of benzyl alcohol by H ₂ O ₂ after 24 h	S52
Figure S29	¹ H NMR spectrum (500 MHz, 25 °C, D ₂ O) of the reaction mixture from entry 2, Table S9	S53

Figure S30	¹ H NMR spectrum (500 MHz, 25 °C, D ₂ O) of the reaction mixture from Table S10 .	S53
Figure S31	IR spectra of Ir2 with and without NaCl	S54
Figure S32	Representative GC traces showing the transfer hydrogenation between HCOONa and compound 1w catalyzed by Ir1 / Ir2	S55
Figure S33	Representative GC traces showing the transfer hydrogenation between HCOONa and compound 1x catalyzed by Ir1 / Ir2	S56
Figure S34	Representative GC traces showing the transfer hydrogenation between HCOONa and compound 1y catalyzed by Ir1 / Ir2	S57
Table S11	Summary of transfer hydrogenation between HCOONa and various biological aldehydes and ketones	S58
NMR Spectroscopic Data		S59-S84
Figure S35	¹ H NMR spectrum of compound L1	S59
Figure S36	¹³ C NMR spectrum of compound L1	S60
Figure S37	¹ H NMR spectrum of compound L2	S61
Figure S38	¹³ C NMR spectrum of compound L2	S62
Figure S39	¹ H NMR spectrum of compound L3	S63
Figure S40	¹³ C NMR spectrum of compound L3	S64
Figure S41	¹ H NMR spectrum of compound L4	S65
Figure S42	¹³ C NMR spectrum of compound L4	S66
Figure S43	¹ H NMR spectrum of compound L5	S67
Figure S44	¹³ C NMR spectrum of compound L5	S68
Figure S45	¹ H NMR spectrum of complex Ir2	S69
Figure S46	¹ H NMR spectrum of compound L6	S70
Figure S47	¹³ C NMR spectrum of compound L6	S71
Figure S48	¹ H NMR spectrum of Ir1'	S72
Figure S49	¹³ C NMR spectrum of complex Ir1'	S73
Figure S50	¹ H NMR spectrum of tetrabutylammonium formate	S74
Figure S51	¹³ C NMR spectrum of tetrabutylammonium formate	S75
Figure S52	¹ H NMR spectrum of 2a	S76
Figure S53	¹ H NMR spectrum of 2c	S77
Figure S54	¹ H NMR spectrum of 2d	S78
Figure S55	¹ H NMR spectrum of 2h	S79
Figure S56	¹ H NMR spectrum of 2l	S80
Figure S57	¹ H NMR spectrum of 2m	S81
Figure S58	¹ H NMR spectrum of 2n	S82
Figure S59	¹ H NMR spectrum of 2p	S83
Figure S60	¹ H NMR spectrum of 2q	S84
Mass Spectrometric Data		S85-S88
Figure S61	Mass spectrum of L5	S85
Figure S62	Mass spectrum of complex Ir2	S85
Figure S63-S71	Mass spectrometric data of alcohols 2a , 2c-d , 2h , 2l-n , 2p-q	S86-S88
X-ray Data Collection and Refinement		S89-S91
Experiment Details		S89
Figure S72	Molecular structure of [(Ir2) ₂ Na(H ₂ O)]Cl (partial)	S89

Figure S73	Molecular structure of $[(\mathbf{Ir2})_2\text{Na}(\text{H}_2\text{O})]\text{Cl}$ (full)	S90
Table S12	Crystal data and structure refinement of $[(\mathbf{Ir2})_2\text{Na}(\text{H}_2\text{O})]\text{Cl}$	S91
Cell Cytotoxic Studies		S92
ICP-MS Analysis		S93
Table S13	Accumulation of Ir2 in NIH-3T3 cells	S93
Figure S74	Comparison of ICP-MS Results for Ir Complexes in NIH-3T3 cells	S94
References		S95

General Procedures

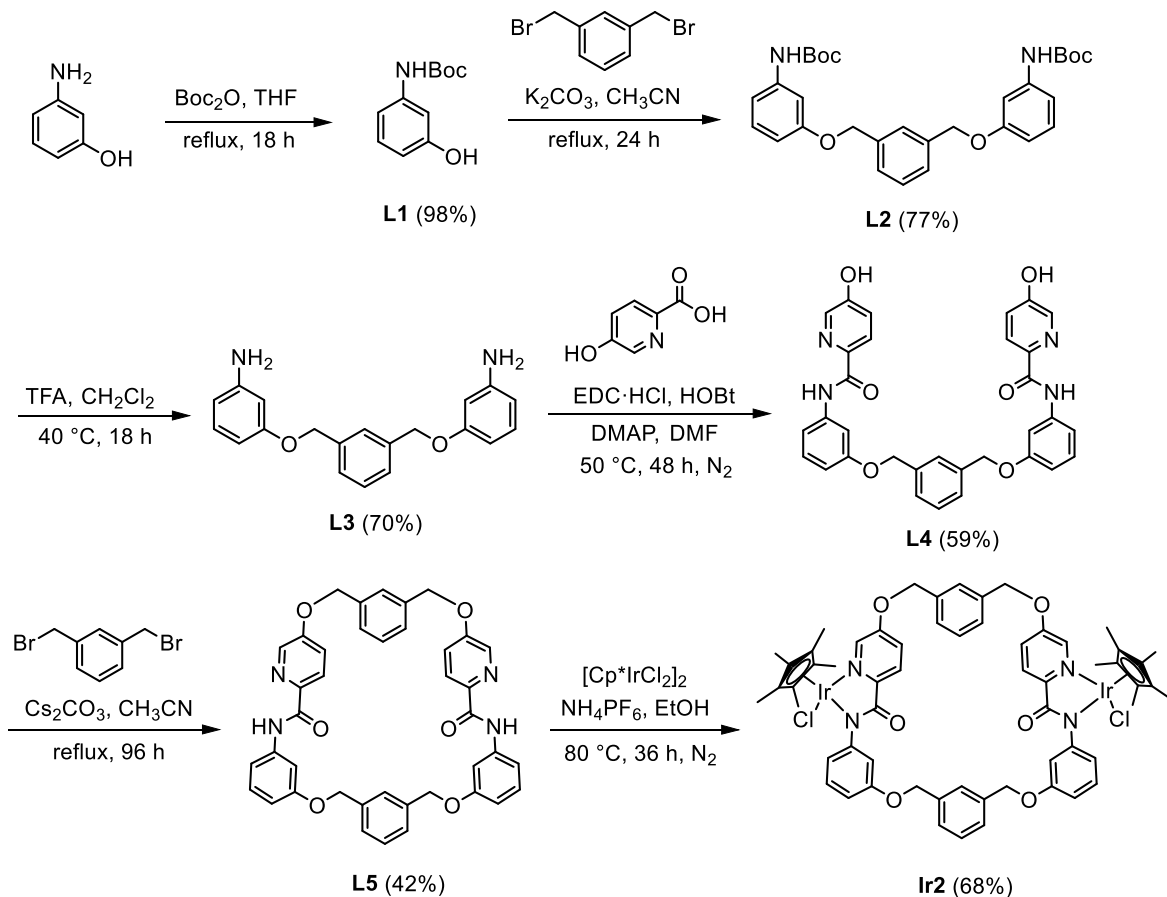
Commercial reagents and solvents were purchased from Sigma Aldrich, Alfa-Aesar, Ambeed Inc., Pressure Chemical, TCI America, Oakwood Chemical, ATCC, Thermo Fisher Scientific, and used as received. Deuterated solvents were purchased from Cambridge Isotope Laboratories Inc. and stored over activated molecular sieves prior to use. Anhydrous solvents were obtained from an Innovative Technology solvent drying system saturated with argon. Nitrogen (ultra-high purity grade) was purchased from Matheson TriGas. Organic solutions were concentrated under reduced pressure using a Heidolph rotary evaporator. Chromatographic purification of products was accomplished by flash chromatography using Silicycle F60 silica gel. Thin-layer chromatography (TLC) was performed on Silicycle 250 μm silica gel plates and visualized using a hand-held UV lamp. All air- and water-sensitive manipulations were performed using standard Schlenk techniques or under a nitrogen atmosphere using a glovebox. Yields refer to purified compounds unless otherwise noted. The iridium precursor $[\text{Cp}^*\text{IrCl}_2]_2$,¹ $[\text{Cp}^*\text{Ir}(N\text{-phenyl-2-pyridinecarboxamidate})\text{Cl}]$ (**Ir1**),² and 2-anthracenecarboxaldehyde³ were prepared as previously described.

Physical Methods

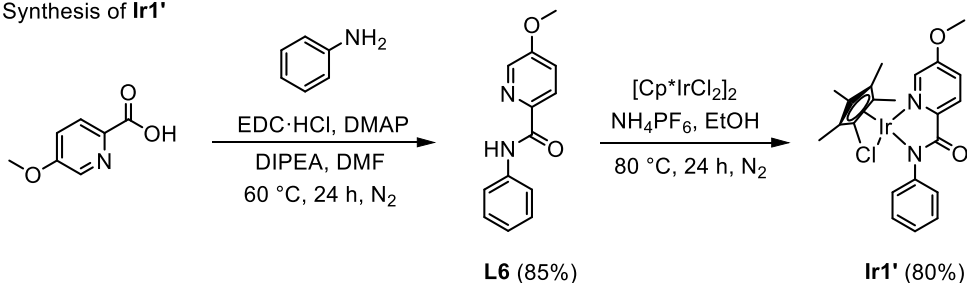
NMR spectra were acquired using JEOL spectrometers (ECA-400, 500, and 600) at room temperature and referenced using residual solvent peaks. All ^{13}C NMR spectra were proton decoupled. High-resolution mass spectra were obtained at the University of Texas-Austin Mass Spectrometry Facility using an Agilent 6546 Q-TOF LC/MS. Gas chromatography-mass spectrometry (GC-MS) was performed using an Agilent 7890 GC/5977A MSD instrument equipped with an HP-5MS capillary column. For the temperature program used for GC-MS analysis, samples were held at 60 $^{\circ}\text{C}$ for 3 min, heated from 60 to 280 $^{\circ}\text{C}$ at 10 $^{\circ}\text{C}/\text{min}$, and then held at 280 $^{\circ}\text{C}$ for 3 min. The inlet temperature was set constant at 280 $^{\circ}\text{C}$. The GC-MS spectra obtained were compared with those in the NIST library. Infrared (IR) spectra were measured by using a Thermo Nicolet Avatar FTIR spectrometer with a diamond ATR. Ultraviolet-visible (UV-vis) absorption spectroscopic studies were performed using an Agilent Cary 60 spectrophotometer. Particles size measurements were performed using dynamic light scattering (DLS) on a Malvern Zetasizer Nano-ZS90. The absorbance of the 96-well plate for cell cytotoxicity studies was measured at 510 nm and 565 nm on a Tecan Infinite M200 Pro microplate reader.

Synthesis and Characterization

A) Synthesis of Ir2

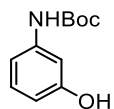


B) Synthesis of Ir1'



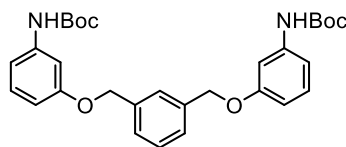
Scheme S1. Synthetic routes for the preparation of complex **Ir1'** and **Ir2**. Boc_2O = di-*tert*-butyl dicarbonate; EDC · HCl = *N*-(3-Dimethylaminopropyl)-*N'*-ethylcarbodiimide hydrochloride; HOBT = hydroxybenzotriazole; DMAP = 4-dimethylaminopyridine; DMF = dimethylformamide; Cp^* = pentamethylcyclopentadienyl anion.

Preparation of Compound L1:



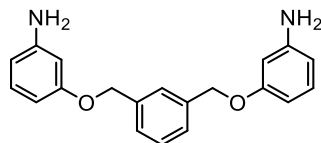
A 20 mL THF solution of di-*tert*-butyl dicarbonate (Boc_2O) (2.60 g, 12 mmol, 1.2 equiv.) was combined with a 25 mL THF solution of 3-aminophenol (1.09 g, 10 mmol, 1.0 equiv.) in a 100 mL round bottom flask at room temperature. The reaction mixture was refluxed for 18 h. After cooling the flask to room temperature and evaporating the solvent to dryness, the brown crude product was purified by silica gel column chromatography using hexanes/ethyl acetate (3:1) as the eluent. The product was obtained as a white solid (2.04 g, 98%). ^1H NMR (500 MHz, $\text{DMSO}-d_6$): δ = 9.21 (br, 1H), 9.15 (br, 1H), 6.98 – 6.93 (m, 2H), 6.79 (d, J = 8.2 Hz, 1H), 6.31 (dd, J = 8.0, 2.7 Hz, 1H), 1.42 (s, 9H) ppm. ^{13}C NMR (126 MHz, $\text{DMSO}-d_6$): δ = 158.14, 153.20, 141.11, 129.70, 109.65, 109.48, 105.78, 79.32, 28.67 ppm. GC-MS: calc. for $\text{C}_{11}\text{H}_{15}\text{NO}_3$ $[\text{M}]^+ = 209.1$, found 209.1. This compound was reported previously.⁴

Preparation of Compound L2:



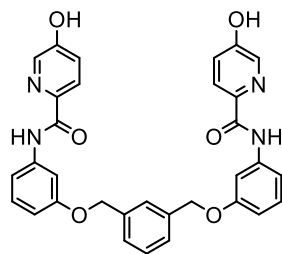
In a 100 mL round bottom flask equipped with a magnetic stir bar, **L1** (1.67 g, 8 mmol, 2 equiv.), *m*-xylylene dibromide (1.06 g, 4 mmol, 1 equiv.), and K_2CO_3 (1.38 g, 10 mmol, 2.5 equiv.) was dissolved in CH_3CN (40 mL) at room temperature. The reaction mixture was refluxed for 24 h to obtain a light yellow mixture. After evaporating the solvent to dryness, ethyl acetate (20 mL) was added, and the mixture was washed with water (3×20 mL). The combined organic layer was subsequently dried over anhydrous Na_2SO_4 , filtered to remove the salt, and then evaporated to dryness. The desired product was obtained as a white solid (1.61 g, 77%) after purification by silica gel column chromatography using hexanes/diethyl ether/ethyl acetate (10:1:1) as the eluent. ^1H NMR (400 MHz, CDCl_3): δ = 7.40 – 7.19 (m, 4H), 7.16 – 7.08 (m, 4H), 6.90 (d, J = 8.0 Hz, 2H), 6.59 (d, J = 8.2, 2H), 4.93 (s, 4H), 1.47 (s, 18H) ppm. ^{13}C NMR (101 MHz, CDCl_3): δ = 159.19, 152.80, 139.81, 137.15, 129.50, 128.54, 126.82, 126.40, 110.94, 109.43, 104.88, 80.10, 69.48, 28.19 ppm. ESI-MS (+): calc. for $\text{C}_{30}\text{H}_{36}\text{N}_2\text{O}_6$ $[\text{M}+\text{H}]^+ = 521.2651$, found 521.2546.

Preparation of Compound L3:



To a 100 mL round bottom flask equipped with a magnetic stir bar containing 45 mL of CH_2Cl_2 , solid **L2** (1.56 g, 3 mmol, 1.0 equiv.) was added, followed by the slow addition of trifluoroacetic acid (TFA, 15 mL). The colorless mixture was continuously stirred for 18 h at 40 °C to obtain a red solution. After evaporating the reaction mixture to dryness (note: 20 mL of a 2 M aqueous of KOH should be added to the rotatory evaporator receiving flask to neutralize TFA), the thick crude liquid was purified by silica gel column chromatography (eluent = starting with hexanes/ethyl acetate/triethylamine (3:1:0.5) and then changing to hexanes/ethyl acetate/triethylamine (1:2:0.5) to obtain the desired product as an off-white solid (680 mg, 70%). ^1H NMR (500 MHz, CDCl_3): δ = 7.49 (s, 1H), 7.39 (s, 3H), 7.07 (t, J = 7.9 Hz, 2H), 6.45 – 6.39 (m, 2H), 6.31 (d, J = 7.5 Hz, 4H), 5.03 (s, 4H), 3.60 (br, 4H) ppm. ^{13}C NMR (126 MHz, CDCl_3): δ = 160.03, 147.94, 137.69, 130.28, 128.94, 127.09, 126.56, 108.37, 104.97, 102.12, 69.77 ppm. GC-MS: calc. for $\text{C}_{20}\text{H}_{20}\text{N}_2\text{O}_2$ $[\text{M}]^+$ = 322.1, found 322.1.

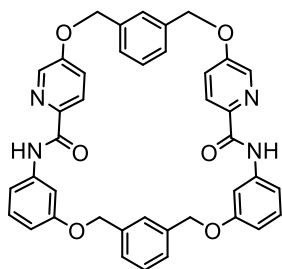
Preparation of Compound L4:



To a 50 mL round bottom flask equipped with a magnetic stir bar contains dry DMF (15 mL), 5-hydroxypicolinic acid (985 mg, 7.1 mmol, 2.2 equiv.), DMAP (786 mg, 6.4 mmol, 2 equiv.), 1-hydroxybenzotriazole (870 mg, 6.4 mmol, 2 equiv.), and EDC·HCl (1.54 g, 8 mmol, 2.5 equiv.) was added sequentially. The mixture was stirred vigorously for 10 min at room temperature to obtain a yellow solution and was then combined with **L3** (1.03 g, 3.2 mmol, 1.0 equiv.). The solution turned dark after 30 min and was stirred for a total of 2 d at 40-50 °C under N_2 to obtain a dark brown mixture. Once the reaction was complete, the mixture was diluted with 50 mL of CH_2Cl_2 + 5 mL of iPrOH and washed with water (5×) until the organic layer become colorless. The combined organic layer was dried over anhydrous Na_2SO_4 , filtered to remove the salt, and evaporated to dryness to obtain a brown viscous oil, which was purified by silica gel chromatography (eluent = starting from hexanes/ethyl acetate (1:1), and then changing to hexanes/ethyl acetate/methanol (1:2:0.1)) to obtain the desired product as an off-white solid (1.06 g, 59%). ^1H NMR (500 MHz, $\text{DMSO}-d_6$): δ = 10.82 – 10.71 (br, 2H), 10.34 (s, 2H), 8.20 (d, J =

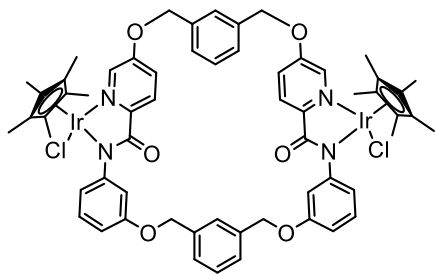
2.7 Hz, 2H), 8.00 (d, $J = 8.5$ Hz, 2H), 7.67 (t, $J = 2.2$ Hz, 2H), 7.54 (s, 1H), 7.47 (dd, $J = 8.0, 1.9$ Hz, 2H), 7.39 (s, 3H), 7.33 (dd, $J = 8.6, 2.8$ Hz, 2H), 7.20 (t, $J = 8.2$ Hz, 2H), 6.72 (dd, $J = 8.3, 2.5$ Hz, 2H), 5.08 (s, 4H) ppm. ^{13}C NMR (126 MHz, DMSO- d_6): $\delta = 162.97, 159.12, 157.18, 141.54, 140.37, 137.86, 137.14, 130.01, 129.13, 127.74, 127.50, 124.51, 123.58, 113.02, 110.42, 107.09, 69.59$ ppm. ESI-MS(+): calc. for $\text{C}_{32}\text{H}_{26}\text{N}_4\text{O}_6$ $[\text{M}+\text{H}]^+ = 563.1930$, found 563.1926.

Preparation of Compound L5:



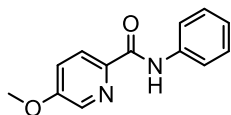
To a 250 mL round bottom flask equipped with a magnetic stir bar contains dry CH_3CN (100 mL), solid **L4** (56 mg, 0.1 mmol, 1 equiv.) and Cs_2CO_3 (164 mg, 0.5 mmol, 5 equiv.) were combined. The mixture was stirred vigorously for 2 h at 70 °C under N_2 to give a cloudy solution. Solid *m*-xylylene dibromide (26 mg, 0.1 mmol, 1 equiv.) was predissolved in 20 mL of dry CH_3CN in a 20 mL screw-capped vial and sonicated for 1 min. Every 2 h, 0.5 mL of this solution was added into the reaction flask via syringe. After completion, the solvent was removed by rotatory evaporation. The crude product was redissolved in water (50 mL) and CH_2Cl_2 (50 mL). The combined organic layer was separated, dried over anhydrous Na_2SO_4 , filtered to remove the salt, and evaporated to dryness. The crude product was purified by silica gel column chromatography (eluent = starting with ethyl acetate/hexanes (1:1), and then changing to ethyl acetate/hexanes/methanol (9:1:0.5) to obtain the desired product as white solid (30 mg, 42%). ^1H NMR (500 MHz, DMSO- d_6): $\delta = 10.33$ (s, 2H), 8.24 (d, $J = 2.6$ Hz, 2H), 7.97 (d, $J = 8.6$ Hz, 2H), 7.57 (s, 1H), 7.54 – 7.50 (m, 7H), 7.40 – 7.35 (m, 4H), 7.35 – 7.32 (m, 2H), 7.21 (t, $J = 8.4$ Hz, 2H), 6.73 (ddd, $J = 8.3, 2.4, 1.1$ Hz, 2H), 5.41 (s, 4H), 5.15 (s, 4H) ppm. ^{13}C NMR (126 MHz, DMSO- d_6): $\delta = 162.56, 158.81, 156.80, 143.05, 140.17, 138.04, 137.60, 137.14, 130.03, 129.58, 128.99, 127.69, 127.04, 126.92, 126.61, 124.08, 123.41, 113.07, 110.36, 107.77, 69.68, 69.10$ ppm. ESI-MS (+): calc. for $\text{C}_{40}\text{H}_{32}\text{N}_4\text{O}_6$ $[\text{M}+\text{H}]^+ = 665.2400$, found 665.2396. IR: $\nu = 438, 578, 680, 781, 832, 1017, 1219, 1261, 1311, 1418, 1489, 1532, 1594, 1668, 3322$ cm^{-1} .

Preparation of Complex Ir2:



In a 50 mL round bottom flask, 15 mL of anhydrous EtOH was purged with nitrogen gas for 30 min. Solid $[\text{Cp}^*\text{IrCl}_2]_2$ (40 mg, 0.05 mmol, 1.0 equiv.) and ligand **L5** (34 mg, 0.05 mmol, 1.0 equiv.) were added and stirred for 15 min at 80 °C. The reaction mixture was then treated with solid ammonium hexafluorophosphate (4.7 equiv.) and stirred for additional 34 h at 80 °C. After cooling to room temperature, the reaction mixture was evaporated to dryness. The crude product was dissolved in 20 mL of CH_2Cl_2 and washed with water (3×20 mL). The organic phase was separated, dried over Na_2SO_4 , filtered, and then evaporated to dryness. The desired product was obtained as a yellow solid after purification by silica gel column chromatography, using 2% methanol in CH_2Cl_2 as the eluent (yield = 46 mg, 68%). ^1H NMR (500 MHz, $\text{DMSO}-d_6$): δ = 8.10 (dd, J = 14.0, 2.0 Hz, 2H), 7.81 (t, J = 2.6 Hz, 3H), 7.75 (d, J = 8.7 Hz, 1H), 7.60 (d, J = 11.7 Hz, 1H), 7.53 (s, 1H), 7.48 (d, J = 5.5 Hz, 2H), 7.41 – 7.32 (m, 4H), 7.21 – 7.11 (m, 2H), 7.04 (s, 1H), 7.00 (t, J = 7.8 Hz, 2H), 6.93 (d, J = 2.5 Hz, 1H), 6.73 (ddd, J = 35.7, 8.4, 2.5 Hz, 2H), 5.60 – 5.42 (m, 4H), 5.14 – 4.99 (m, 4H), 1.12 (d, J = 1.2 Hz, 30H) ppm. The ^{13}C NMR spectrum of **Ir2** could not be obtained due to its low solubility in $\text{DMSO}-d_6$ and other typical NMR solvents (e.g., acetonitrile, acetone, benzene, chloroform, methanol). ESI-MS(+): calc. for $\text{C}_{60}\text{H}_{60}\text{Ir}_2\text{N}_4\text{O}_6\text{Cl}_2$ $[\text{M}-2\text{Cl}]^{2+}$ = 659.188, found 659.192. IR: ν = 687, 791, 1023, 1256, 1372, 1459, 1586, 1718, 2858, 2920 cm^{-1} .

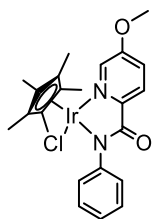
Preparation of Compound L6:



To a 50 mL round bottom flask equipped with a magnetic stir bar containing dry DMF (15 mL), 5-methoxypicolinic acid (385 mg, 2.5 mmol, 1.0 equiv.), DMAP (76 mg, 0.25 equiv.), and EDC·HCl (580 mg, 3 mmol, 1.5 equiv.) were combined. The mixture was then treated with aniline (235 μL , 1.1 equiv.) and *N,N*-diisopropylethylamine (1.2 mL, 3.0 equiv.), and was stirred for 24 h at 60 °C under N_2 to obtain a brown mixture. Once the reaction was complete, the mixture was diluted with 50 mL of ethyl acetate and washed with water (3×) until the organic layer become

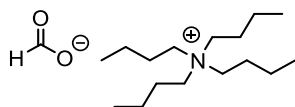
colorless. The combined organic layer was mixed with aqueous HCl (1 M) until the pH of the water layer was ~6.0. After removing the aqueous layer, the organic layer was dried over anhydrous Na₂SO₄, filtered to remove the salt, and evaporated to dryness to obtain the desired product as an off-white solid (580 mg, 85%). ¹H NMR (400 MHz, CDCl₃): δ = 9.83 (br, 1H), 8.28 – 8.19 (m, 2H), 7.79 – 7.73 (m, 2H), 7.41 – 7.30 (m, 3H), 7.12 (tt, *J* = 7.3, 1.3 Hz, 1H), 3.91 (s, 3H) ppm. ¹³C NMR (101 MHz, CDCl₃): δ = 162.15, 158.20, 142.50, 138.05, 136.51, 129.16, 124.18, 123.73, 120.49, 119.67, 55.93 ppm. GC-MS: calc. for C₁₃H₁₂N₂O₂ [M]⁺ = 228.1, found 228.0. IR: ν = 512, 559, 679, 748, 838, 897, 1023, 1124, 1206, 1262, 1317, 1435, 1523, 1588, 1666, 2924, 3310 cm⁻¹.

Preparation of Complex Ir1':



In a 50 mL round bottom flask, 15 mL of anhydrous EtOH was purged with nitrogen gas for 30 min. Solid [Cp*IrCl₂]₂ (80 mg, 0.1 mmol, 1.0 equiv.), ligand **L6** (50 mg, 0.22 mmol, 2.2 equiv.), and ammonium hexafluorophosphate (98 mg, 6.0 equiv.) were combined and stirred for 24 h at 80 °C under N₂. After cooling to room temperature, the reaction mixture was evaporated to dryness. The desired product was obtained as a yellow solid after purification by silica gel column chromatography, using 2% methanol in ethyl acetate as the eluent (yield = 94 mg, 80%). ¹H NMR (500 MHz, DMSO-*d*₆): δ = 8.25 (d, *J* = 2.6 Hz, 1H), 7.82 (d, *J* = 8.7 Hz, 1H), 7.74 (dd, *J* = 8.8, 2.6 Hz, 1H), 7.45 – 7.42 (m, 2H), 7.26 – 7.22 (m, 2H), 7.01 (tt, *J* = 7.2, 1.3 Hz, 1H), 3.96 (s, 3H), 1.30 (s, 15H) ppm. ¹³C NMR (126 MHz, DMSO-*d*₆): δ = 168.06, 158.76, 149.18, 147.78, 138.87, 128.00, 127.61, 126.74, 124.00, 123.61, 86.79, 57.00, 8.55 ppm. IR: ν = 515, 584, 685, 762, 854, 1022, 1106, 1254, 1361, 1483, 1587, 2919 cm⁻¹.

Preparation of tetrabutylammonium formate:

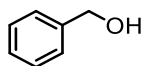


To a 50 mL round bottom flask equipped with a magnetic stir bar containing methanol (10 mL), formic acid (reagent grade, 200 μL, 5.5 mmol, 1.1 equiv.) and tetrabutylammonium hydroxide solution (25 wt.% in methanol, 1800 μL, 5 mmol, 1.0 equiv.) were combined. The flask was sealed with a septum stopper and the mixture was stirred for 24 h at RT. The solution was then evaporated to dryness under reduced pressure, giving a colorless amorphous salt. The solid was rinsed with hexanes and then dried under high vacuum at room temperature overnight to afford the desired the

salts as white solid in quantitative yield (1.5 g, >99%). ^1H NMR (500 MHz, $\text{DMSO-}d_6$): δ = 8.39 (br, 1H), 3.25 – 3.04 (m, 8H), 1.56 – 1.50 (m, 8H), 1.31 – 1.25 (m, 8H), 0.89 (t, J = 7.4 Hz, 12H) ppm. ^{13}C NMR (126 MHz, $\text{DMSO-}d_6$): δ = 165.63, 58.04, 23.60, 19.73, 14.03 ppm. These data match those reported in the literature.⁵

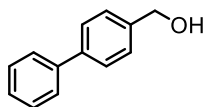
Characterization Data for Alcohol Products

Compound 2a



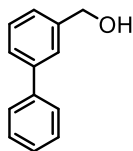
Compound **2a** was obtained as a colorless liquid. ^1H NMR (400 MHz, $\text{DMSO-}d_6$): δ = 7.31 – 7.27 (m, 4H, ArH), 7.22 – 7.17 (m, 1H, ArH), 5.17 (t, J = 5.7 Hz, 1H, OH), 4.47 (d, J = 5.7 Hz, 2H, CH_2) ppm. GC-MS (EI): calc. for $\text{C}_7\text{H}_8\text{O}$ $[\text{M}]^+$ = 108.1, found 107.8. These data matched those reported in the literature.⁶

Compound 2c



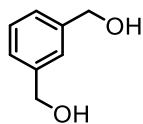
Compound **2c** was obtained as a white solid. ^1H NMR (400 MHz, $\text{DMSO-}d_6$): δ = 7.63 – 7.57 (m, 4H, ArH), 7.44 – 7.29 (m, 5H, ArH), 5.19 (t, J = 5.7 Hz, 1H, OH), 4.50 (d, J = 5.7 Hz, 2H, CH_2) ppm. GC-MS (EI): calc. for $\text{C}_{13}\text{H}_{12}\text{O}$ $[\text{M}]^+$ = 184.1, found 184.3. These data matched those reported in the literature.⁷

Compound 2d



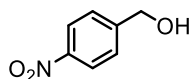
Compound **2d** was obtained as a white solid. ^1H NMR (400 MHz, $\text{DMSO-}d_6$): δ = 7.62 – 7.56 (m, 3H, ArH), 7.49 – 7.27 (m, 6H, ArH), 4.53 (s, 2H, CH_2) ppm. GC-MS (EI): calc. for $\text{C}_{13}\text{H}_{12}\text{O}$ $[\text{M}]^+$ = 184.1, found 184.0. These data matched those reported in the literature.⁸

Compound 2h



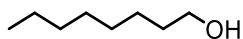
Compound **2h** was obtained as a colorless liquid. ^1H NMR (400 MHz, DMSO- d_6): δ = 7.29 – 7.12 (m, 4H, ArH), 4.45 (s, 4H, 2CH₂) ppm. GC-MS (EI): calc. for C₈H₁₀O₂ [M]⁺ = 138.1, found 138.2. These data matched those reported in the literature.⁹

Compound 2l



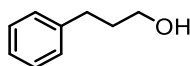
Compound **2l** was obtained as a white solid. ^1H NMR (400 MHz, DMSO- d_6): δ = 8.22 – 8.08 (m, 2H, ArH), 7.57 – 7.48 (m, 2H, ArH), 5.51 (t, J = 5.7 Hz, 1H, OH), 4.60 (d, J = 5.7 Hz, 2H, CH₂) ppm. GC-MS (EI): calc. for C₇H₇NO₃ [M]⁺ = 153.0, found 152.9. These data matched those reported in the literature.⁶

Compound 2m



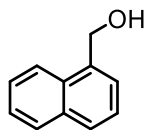
Compound **2m** was obtained as a colorless liquid. ^1H NMR (400 MHz, DMSO- d_6): δ = 4.30 (t, J = 5.2 Hz, 1H, OH), 3.38 – 3.29 (m, 2H, CH₂), 1.37 – 1.32 (m, 2H, CH₂), 1.26 – 1.17 (m, 10H), 0.82 (t, J = 6.9 Hz, 3H, CH₃) ppm. GC-MS (EI): calc. for C₈H₁₈O [M-OH]⁺ = 112.1, found 112.1. These data matched those reported in the literature.⁷

Compound 2n



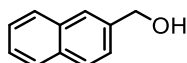
Compound **2n** was obtained as a colorless liquid. ^1H NMR (400 MHz, DMSO- d_6): δ = 7.26 – 7.20 (m, 2H, ArH), 7.17 – 7.09 (m, 3H, ArH), 4.47 (t, J = 5.2 Hz, 1H, OH), 3.38 (td, J = 6.5, 5.0 Hz, 2H, CH₂), 2.62 – 2.53 (m, 2H, CH₂), 1.75 – 1.62 (m, 2H, CH₂) ppm. GC-MS: calc. for C₉H₁₂O [M]⁺ = 136.1, found 136.1. These data matched those reported in the literature.⁷

Compound 2p



Compound **2p** was obtained as a colorless liquid. ^1H NMR (400 MHz, $\text{DMSO-}d_6$): δ = 8.11 – 8.00 (m, 1H, *ArH*), 7.96 – 7.85 (m, 1H, *ArH*), 7.79 (d, J = 8.0 Hz, 1H, *ArH*), 7.60 – 7.40 (m, 4H, *ArH*), 5.36 (t, J = 5.2 Hz, 1H, *OH*), 4.97 (d, J = 3.7 Hz, 2H, *CH*₂) ppm. GC-MS: calc. for $\text{C}_{11}\text{H}_{10}\text{O}$ $[\text{M}]^+$ = 158.1, found 158.0. These data matched those reported in the literature.⁷

Compound 2q



Compound **2q** was obtained as a white solid. ^1H NMR (400 MHz, $\text{DMSO-}d_6$): δ = 7.88 – 7.75 (m, 4H, *ArH*), 7.49 – 7.37 (m, 3H, *ArH*), 5.35 (br, 1H, *OH*), 4.63 (s, 2H, *CH*₂) ppm. GC-MS: calc. for $\text{C}_{11}\text{H}_{10}\text{O}$ $[\text{M}]^+$ = 158.1, found 158.0. These data matched those reported in the literature.⁷

Table S1. Screening Conditions for Amide Coupling using Model Substrates

Entry	Condition	Yield (%) ^a
1	a) (COCl) ₂ , DMF, CH ₂ Cl ₂ , 0 °C, 24 h b) Et ₃ N, then aniline, RT, 6 h	0
2	a) NHS, DCC, DMAP, CH ₂ Cl ₂ , RT, 12 h b) aniline, 12 h	0
3	a) Et ₃ N, CH ₂ Cl ₂ , 0°C, 10 min b) ClCOOEt, N ₂ , RT, 2 h c) aniline, 18 h	trace
4	a) I ₂ , PPh ₃ , CH ₂ Cl ₂ b) 5-Hydroxypicolinic acid, 30 min, RT c) aniline, 1 h, then Et ₃ N	trace
5	CMPI, DMAP, CH ₂ Cl ₂	0
6	HBTU, DMAP, CH ₂ Cl ₂	17
7 ^b	DCC, DMAP, CH ₂ Cl ₂	68
8 ^b	DCC, HOBt, DMAP, CH ₂ Cl ₂	70
9	EDC · HCl, HOBt, DMAP, CH ₂ Cl ₂	45
10	EDC · HCl, HOBt, DMAP, DMF	82

The reactions were performed in 0.5 mmol scale of 5-hydroxypicolinic acid in 10 mL round-bottom flasks sealed with a rubber septum and were analyzed by GC-MS after completion. ^aIsolated yields. ^bThe dicyclohexylurea (DCU) byproduct could not be removed from the isolated product even after purification. Abbreviation: NHS = *N*-hydroxysuccinimide, DCC = *N,N'*-dicyclohexylcarbodiimide, DMAP = 4-dimethylaminopyridine, CMPI = 2-chloro-1-methylpyridinium iodide, HBTU = hexafluorophosphate benzotriazole tetramethyl uronium, HOBt = *N*-hydroxybenzotriazole, EDC = *N*-(3-Dimethylaminopropyl)-*N'*-ethylcarbodiimide hydrochloride.

General Procedure for Transfer Hydrogenation Studies

Stock solutions of the substrate (100 mM) and iridium complexes (**Ir1** or **Ir1'** = 10 mM, **Ir2** = 5 mM) were prepared in DMSO and stored in the freezer for subsequent use. Stock solutions of HCOONa (100 mM) in millipore water were prepared fresh each time. The appropriate volumes of the following stock solutions were combined sequentially in a 3 mL vial: Ir catalyst, substrate, and HCOONa. Additional solvent was added to achieve a mixture containing 10% DMSO in water with a total volume of 3.0 mL. The reaction vials were sealed tightly with screw caps and allowed to proceed at 37 °C. After an allotted amount of time, diphenyl ether (0.2 equiv. relative to the substrate) was added as an internal standard (IS) and the reaction mixture was transferred to a test tube, which was further diluted with 3 mL of ethyl acetate. The combined organic layer was filtered through a pipette plug containing celite + Na₂SO₄, and the sample was analyzed by GC-MS. GC yields were calculated as follows:

$$\text{Yield of alcohol} = \frac{\text{moles of alcohol}}{(\text{moles of unreacted aldehyde}) + (\text{moles of alcohol})} \times 100\%$$

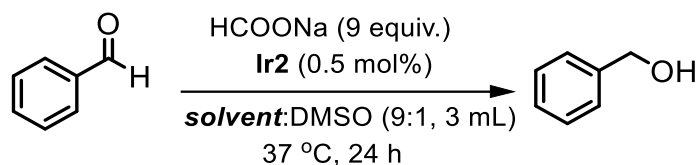
$$\text{moles of alcohol} = \text{RF}_{\text{alcohol}} \times \frac{\text{Area}_{\text{alcohol}}}{\text{Area}_{\text{internal standard}}} \times (\text{moles of internal standard})$$

$$\text{moles of unreacted aldehyde} = \text{RF}_{\text{aldehyde}} \times \frac{\text{Area}_{\text{unreacted aldehyde}}}{\text{Area}_{\text{internal standard}}} \times (\text{moles of internal standard})$$

$\text{RF}_{\text{alcohol}}$ = GC retention factor of the alcohol

$\text{RF}_{\text{aldehyde}}$ = GC retention factor of the aldehyde

For substrates giving nearly full conversion with catalyst **Ir2** (**1a**, **1c**, **1d**, **1h**, **1l**, **1m**, **1n**) or more sterically hindered aldehydes (**1p**, **1q**), further characterization of the corresponding alcohols by ¹H NMR spectroscopy was conducted. The reaction was performed in a 0.3 mmol scale of aldehyde, using 10 mL of H₂O:DMSO (9:1, v/v) in a 20 mL borosilicate glass scintillation vial sealed with a polyethylene cap. When the reaction was complete, the sample was diluted with 10 mL of ethyl acetate. The organic layer was separated, dried over Na₂SO₄, filtered, and evaporated to dryness. For NMR spectroscopic studies (for substrates **1o**, **1v**), deuterated solvents (D₂O and DMSO-*d*₆) were used instead to prepare the stock solutions so that the reaction mixtures could be analyzed in situ. After the reactions were stirred for an allotted amount of time, 1,3,5-trimethoxybenzene (0.5 equiv. relative to the substrate) was added and the reaction mixture was transferred to an NMR tube for ¹H NMR spectroscopic analysis.

Table S2. Biocompatibility Evaluation of **Ir2**

Entry	Solvent/Additives	Yield (%) ^a
1	H ₂ O as solvent	90 ± 1
2	PBS as solvent	81 ± 5
3	RPMI-1640 as solvent	48 ± 2
4	DMEM as solvent	45 ± 2
5	DMEM + 10% FBS + 1% antibiotics ^b as solvent	40 ± 1
6	Gln (4 mM) + Lys (0.8 mM) in PBS as solvent	78 ± 2
7	Gln (2 mM) + Arg (1 mM) in PBS as solvent	72 ± 4
8	Glucose (5 mM) in PBS as solvent	52 ± 2
9	Glucose (25 mM) in PBS as solvent	41 ± 3
10 ^c	NADH (9 equiv.) as hydride source	74 ± 2

Reaction conditions used: benzaldehyde (15 μmol), HCOONa (135 μmol), Ir complex (0.075 μmol), 37 °C, 24 h. The reaction yields were determined by gas chromatography using diphenyl ether as an internal standard. ^aYields are average of duplicate runs. ^bPenicillin-Streptomycin 10/10 solution (100×). ^cNADH was used as hydride source instead of sodium formate and the reaction was performed in H₂O/DMSO (9:1, 3 mL). Abbreviation: PBS = Phosphate-Buffered Saline, RPMI = Roswell Park Memorial Institute, DMEM = Dulbecco's Modified Eagle Medium, FBS = Fetal Bovine Serum, Gln = glutamine, Lys = lysine, Arg = arginine, NADH = reduced nicotinamide adenine dinucleotide.

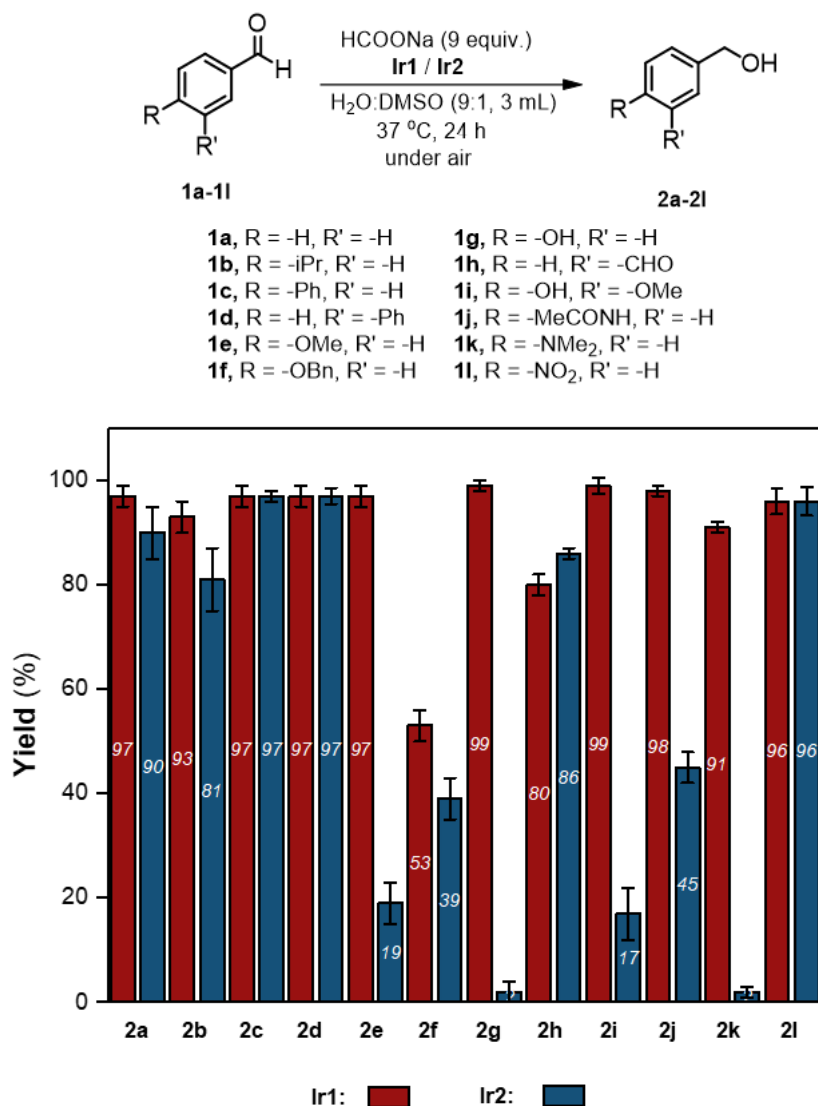


Figure S1. Substrate scope studies of benzaldehyde and its derivatives. Reaction conditions used: substrate (5 mM, 15 μ mol), HCOONa (135 μ mol), Ir complex (0.15 μ mol for **Ir1**, 0.075 μ mol for **Ir2**), 37 °C, 24 h. The reaction yields were determined by GC-MS using diphenyl ether as an internal standard, except for substrate **1b** and **1i**, biphenyl was used as an internal standard. Yields are average of triplicate independent runs.

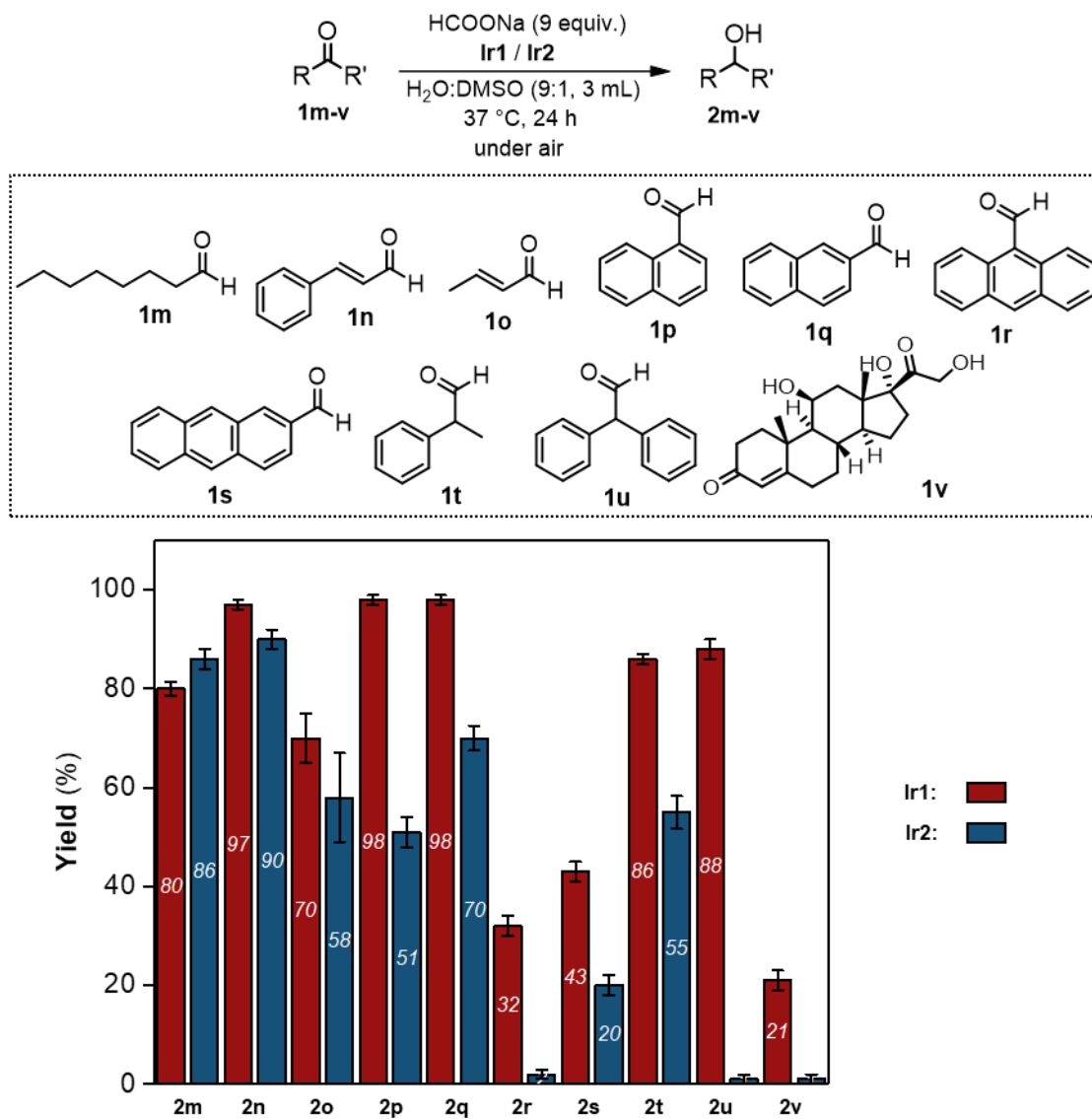
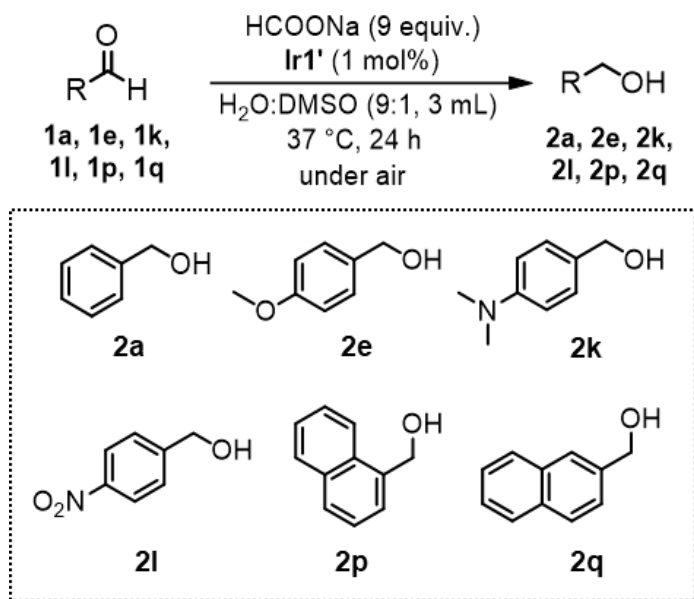


Figure S2. Substrate scope studies of various aldehydes and ketones. Reaction conditions used: substrate (5 mM, 15 μmol), HCOONa (135 μmol), Ir complex (0.15 μmol for **Ir1**, 0.075 μmol for **Ir2**), 37 $^\circ\text{C}$, 24 h. The reaction yields were determined by GC-MS using diphenyl ether as an internal standard. Yields are average of triplicate independent runs. For substrate **1o** and **1v**, samples were prepared in D_2O : $\text{DMSO}-d_6$ (9:1, 1 mL) and yields were determined by ^1H NMR spectroscopy, using 1,3,5-trimethoxybenzene as an internal standard. Yields of **2o** were determined after 6 h for **Ir1** and 12 h for **Ir2**. Full conversion of crotonaldehyde **1o** to its corresponding alcohol **2o** was observed; however, the calculated yields are not accurate due to starting material evaporation.

Table S3. Comparing the Activity of Ir Catalysts

Entry	Catalyst	Substrate	Yield (%)
1	Ir1'	1a	91 ± 3
2		1e	95 ± 1
3		1k	90 ± 2
4		1l	96 ± 1
5		1p	81 ± 6
6		1q	85 ± 2
7	Ir1	1a	97 ± 2
8		1e	97 ± 2
9		1k	91 ± 1
10		1l	96 ± 3
11		1p	98 ± 1
12		1q	98 ± 1
13	Ir2	1a	90 ± 5
14		1e	19 ± 4
15		1k	trace
16		1l	96 ± 3
17		1p	51 ± 3
18		1q	70 ± 2

Reaction conditions used: substrate (5 mM, 15 μmol), HCOONa (135 μmol), **Ir1'** (0.15 μmol), 37 °C, 24 h. The reaction yields were determined by GC-MS using diphenyl ether as an internal standard. Yields are average of triplicate independent runs. Data from entry 7 – entry 18 were used for comparison, which were previously shown in **Figure S1** and **Figure S2**.

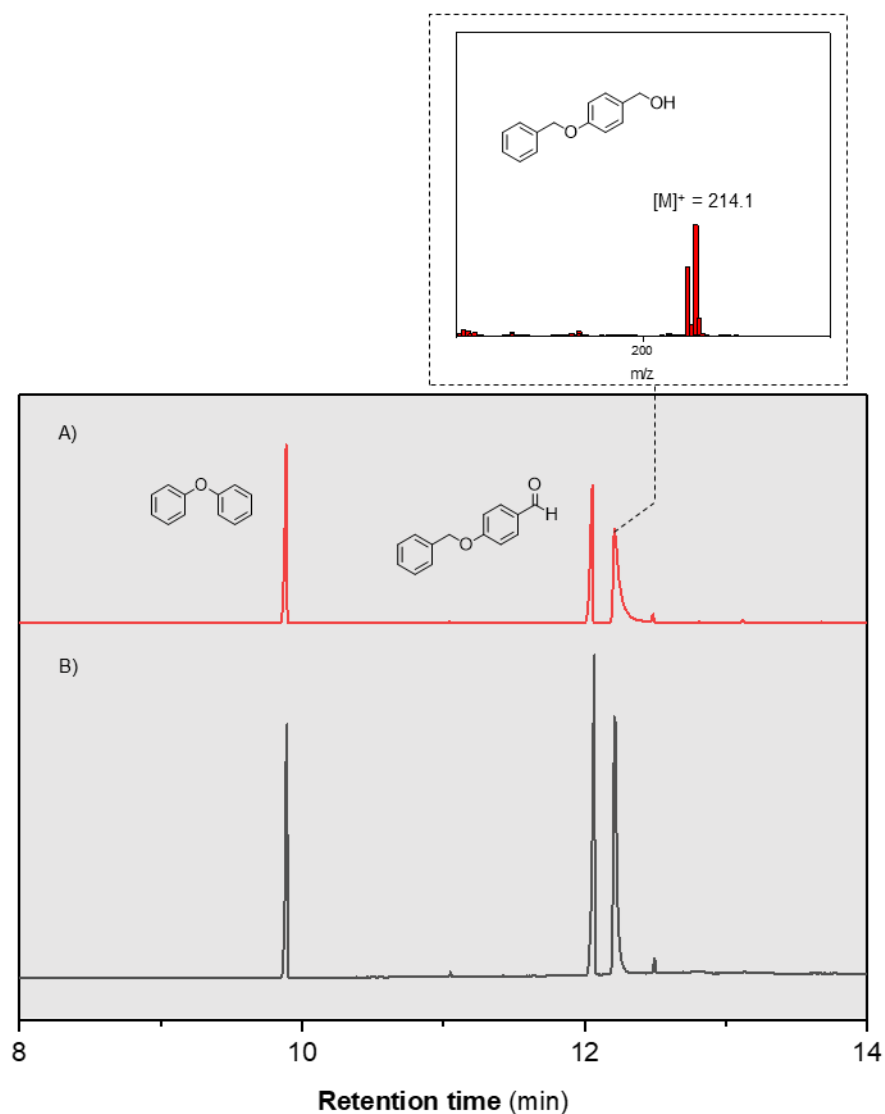


Figure S3. Representative GC plots showing products obtained from the transfer hydrogenation between 4-benzyloxybenzaldehyde **1f** and HCOONa using **Ir1** (a) or **Ir2** (b). The inset shows the mass spectrum of 4-benzyloxybenzyl alcohol **2f**. These results also suggest that the benzyl ether moiety is stable under our reaction condition since 4-hydroxybenzyl alcohol was not detected.

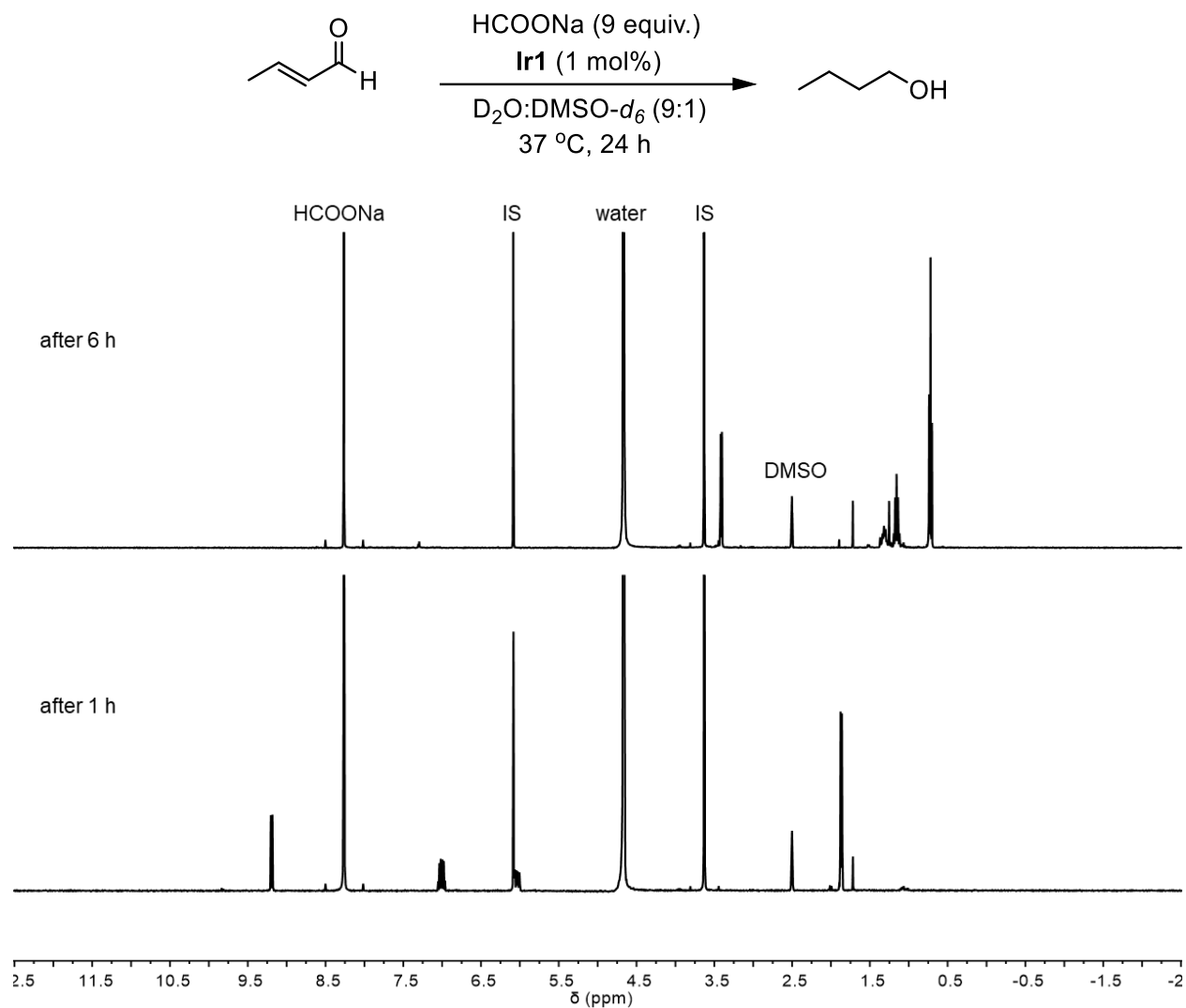


Figure S4. ^1H NMR spectra ($\text{D}_2\text{O:DMSO-}d_6$ (9:1), 400 MHz) of **Ir1** + crotonaldehyde. Internal standard (IS) = 1,3,5-trimethoxybenzene.

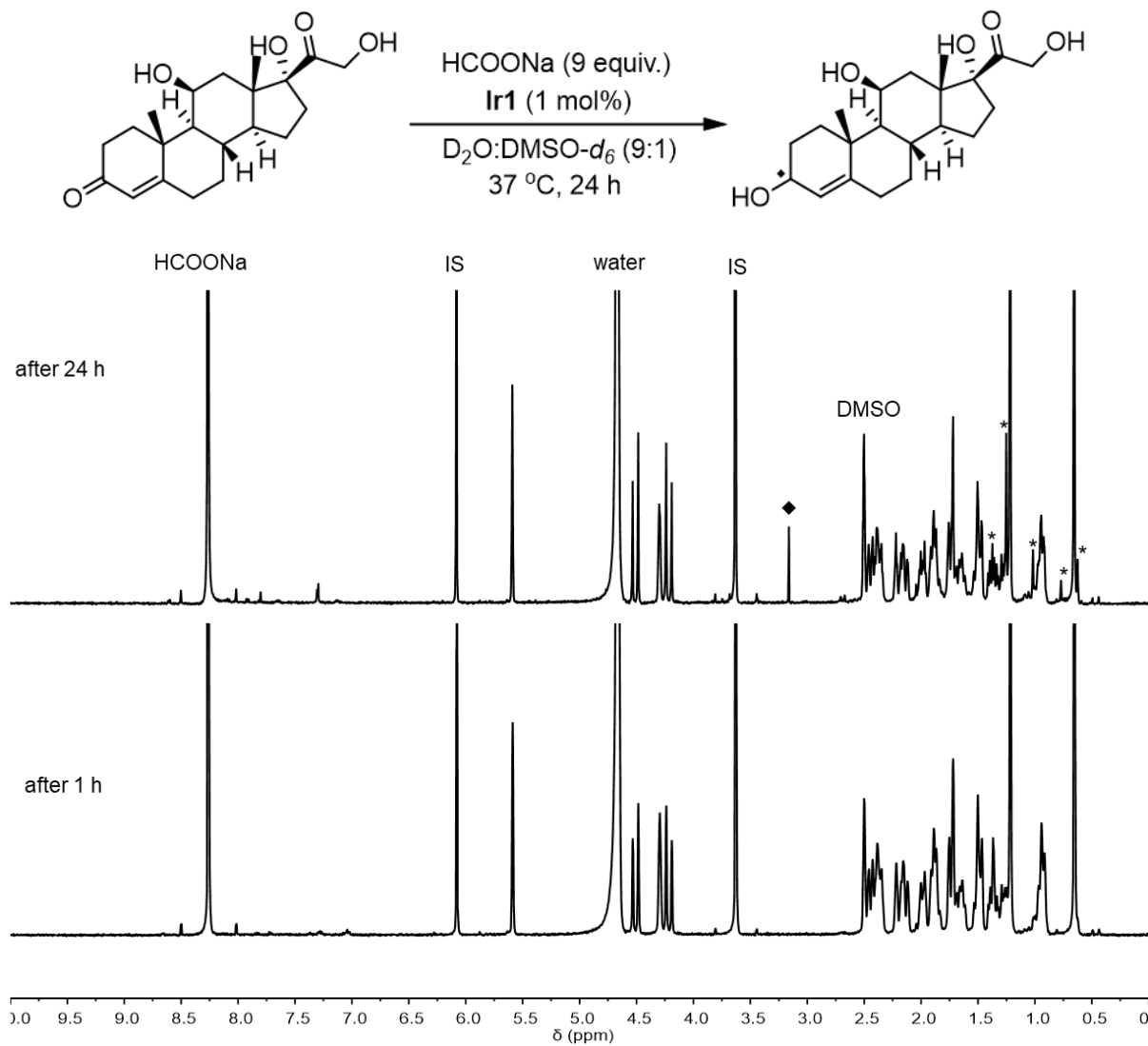


Figure S5. ¹H NMR spectra (D₂O:DMSO-*d*₆ (9:1), 400 MHz) of Ir1 + hydrocortisone. Internal standard (IS) = 1,3,5-trimethoxybenzene. Peaks marked with asterisks (*) were assigned to the singly reduced product.

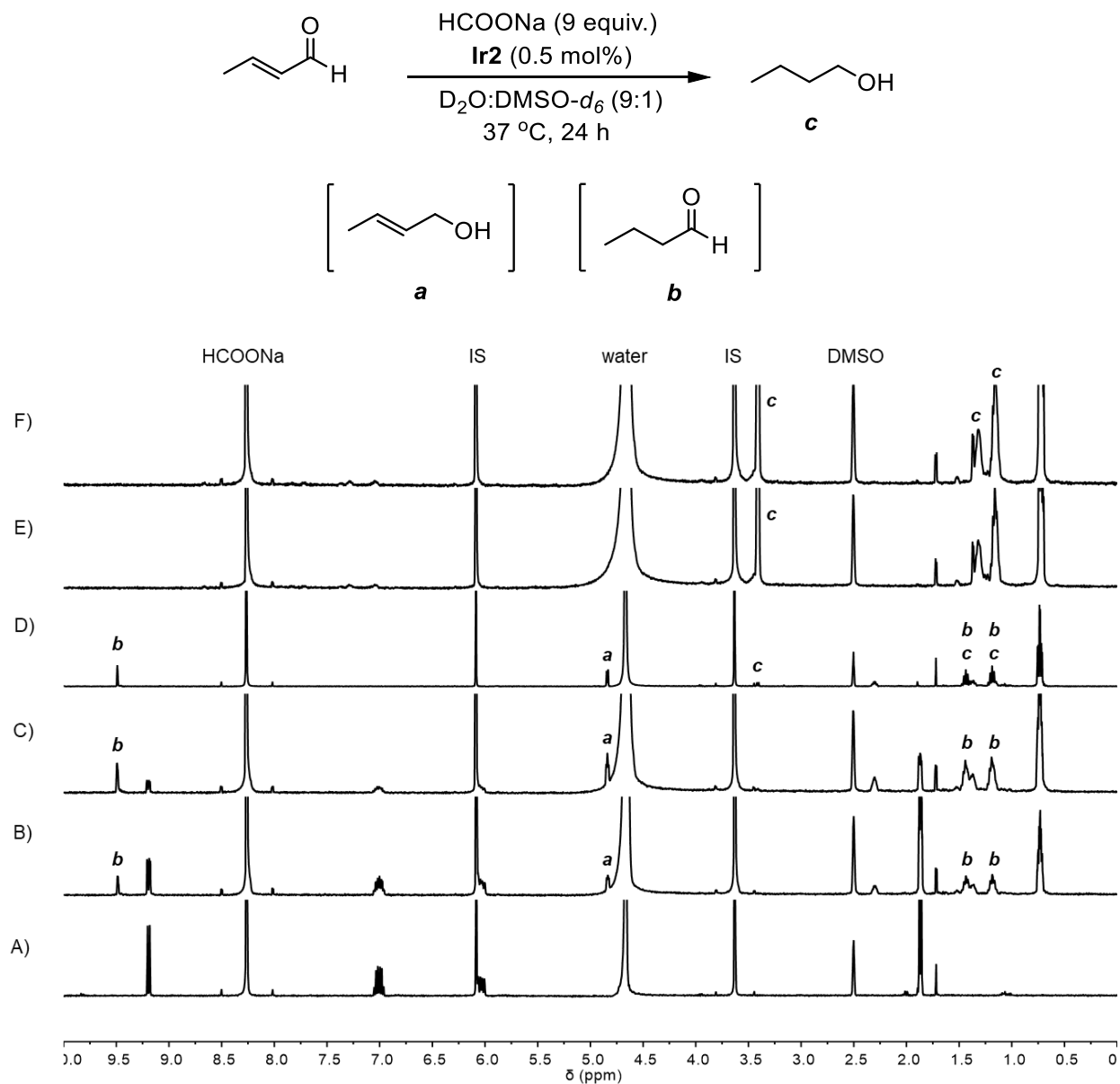


Figure S6. ^1H NMR spectra ($\text{D}_2\text{O:DMSO-}d_6$ (9:1), 400 MHz) of **Ir2** + crotonaldehyde. Internal standard (IS) = 1,3,5-trimethoxybenzene. A) crotonaldehyde + HCOONa + IS; B-F) reactions after 2 h (B), 4 h (C), 6 h (D), 12 h (E), and 24 h (F). Full conversion of crotonaldehyde to its corresponding butanol was observed after 12 h.

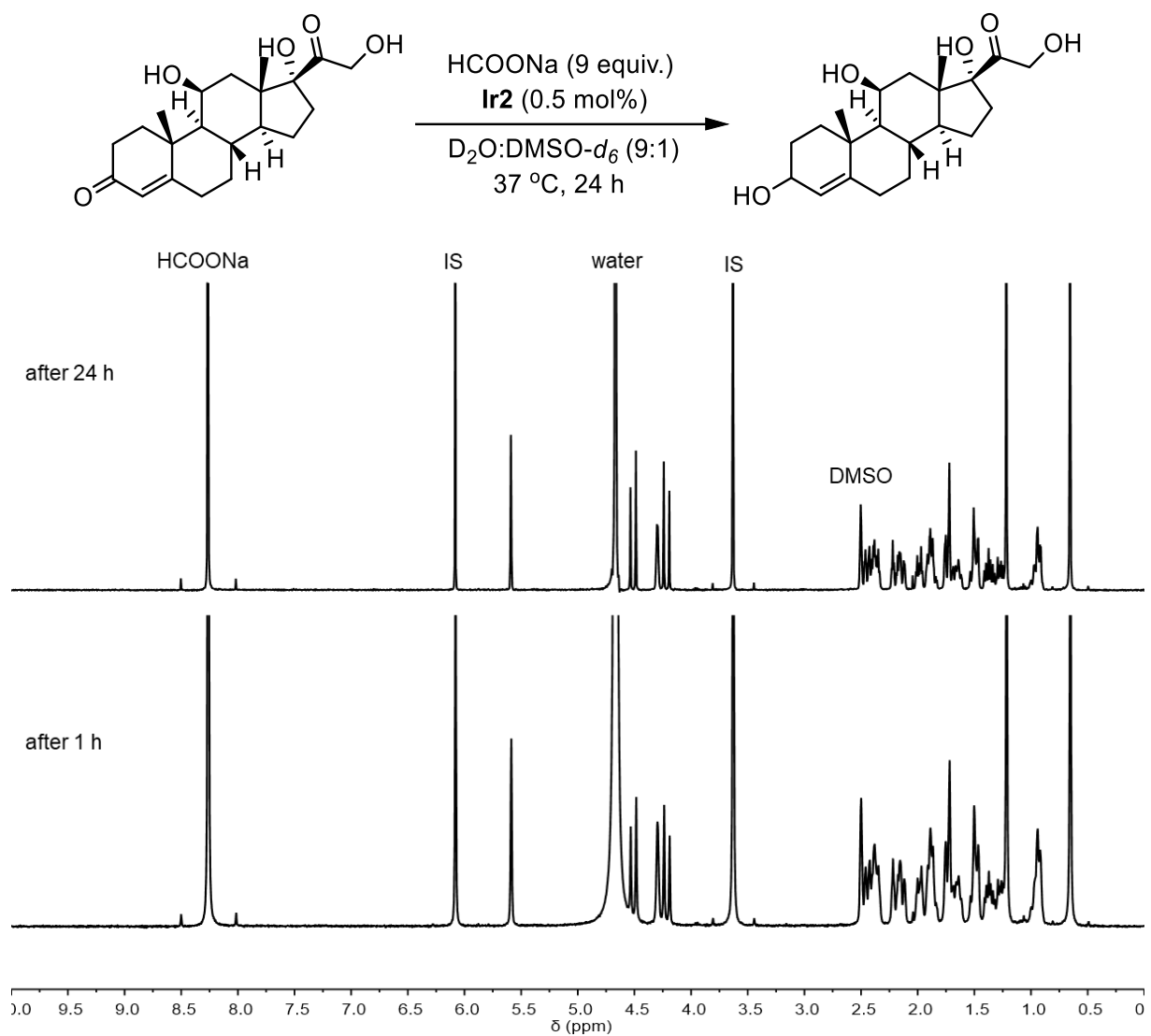


Figure S7. ¹H NMR spectra (D₂O:DMSO-*d*₆ (9:1), 400 MHz) of **Ir2** + hydrocortisone. Internal standard (IS) = 1,3,5-trimethoxybenzene.

General Procedure for Glutathione Tolerance Studies

Stock solutions of benzaldehyde (100 mM), **Ir1** (10 mM), and **Ir2** (5 mM) were prepared in DMSO and stored in the freezer for subsequent use. Stock solutions of HCOONa (100 mM) and GSH (100 mM) in millipore water were freshly prepared each time. Reactions were performed in 3 mL vials at 37 °C. The appropriate volumes of the following stock solutions were combined sequentially: Ir catalyst, additive, substrate, and HCOONa. Additional solvent was added to achieve a mixture containing 10% DMSO in water with a total volume of 3.0 mL. The reaction vial was sealed tightly with a septum screw cap and allowed to proceed at 37 °C under N₂. After the reaction was stirred for an allotted amount of time, diphenyl ether (0.2 equiv. relative to the substrate) was added and the reaction mixture was transferred to a test tube, which was further diluted with 3 mL of ethyl acetate. The combined organic layer was filtered through a pipette plug containing celite + Na₂SO₄, and the sample was analyzed by GC-MS.

Determination of H₂O₂ Concentration by Quantofix® Peroxides Test Strips

Stock solutions of benzaldehyde (100 mM), **Ir1** (10 mM), and **Ir2** (5 mM) were prepared in DMSO and stored in the freezer for subsequent use. Stock solutions of HCOONa (100 mM) and GSH (100 mM) in millipore water were freshly prepared each time. Reactions were performed in 3 mL vials at 37 °C. In each experiment, substrate, additives (GSH, HCOONa), and Ir catalyst stock solutions were diluted to a desired concentration. Additional solvent was added to achieve a mixture containing 10% DMSO in water with a total volume of 3.0 mL. The H₂O₂ concentration was monitored using Quantofix® peroxides 25 test strips at specific time intervals. The amount of peroxide present was determined based on the color of the test strip after exposure to the reaction mixture for 30 sec. Each set of experiments was repeated two times to confirm that the trends observed were consistent and reproducible. Photos of the original test strips were taken using an iPhone 11 Pro under normal laboratory lighting. This method of peroxide concentration determination is semi-quantitative since errors associated with inhomogeneous photo lighting, test strip response, and other uncontrolled experimental factors could affect its accuracy. To estimate the amount of H₂O₂ in each sample, photos of the test strips were converted to grayscale and the program ImageJ was used to measure the grayscale intensity. This value was converted to H₂O₂ concentration using a calibration curve created using the manufacture's color scale (which was also converted to grayscale). The following formula was used to convert grayscale intensity values into H₂O₂ concentration:

$$[\text{H}_2\text{O}_2] (\mu\text{M}) = 10^{(\text{intensity} - 256.36)/56.59}$$

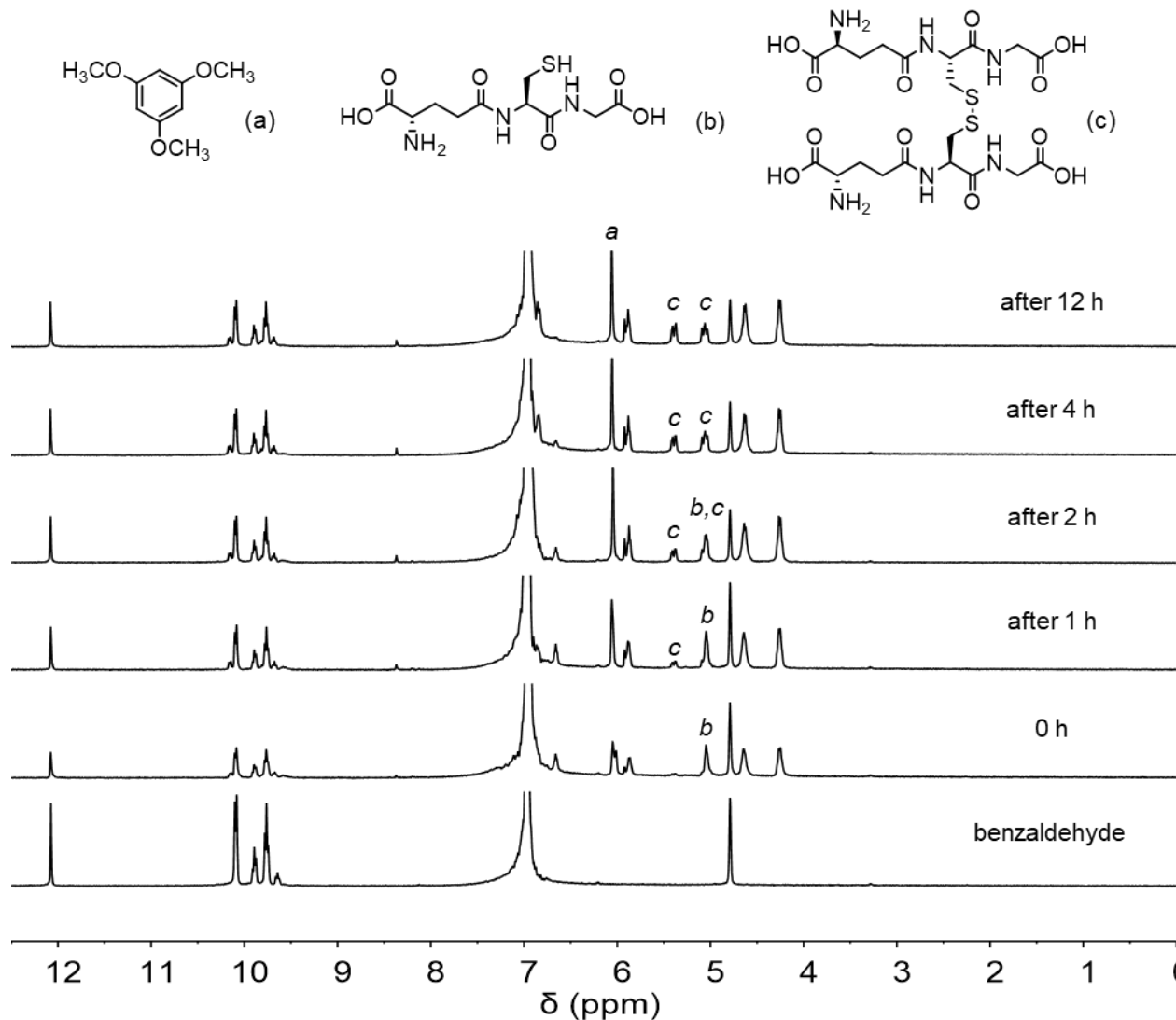
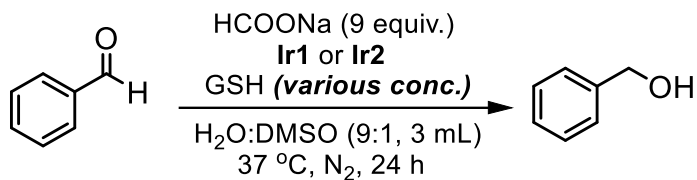


Figure S8. ^1H NMR spectra ($\text{DMSO-}d_6$: D_2O (1:9), 500 MHz) of GSH (50 mM) + benzaldehyde (50 mM) + 1,3,5-trimethoxybenzene (25 mM). The peak assignments are shown using letters corresponding to the chemical structures depicted above. The oxidation of GSH to GSSG under ambient conditions is complete within 4 h. No significant interaction between benzaldehyde and GSH was observed after 12 h, suggesting that benzaldehyde is a suitable substrate for the GSH tolerance studies.

Table S4. GSH Tolerance of Different Ir Complexes in H₂O

Entry	Condition ^a	Yield (%) ^b
1	Ir1 (1 mol%)	98 ± 2
2	Ir1 (1 mol%) + GSH (0.5 mM)	29 ± 5
3	Ir1 (1 mol%) + GSH (1.0 mM)	11 ± 3
4	Same as entry 2, 48 h	35 ± 4
5	Ir2 (0.5 mol%)	81 ± 5
6	Ir2 (0.5 mol%) + GSH (0.5 mM)	63 ± 4
7	Ir2 (0.5 mol%) + GSH (1.0 mM)	40 ± 5
8	Same as entry 5, 48 h	72 ± 5

^aReaction conditions used: benzaldehyde (5 mM, 15 μmol), HCOONa (135 μmol), Ir complex (0.15 μmol for **Ir1**, 0.075 μmol for **Ir2**), 37 °C, 24 h, under N₂. ^bThe reaction yields were determined by GC-MS using diphenyl ether as an internal standard.

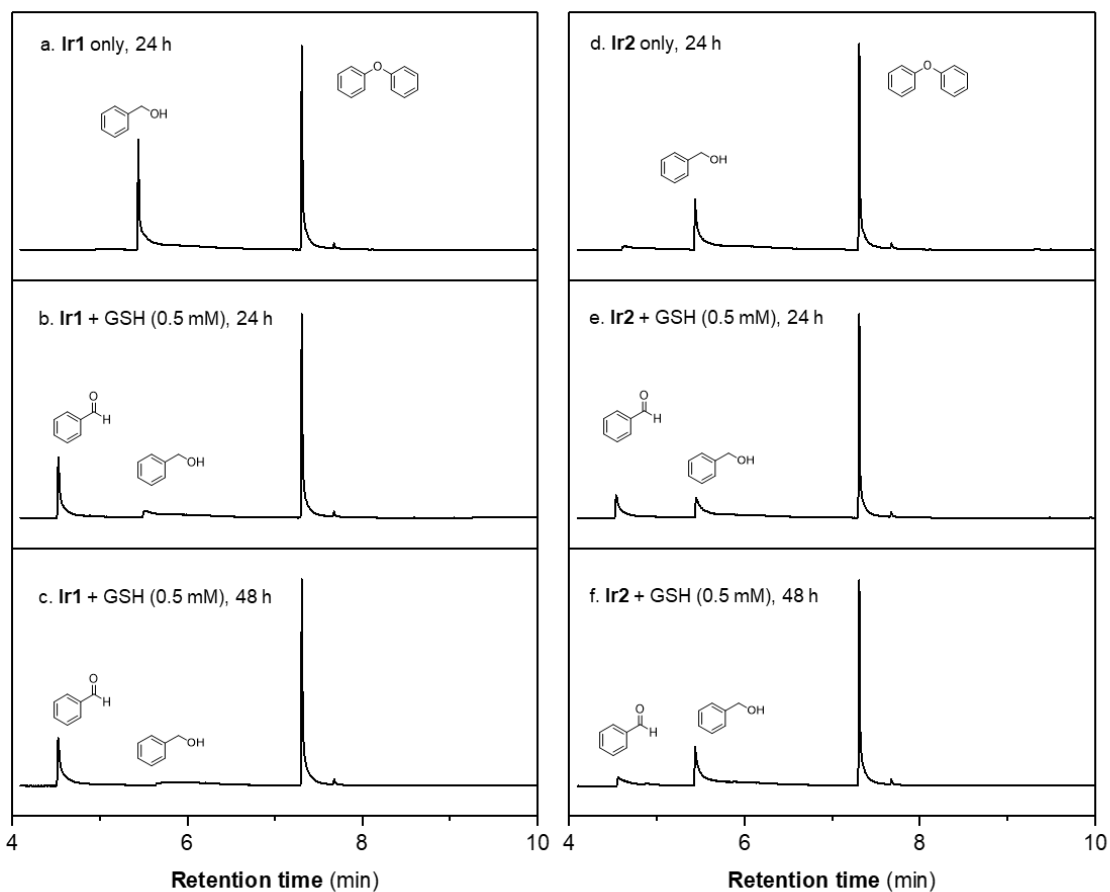


Figure S9. Representative GC plots showing the transfer hydrogenation between HCOONa and benzaldehyde catalyzed by **Ir1**/**Ir2** in the presence of GSH.

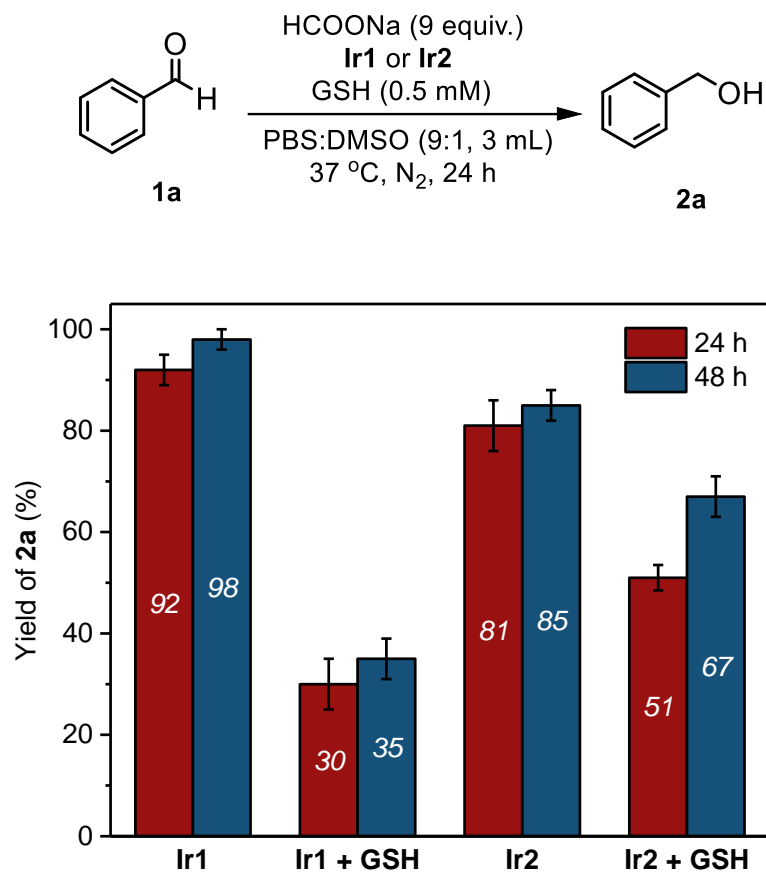


Figure S10. GSH tolerance of different Ir complexes in PBS/DMSO (9:1). Reaction conditions used: **1a** (5 mM, 15 μ mol), HCOONa (135 μ mol), Ir complex (0.15 μ mol for **Ir1**, 0.075 μ mol for **Ir2**), GSH (0.5 mM), 37 $^{\circ}$ C, 24 h or 48 h, under N₂. The reaction yields were determined by gas chromatography using diphenyl ether as an internal standard. Yields are average of triplicate runs. Abbreviation: GSH = glutathione, PBS = phosphate-buffered saline.

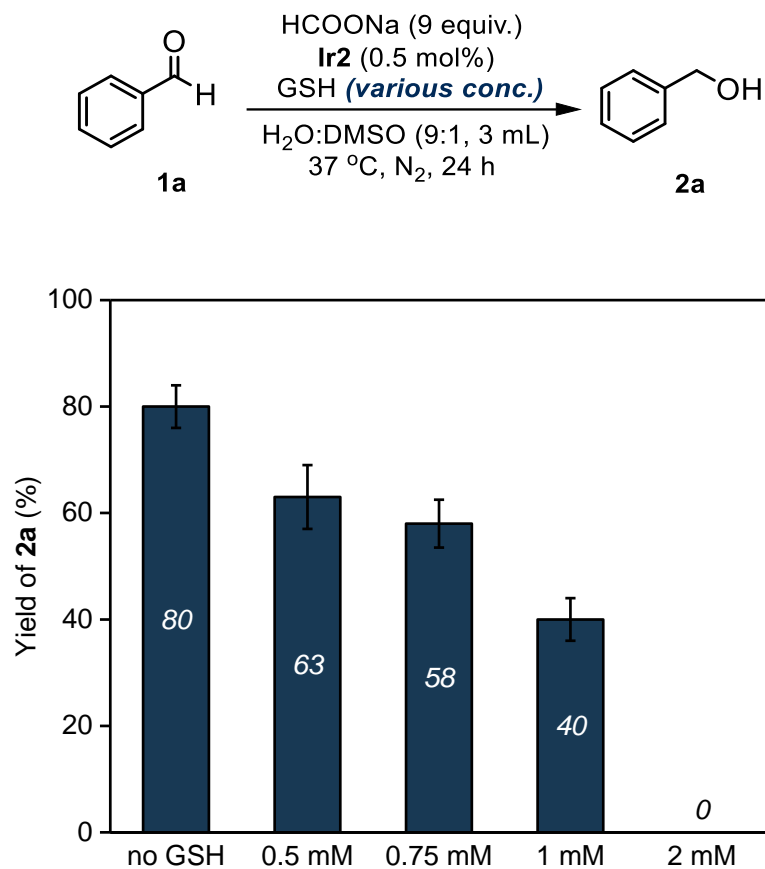


Figure S11. Maximum tolerance of **Ir2** to GSH in H₂O/DMSO (9:1). Reaction condition used: benzaldehyde (15 μ mol), HCOONa (135 μ mol), Ir complex (0.075 μ mol), 37 °C, 24 h, under N₂. The reaction yields were determined by gas chromatography using diphenyl ether as an internal standard. Yields are average of triplicate runs.

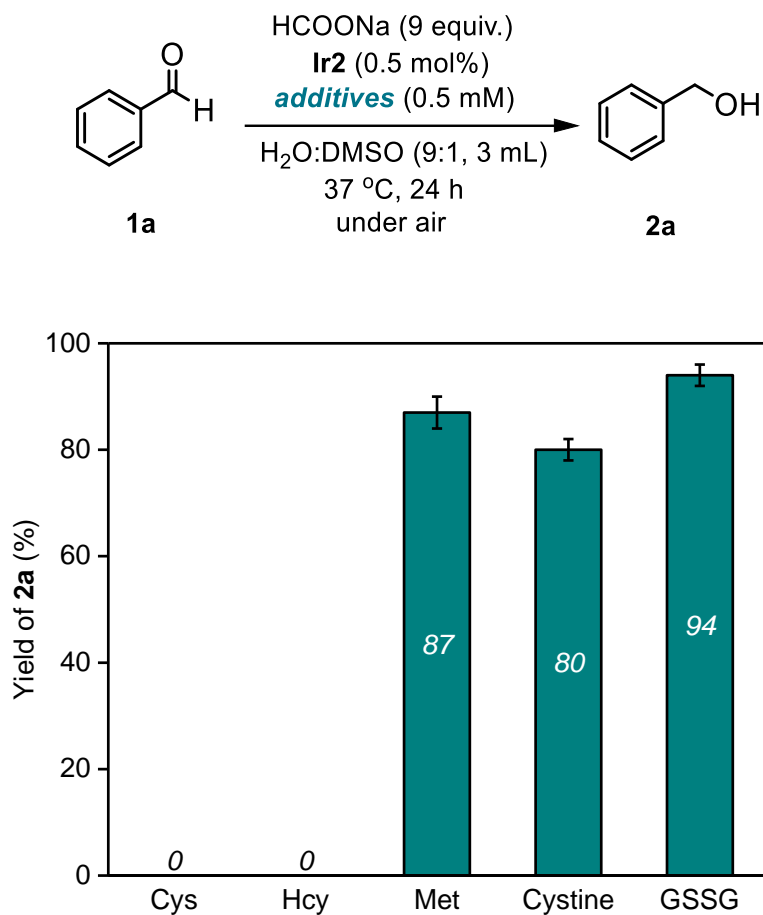


Figure S12. Tolerance of **Ir2** to various biological S-containing nucleophiles. Reaction condition used: benzaldehyde (15 μ mol), HCOONa (135 μ mol), Ir complex (0.075 μ mol), 37 °C, 24 h, under air. The reaction yields were determined by gas chromatography using diphenyl ether as an internal standard. Yields are average of triplicate runs. Abbreviation: Cys = *L*-cysteine, Hcy = *DL*-homocysteine, Met = *L*-methionine, GSSG = glutathione disulfide

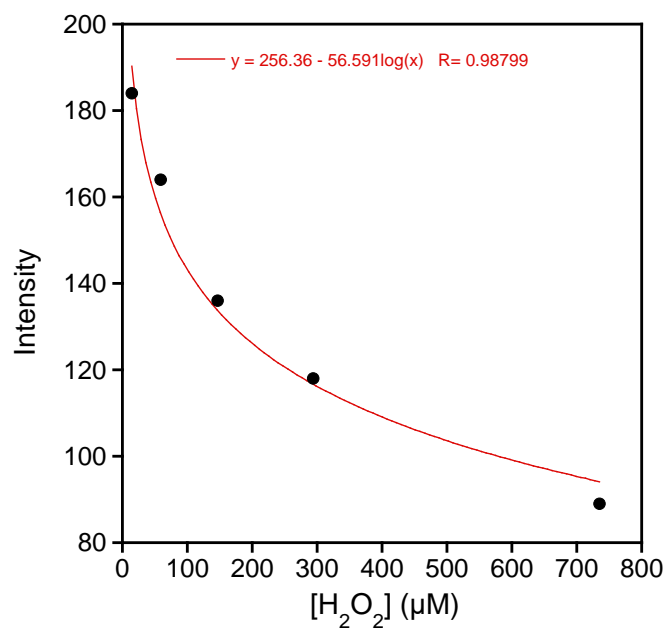


Figure S13. Calibration curve used to determine the hydrogen peroxide concentration from the test strips.

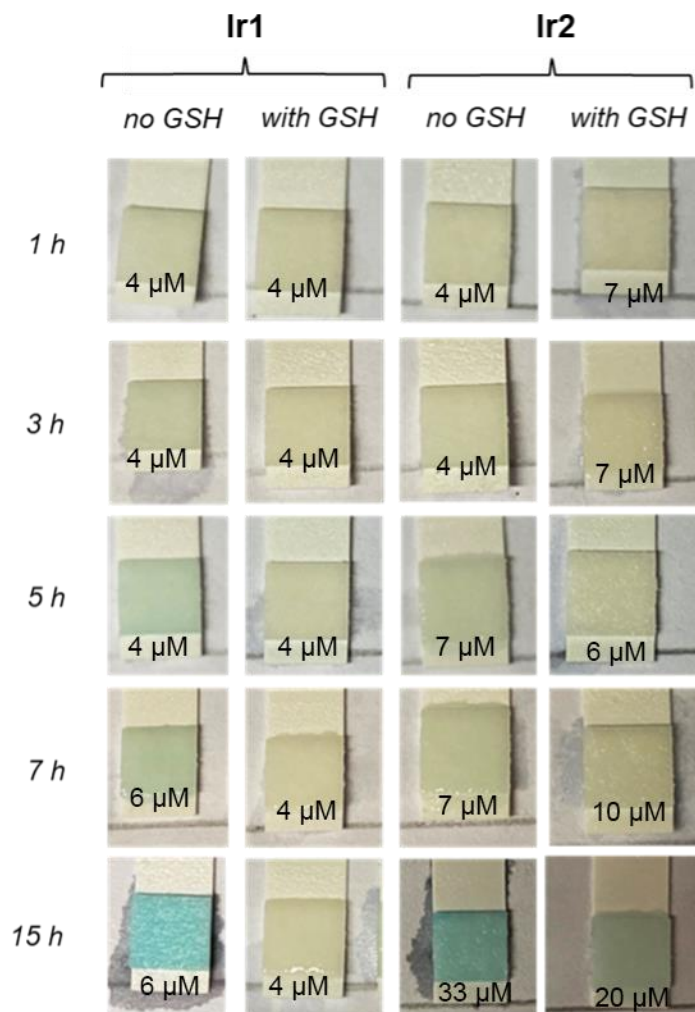


Figure S14. Peroxide color-strips obtained from solutions containing **Ir1** or **Ir2** in the presence of benzaldehyde after various times. Each reaction mixture tested contains: 10% DMSO in water (3.0 mL), Ir complex (0.15 μ mol for **Ir1**, 0.075 μ mol for **Ir2**), benzaldehyde (5 mM, 15 μ mol), GSH (0.5 mM, 0.15 μ mol), HCOONa (135 μ mol). Due to variations in room lighting some photos appear darker than they are, which may affect the estimated H₂O₂ concentrations.

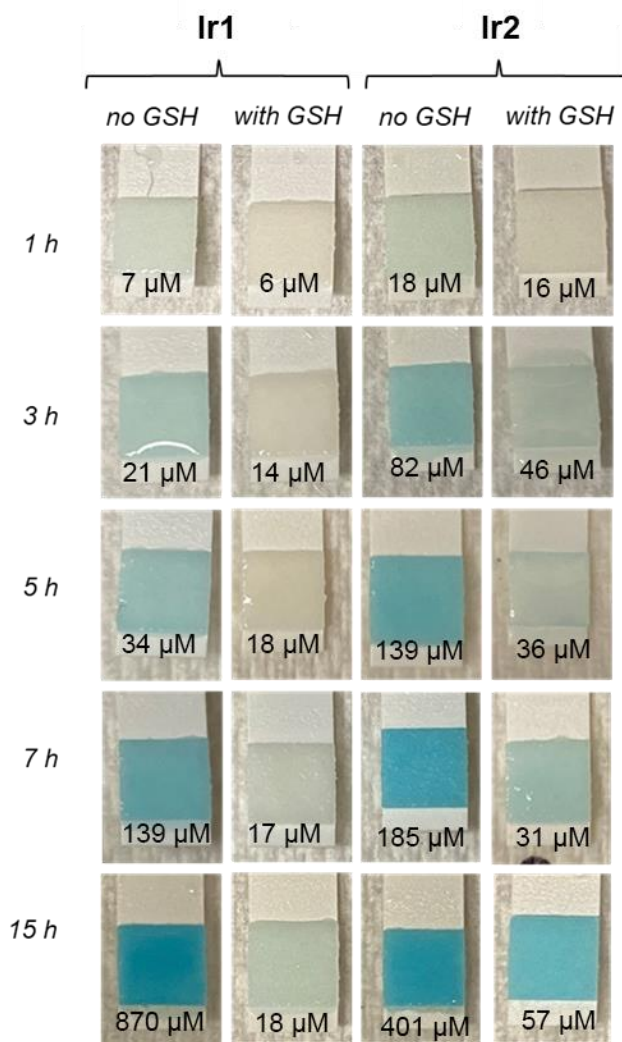
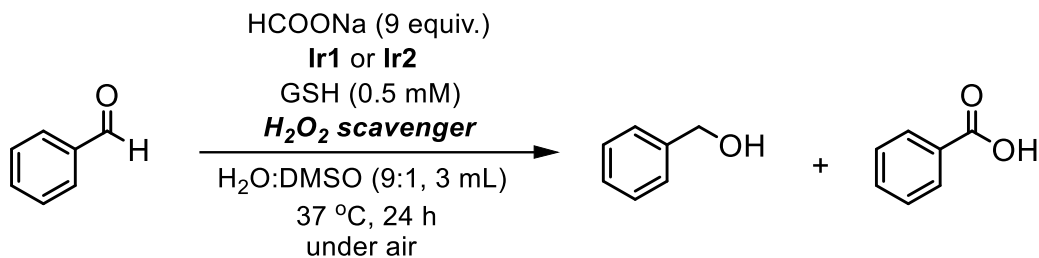
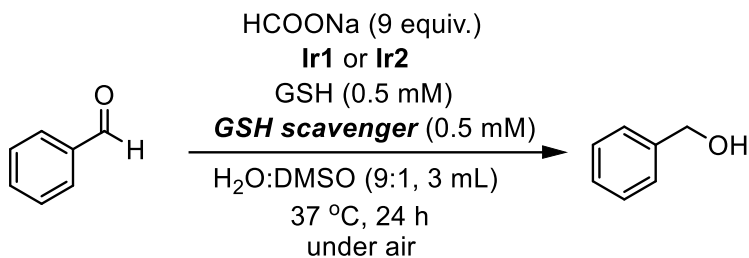


Figure S15. Peroxide color-strips obtained from solutions containing **Ir1/Ir2** in the absence of benzaldehyde after various times. In a mixture containing 10% DMSO in water with a total volume of 3.0 mL of sample contains: Ir complex (0.15 μ mol for **Ir1**, 0.075 μ mol for **Ir2**), GSH (0.5 mM, 0.15 μ mol), HCOONa (135 μ mol).

Table S5. Effect of GSH on **Ir1/Ir2** in the Presence of H₂O₂ Scavengers

Entry	Condition	Yield of alcohol (%)	Yield of acid (%)
1	Ir1 (1 mol%) + sodium ascorbate (2 mM)	0	6
2	Ir1 (1 mol%) + catalase (1000 units/mL)	11	5
3	Ir2 (0.5 mol%) + sodium ascorbate (2 mM)	17	5
4	Ir2 (0.5 mol%) + catalase (1000 units/mL)	28	7

Reaction conditions used: benzaldehyde (5 mM, 15 μ mol), HCOONa (135 μ mol), Ir complex (0.15 μ mol for **Ir1**, 0.075 μ mol for **Ir2**), 37 °C, 24 h. The reaction yields were determined by gas chromatography using diphenyl ether as an internal standard. Yields are average of duplicate runs.

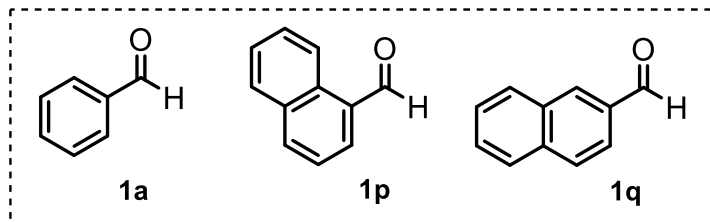
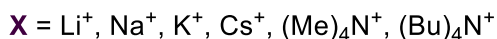
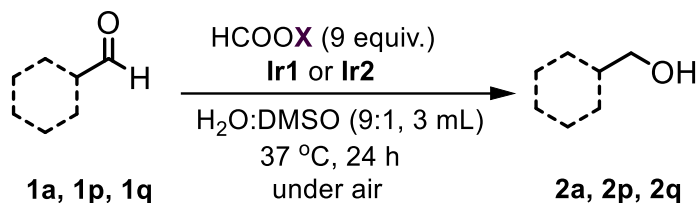
Table S6. Effect of GSH on **Ir1** and **Ir2** in the Presence of GSH Scavengers

Entry	Condition	Yield (%) ^a
1	Ir1 (1 mol%)	27
2	Ir1 (1 mol%) + maleimide (0.5 mM)	97
3 ^b	Ir1 (1 mol%) + phenyl vinyl sulfone (0.5 mM)	91
4 ^c	Ir1 (1 mol%) + benzoquinone (0.5 mM)	90
5	Ir1 (1 mol%) + KHSO ₅ (0.5 mM)	94
6	Ir2 (0.5 mol%)	63

Reaction conditions used: benzaldehyde (5 mM, 15 μmol), HCOONa (135 μmol), Ir complex (0.15 μmol for **Ir1**, 0.075 μmol for **Ir2**), GSH scavenger (0.5 mM), 37 °C, 24 h. The reaction yields were determined by gas chromatography using diphenyl ether as an internal standard. ^aYields are average of duplicate runs. ^bPhenyl ethyl sulfone was observed as a reaction product. ^cBenzoic acid was observed as a minor side product.

General Procedure for Cation Effect Studies

Stock solutions of benzaldehyde, 1-naphthaldehyde, 2-naphthaldehyde (100 mM), **Ir1** (10 mM), and **Ir2** (5 mM) were prepared in DMSO and stored in the freezer for subsequent use. Stock solutions of HCOOX (100 mM) (where X = Li⁺, Na⁺, K⁺, Cs⁺, NMe₄⁺, NBu₄⁺) in millipore water were freshly prepared each time. Reactions were performed in 3 mL vials at 37 °C for 24 h. The appropriate volumes of the following stock solutions were combined sequentially: catalyst, substrate, and HCOOX. Additional solvent was added to achieve a mixture containing 10% DMSO in water with a total volume of 3.0 mL. The reaction vial was sealed tightly with a septum screw cap and allowed to proceed at 37 °C under N₂. After the reaction had proceeded for an allotted amount of time, diphenyl ether (0.2 equiv. relative to the substrate) was added, and the reaction mixture was transferred to a test tube and further diluted with 3 mL of ethyl acetate. The combined organic layer was filtered through a pipette plug containing celite + Na₂SO₄, and the sample was analyzed by GC-MS.

Table S7. Reactions of **Ir1** and **Ir2** in the Presence of Different Formate Salts

Entry	Formates	Substrates	Yield (%)	
			Ir1	Ir2
1	HCOOLi	1a	98 ± 2	91 ± 3
2		1p	98 ± 2	17 ± 1
3		1q	98 ± 2	77 ± 4
4	HCOONa	1a	98 ± 2	89 ± 2
5		1p	97 ± 2	38 ± 2
6		1q	98 ± 2	79 ± 3
7	HCOOK	1a	96 ± 1	84 ± 2
8		1p	98 ± 2	34 ± 7
9		1q	98 ± 2	81 ± 2
10	HCOOCs	1a	95 ± 1	80 ± 3
11		1p	91 ± 4	41 ± 5
12		1q	92 ± 2	75 ± 2
13	HCOONMe ₄	1a	97 ± 2	90 ± 2
14		1p	97 ± 2	85 ± 1
15		1q	97 ± 2	91 ± 2
16	HCOONBu ₄	1a	95 ± 2	89 ± 2
17		1p	94 ± 3	72 ± 3
18		1q	97 ± 2	85 ± 2

Reaction conditions used: substrate (5 mM, 15 μmol), formate salt (135 μmol), Ir complex (0.15 μmol for **Ir1**, 0.075 μmol for **Ir2**), 37 °C, 24 h. The reaction yields were determined by GC-MS using diphenyl ether as an internal standard.

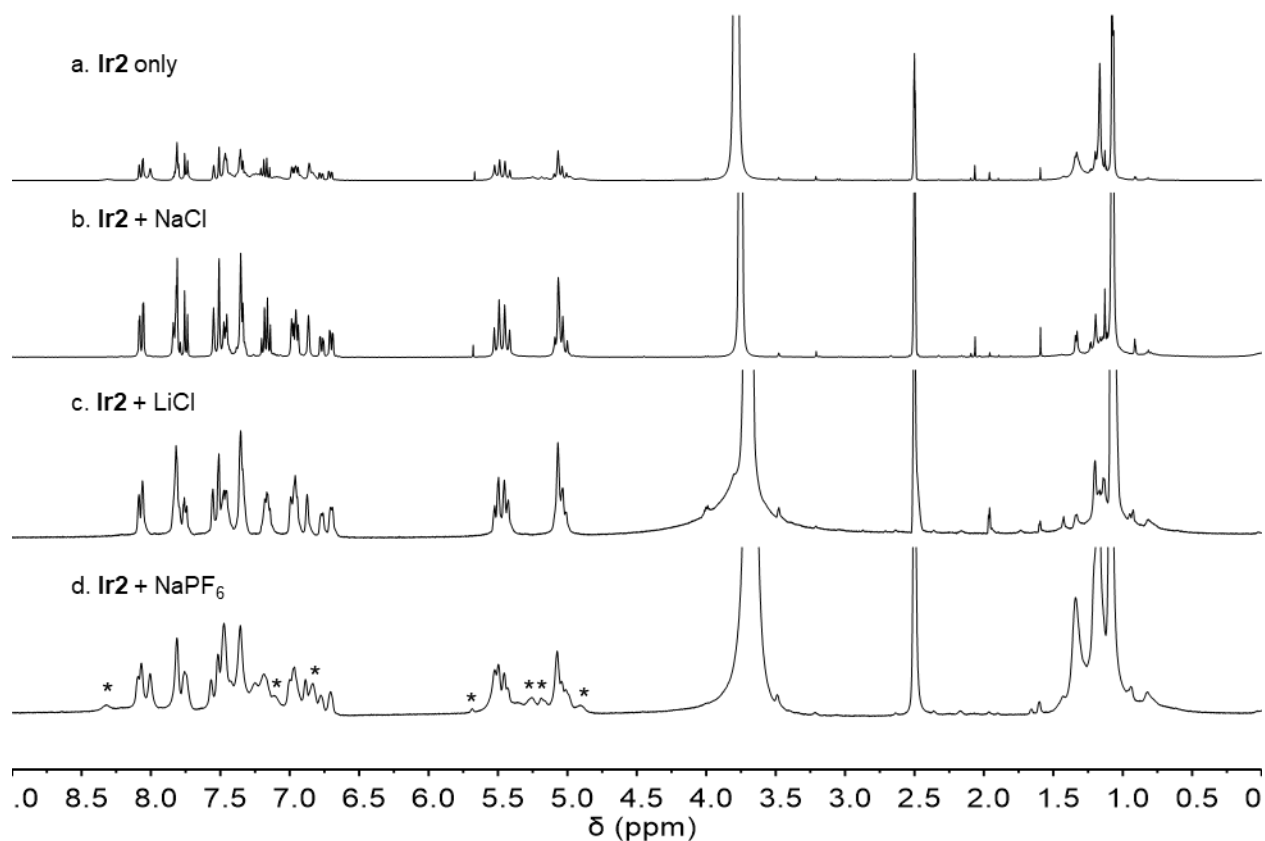


Figure S16. ^1H NMR spectra (500 MHz) of **Ir2** (10 mM) with different salts (100 mM) in D_2O : $\text{DMSO-}d_6 = 1:9$. Broad peaks were observed in most cases due to precipitate formation. The peaks marked with asterisks in spectra d may be due to formation of the corresponding Ir- H_2O species since there is a low concentration of chloride ions.

Titration Studies by UV-Vis Absorption Spectroscopy

Stock solutions of **Ir1** (10 mM) and **Ir2** (5 mM) were prepared separately in DMSO and sonicated for 10 min to obtain homogenous yellow mixtures. Stock solutions of NaX (where X = Cl, PF₆, 1 M) or NMe₄⁺ (1 M) were freshly prepared using millipore water. A 3.0 mL solution of **Ir1** or **Ir2** (0.1 mM) in DMSO/H₂O (1:9, v/v) was prepared in a 10 mm path length quartz cuvette by diluting 30 μ L of the **Ir1** (10 mM) or 60 μ L of **Ir2** (5 mM) stock solution with the appropriate amounts of DMSO and water. The cuvette was sealed with a septum screw cap, placed inside a UV-Vis spectrophotometer, and the spectrum was recorded at 37 °C. Aliquots containing NaX or NMe₄Cl (10 μ L) were added into the cuvette using a 10 μ L Hamilton syringe until a final concentration of 4.0 mM salt concentration was achieved. Photos of the cuvette were taken using an iPhone 11 Pro.

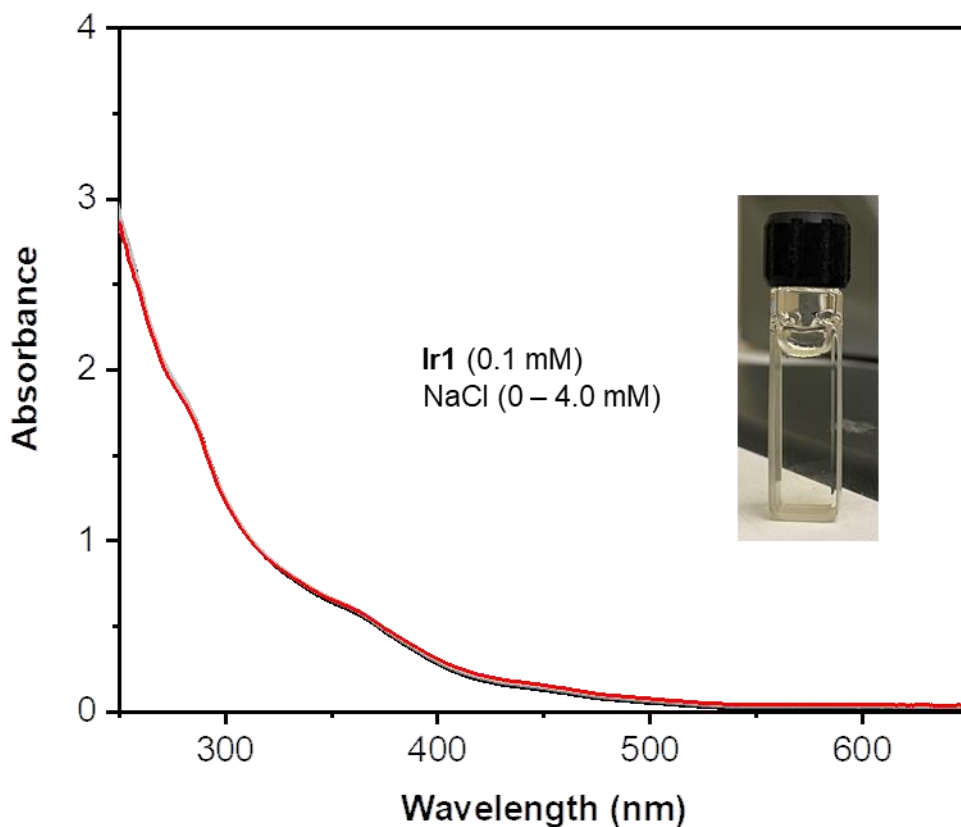


Figure S17. UV-vis absorbance spectra of **Ir1** (0.1 mM) in DMSO/H₂O (1:9, v/v) before (black trace) and after (red trace) the addition of 4.0 mM of NaCl at 37 °C. No significant spectral changes were observed upon the addition of NaCl (photo of cuvette shown).

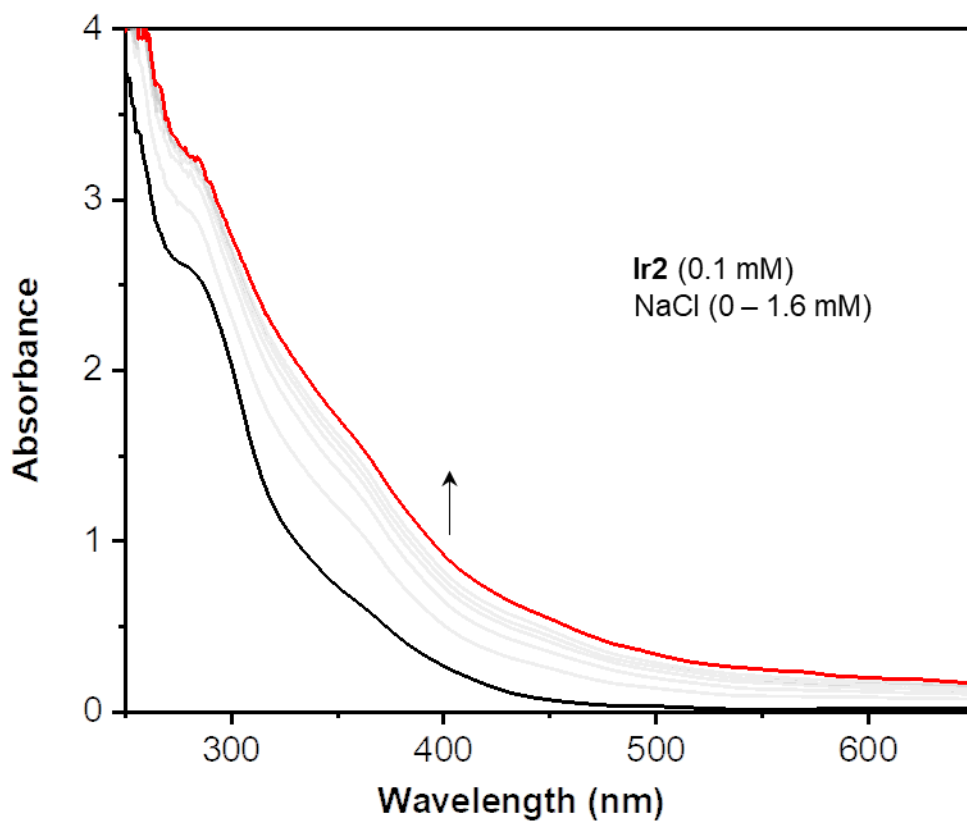


Figure S18. UV-vis absorbance spectra of **Ir2** (0.1 mM) in DMSO/H₂O (1:9, v/v) before (black trace) and after the addition of up to 16 equiv. of NaCl (red trace, final) at 37 °C. The arrow indicates the absorbance change upon the addition of increasing amounts of NaCl.

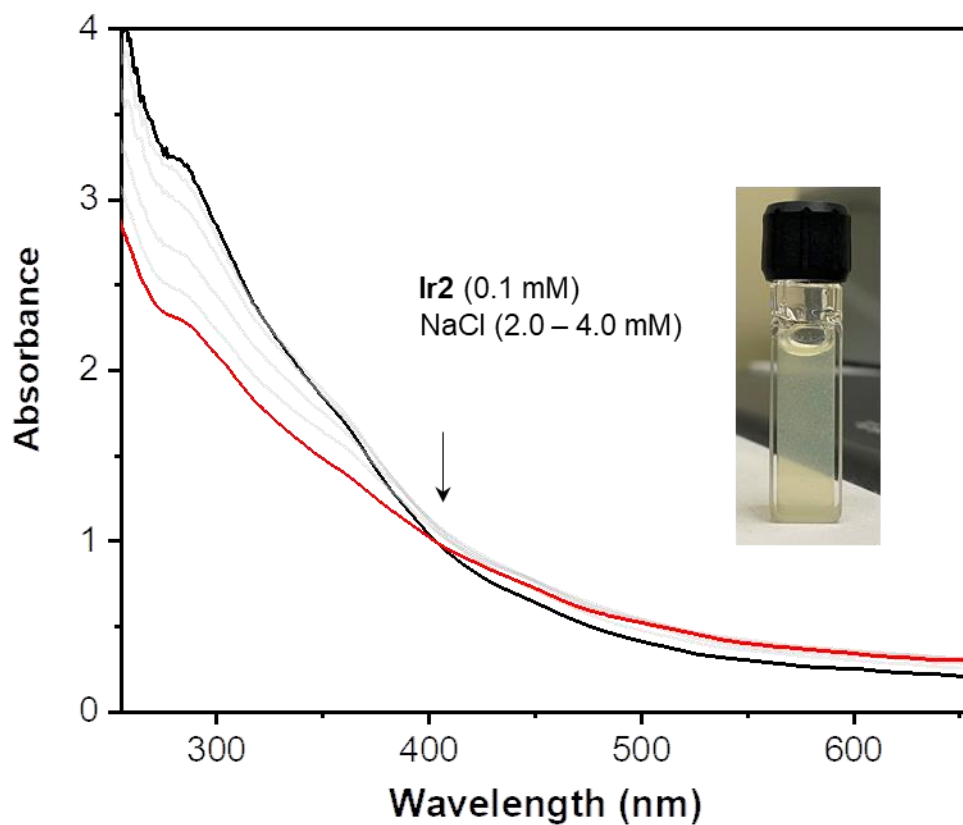


Figure S19. UV-vis absorbance spectra of **Ir2** (0.1 mM) in DMSO/H₂O (1:9, v/v) before (black trace) and after the addition of 20-40 equiv. of NaCl (red trace) at 37 °C. The arrow indicates the absorbance change upon the addition of increasing amounts of NaCl. Significant precipitation was observed when a large excess of NaCl was added to **Ir2** (photo of cuvette shown).

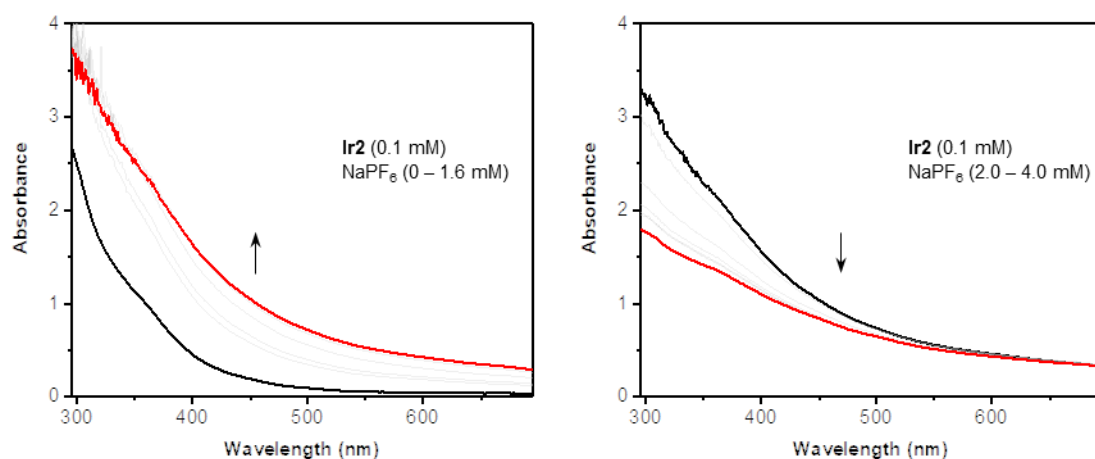


Figure S20. UV-vis absorbance spectra of **Ir2** (0.1 mM) in DMSO/H₂O (1:9, v/v) before (black trace) and after the addition of up to 40 equiv. of NaPF₆ (red trace) at 37 °C. The arrows indicate the absorbance changes after the addition of increasing amount of NaPF₆.

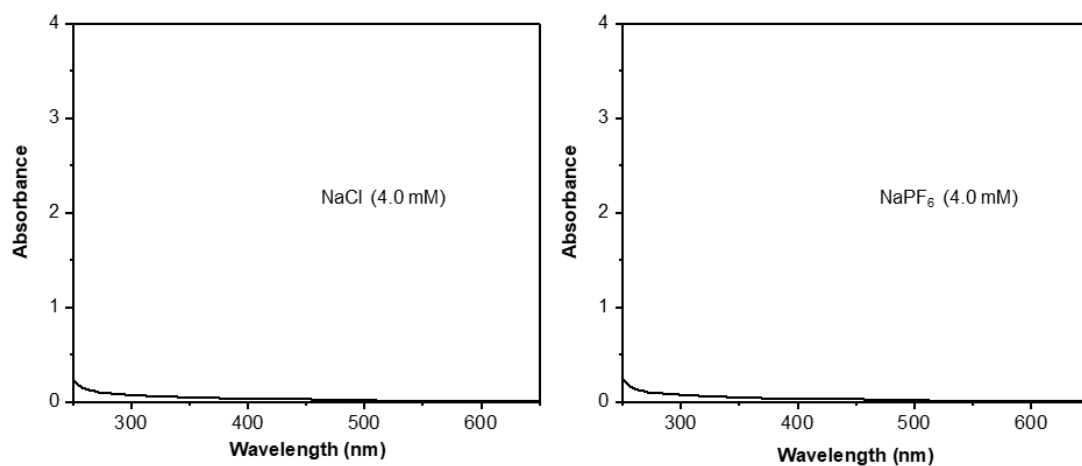


Figure S21. UV-vis absorbance spectra of NaCl (4.0 mM, left) and NaPF₆ (4.0 mM, right) in DMSO/H₂O (1:9, v/v) at 37 °C.

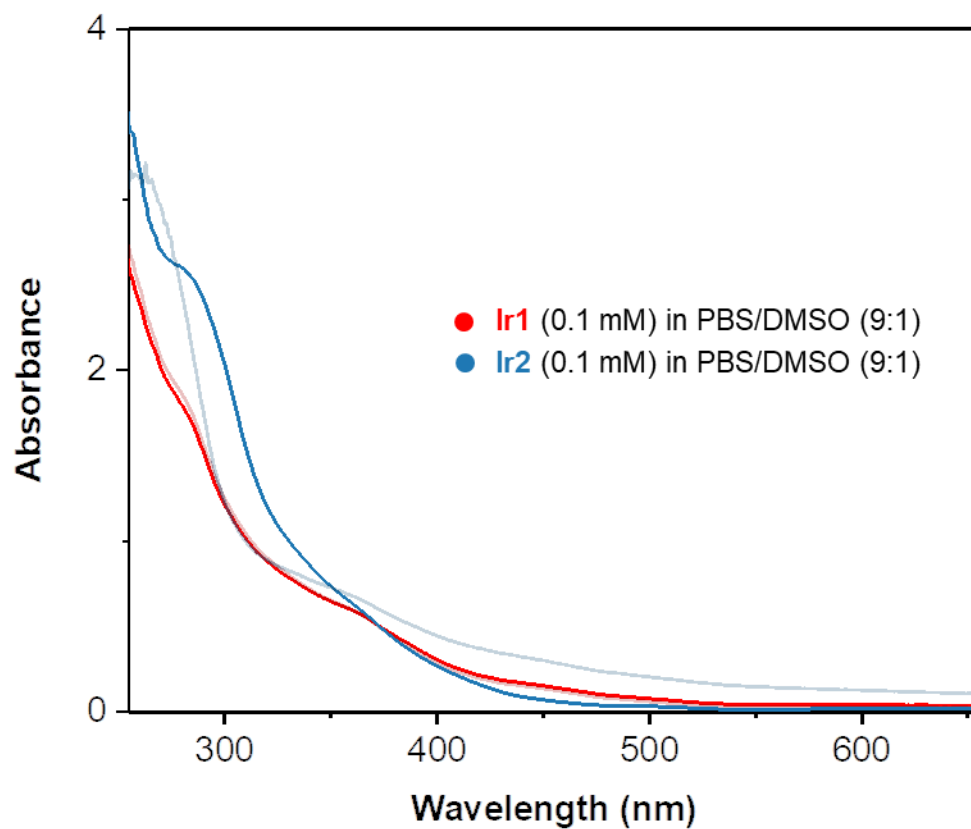


Figure S22. UV-vis absorbance spectra of **Ir1** (red trace, 0.1 mM) and **Ir2** (blue trace, 0.1 mM) in DMSO/PBS (1:9, v/v) at 37 °C. UV-vis absorbance spectra of **Ir1** and **Ir2** in DMSO: H₂O (1:9, v/v) were illustrated as dimmed corresponding-colored traces for comparison.



● **Ir1** (0.1 mM) in PBS/DMSO (9:1)



● **Ir2** (0.1 mM) in PBS/DMSO (9:1)

Figure S23. Images of cuvettes containing **Ir1** (left) and **Ir2** (right) in DMSO/PBS (1:9, v/v) at 37 °C.

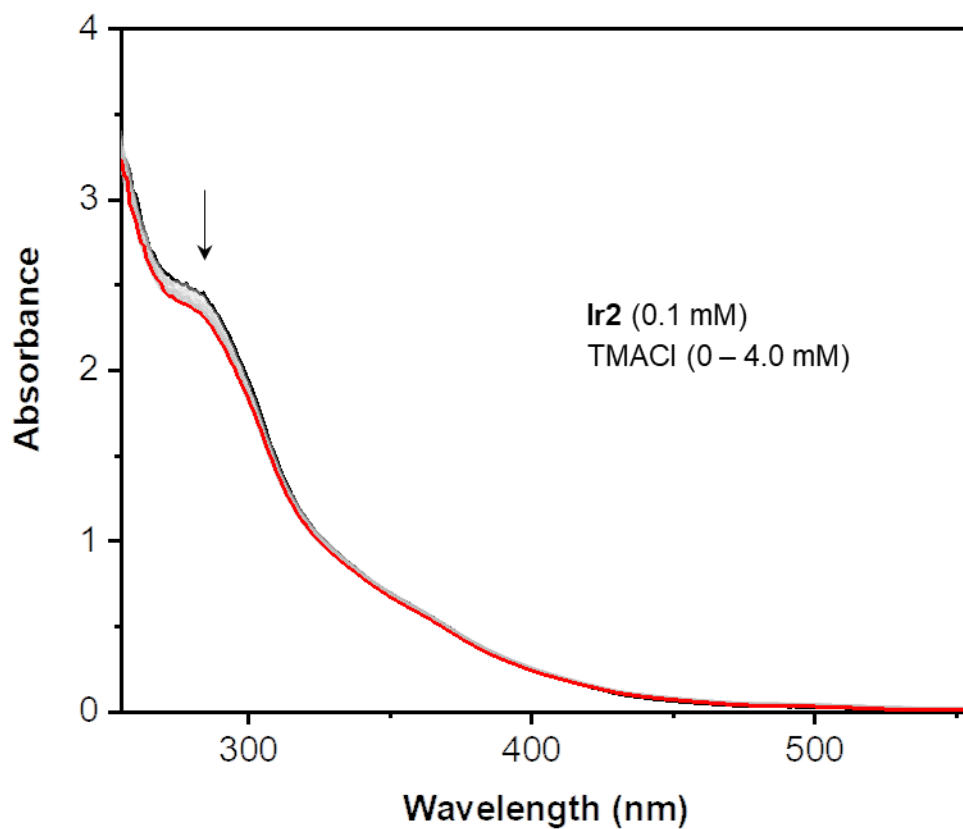


Figure S24. UV-vis absorbance spectra of **Ir₂** (0.1 mM) in DMSO/H₂O (1:9, v/v) before (black trace) and after the addition of up to 40 equiv. of tetramethylammonium chloride (red trace) at 37 °C. The absorbance changes upon the addition of NMe₄Cl (TMACl) were insignificant.

Particle Size Measurements Using Dynamic Light Scattering (DLS)

DLS samples were prepared using stock solutions of **Ir2** (5 mM) in DMSO and NaCl (1000 mM) in DI water. A diluted solution of macrocyclic **Ir2** complex (0.1 mM) in the presence of NaCl (4.0 mM) was prepared in 3 mL of DMSO:H₂O. This sample was further diluted 2× (1.5 mL of solution was taken, followed by the addition of 1.5 mL of DMSO:H₂O (1:9)) and sonicated for 5 min before measuring the size distribution by DLS. For measuring the size distribution of **Ir2** aggregates in biorelevant media (PBS, DMEM), **Ir2** complex (0.1 mM) were prepared in 3 mL of PBS or DMEM and was further diluted 5× (1 mL of solution was taken, followed by the addition of 4 mL of DMSO:media (1:9)) to obtain particle sizes that do not exceed the upper detection limit of the instrument.

All measurements were performed on a Malvern Zetasizer Nano-ZS90. Samples were irradiated with red light (HeNe laser, wavelength $\lambda = 632.8$ nm) and the intensity fluctuations of the scattered light (backscattering angle = 173°) were analyzed to obtain an autocorrelation function. The software provided both the size mean and polydispersity, using the cumulants analysis (according to the international standard ISO 13321:19963) and a size distribution using a regularization scheme by intensity. The following assumptions were made in the analysis: the solution viscosity was assumed to be that of water; the solution refractive index was that of water (RI = 1.33); the refractive index of the particle was selected to be 1.45 with an absorption of 0.001. Samples were measured in disposable polystyrene cuvettes within 90 s at a temperature of 25 °C, and this temperature was actively maintained within 0.1 °C in the sample chamber. Data were acquired in automatic mode, ensuring enough photons were accumulated for the result to be statistically relevant. The software generated a ‘data quality report’ that indicated good quality for all data obtained.

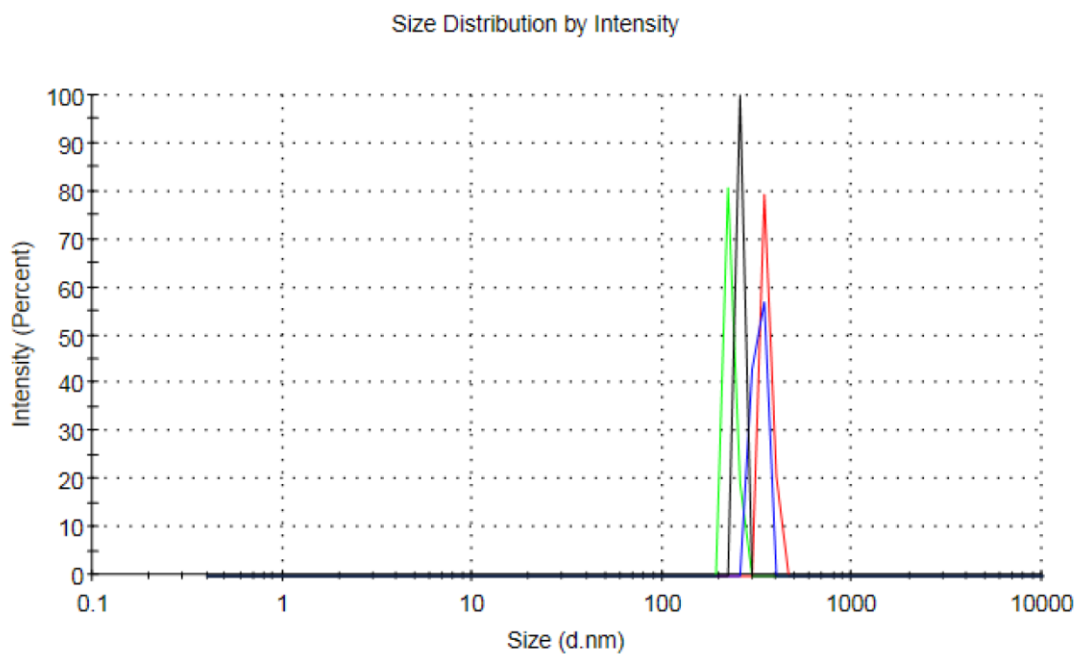


Figure S25. Size distribution vs. intensity data obtained from DLS analysis of **Ir2** (0.05 mM) in the presence of NaCl (2.0 mM) in DMSO:H₂O (1:9). Based on measurements of 4 independently prepared samples, the average particle size is 290 nm.

Table S8. Relative Size of Particles Formed from **Ir2** + NaCl in DMSO:H₂O (1:9)

	Size (diameter, nm)	Standard Deviation (diameter, nm)
Peak 1 (green color)	226.9	13.73
Peak 2 (black color)	255.0	-
Peak 3 (blue color)	321.9	23.11
Peak 4 (red color)	356.8	43.74

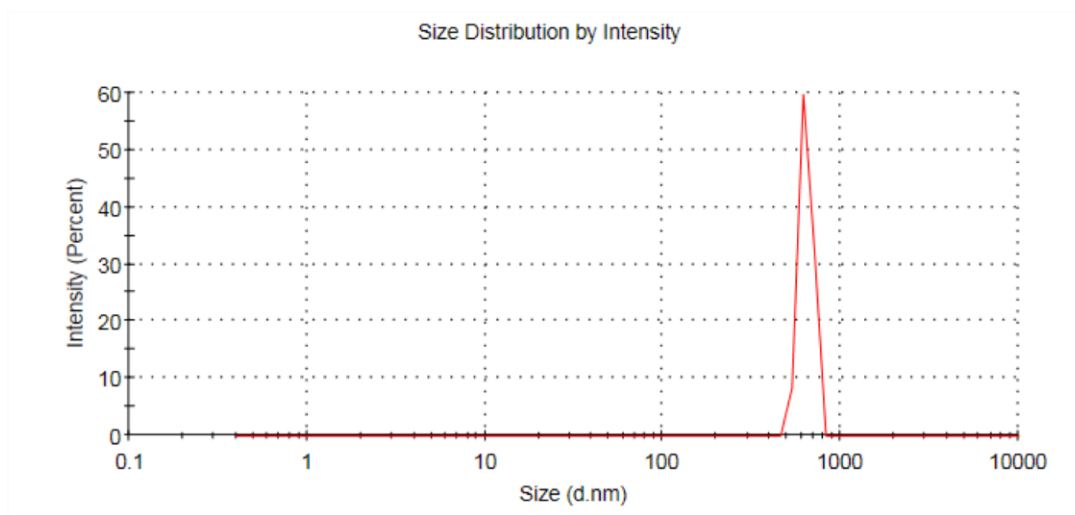


Figure S26. Size distribution vs. intensity data obtained from DLS analysis of **Ir2** (0.02 mM) in in DMSO:PBS (1:9) with no additional NaCl. The average particle size is 639.3 ± 55.08 nm. Commercial Dulbecco's PBS 1 \times (D8537 – Sigma-Aldrich) contains KCl (2.7 mM), NaCl (137 mM), Na₂HPO₄ (10 mM), and KH₂PO₄ (1.8 mM)

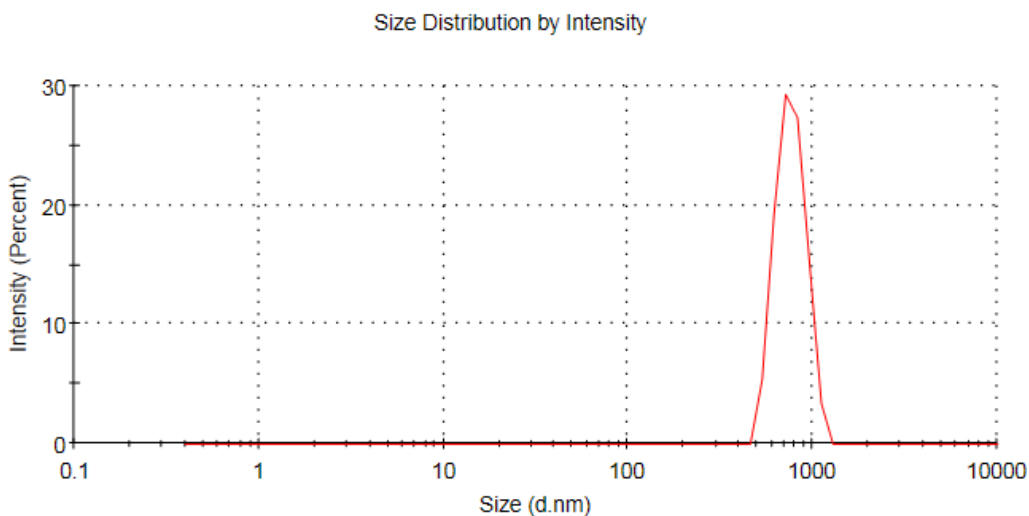


Figure S27. Size distribution vs. intensity data obtained from DLS analysis of **Ir2** (0.02 mM) in DMSO: modified DMEM (1:9). The average particle size is 765.6 ± 136.6 nm. The modified Dulbecco's Modified Eagle Medium 1 \times (Gibco A1443001, without glucose, glutamine, phenol red, and sodium pyruvate) was used. As a control, DLS measurements of the DMEM solution without **Ir2** showed no detectable particles.

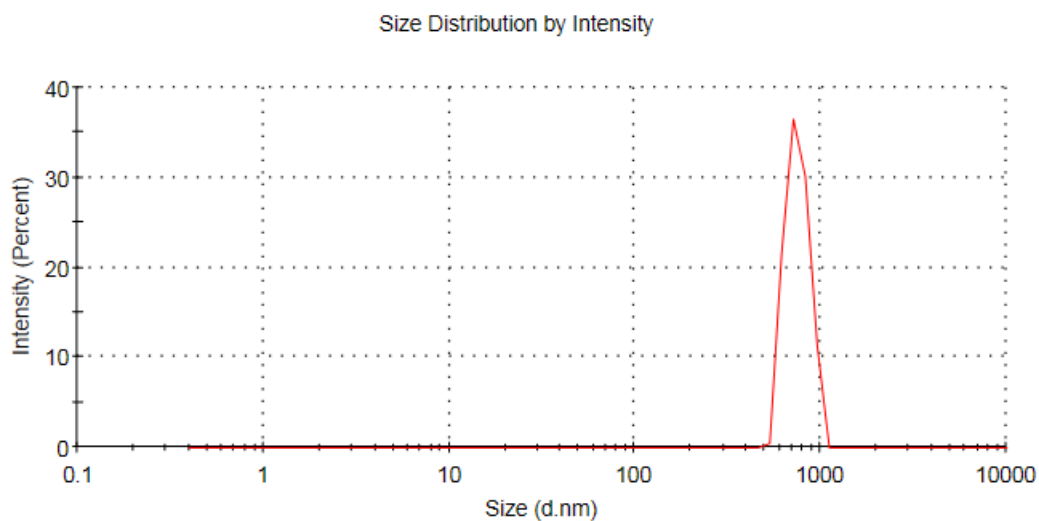
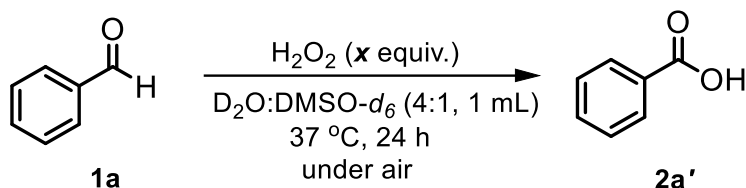


Figure S28. Size distribution vs. intensity data obtained from DLS analysis of **Ir2** (0.02 mM) in in DMSO: DMEM (1:9). The average particle size is 752.2 ± 105.7 nm. The Dulbecco's Modified Eagle Medium 1 \times (ATCC 30-2002, high glucose, with glutamine, phenol red, and sodium pyruvate) was used.

Control Experiments

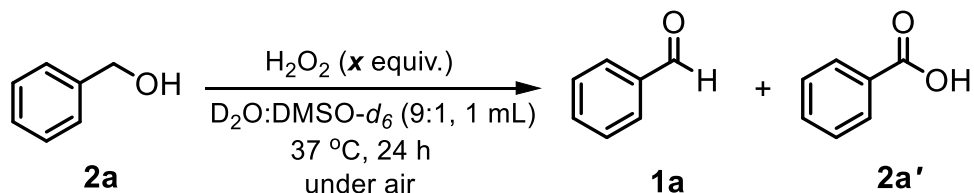
Table S9. Oxidation of Benzaldehyde by H₂O₂



Entry	Condition ^a	Yield of 2a' (%)
1	Using 1 equiv. of H ₂ O ₂ (30% in water)	15
2	Using 2 equiv. of H ₂ O ₂ (30% in water)	33

^aReaction condition used: benzaldehyde **1a** (51 μL, 0.5 mmol, 1 equiv.), H₂O₂ (60 - 120 μL), D₂O: DMSO-*d*₆ (4:1, 1 mL), performed in 1.5-dram vials, 37 °C, 24 h. The solvent ratio was changed to improve the solubility. Yields were determined by ¹H NMR spectroscopy using 1,3,5-trimethoxybenzene as internal standard.

Table S10. Oxidation of Benzyl Alcohol by H₂O₂



Entry	Condition	Yield of 1a (%)	Yield of 2a' (%)
1	Using 1 equiv. of H ₂ O ₂ (30% in water)	0	0
2	Using 2 equiv. of H ₂ O ₂ (30% in water)	0	0

^aReaction condition used: benzyl alcohol **2a** (52 μL, 0.5 mmol, 1 equiv.), H₂O₂ (60 - 120 μL), D₂O: DMSO-*d*₆ (9:1, 1 mL), performed in 1.5-dram vials, 37 °C, 24 h. Yields were determined by ¹H NMR spectroscopy using 1,3,5-trimethoxybenzene as internal standard.

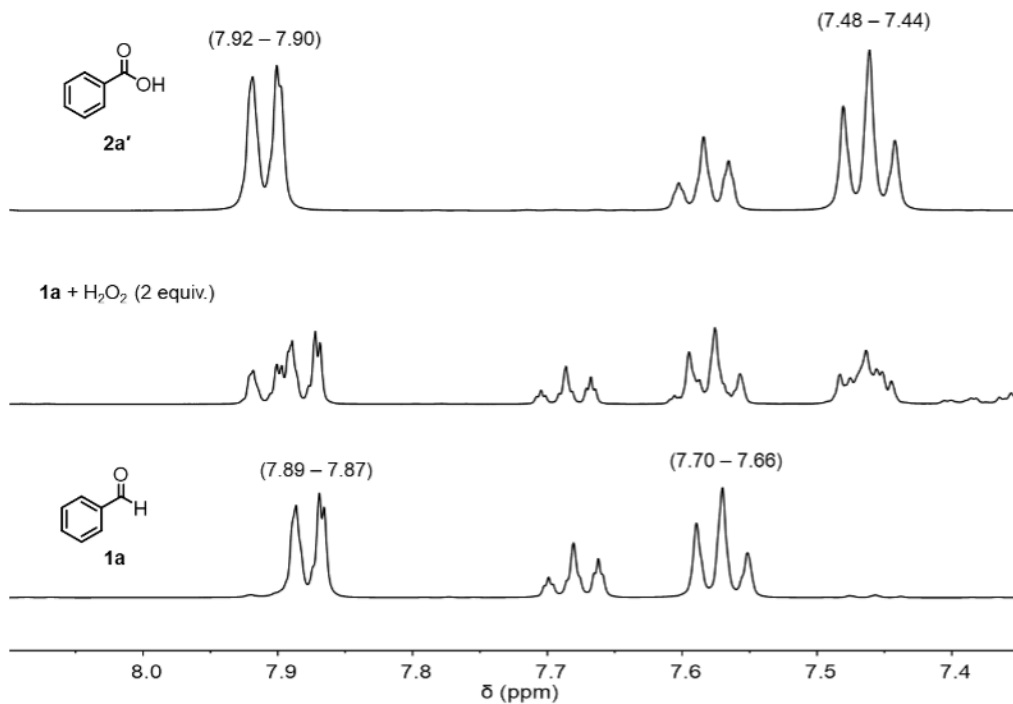


Figure S29. ^1H NMR spectrum (500 MHz, 25 °C, D_2O) of the reaction mixture from entry 2 in Table S9 (middle trace). The top and bottom traces are the ^1H NMR spectra of **2a'** and **1a** only, respectively.

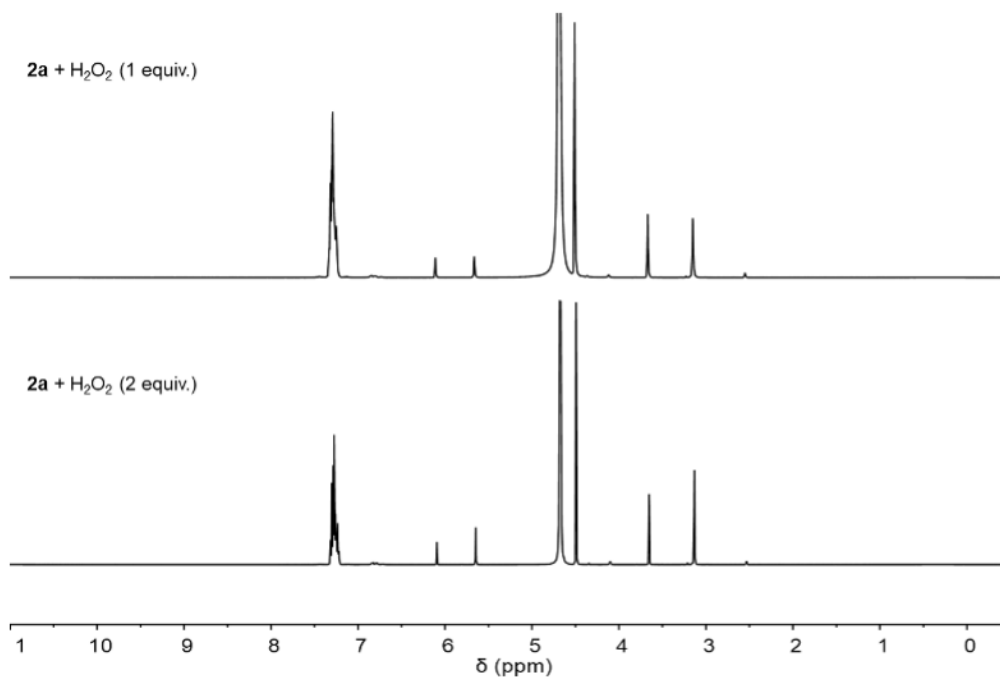


Figure S30. ^1H NMR spectra (500 MHz, 25 °C, D_2O) of the reaction mixtures from Table S10. Our results indicate that H_2O_2 does not react with benzyl alcohol **2a** under these reaction conditions.

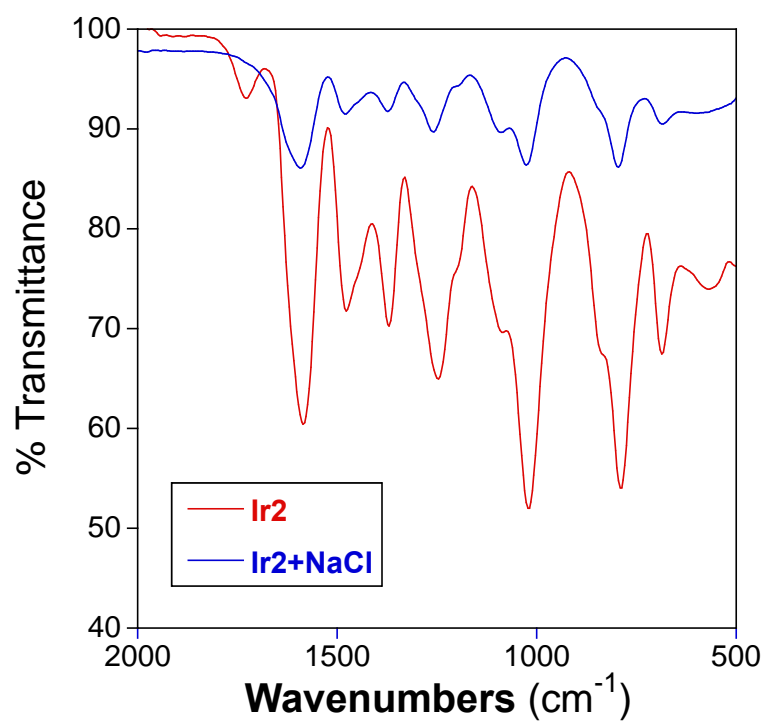


Figure S31. IR spectra of **Ir2** (red trace) and **Ir2** + NaCl (premixed in solution and dried for IR spectroscopic analysis; blue trace). No significant differences were observed between the two spectra.

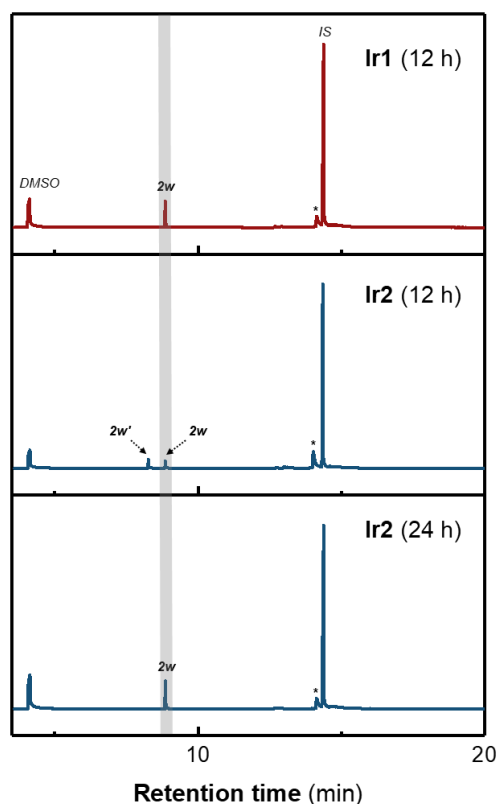
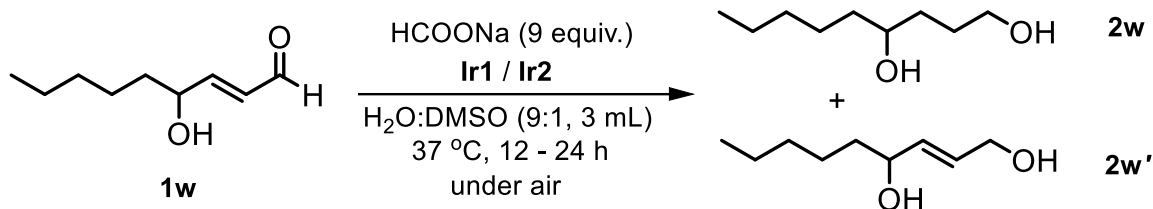


Figure S32. Representative GC traces showing the transfer hydrogenation between HCOONa and compound **1w** catalyzed by **Ir1** after 12 h (*top trace*) and by **Ir2** after 12 h (*middle trace*) and 24 h (*bottom trace*). 1,3,5-Trimethoxybenzene (0.5 equiv. relative to the substrate) was added as an internal standard (IS), which showed a peak at ~14.37 min. Other peaks at 8.27, 8.85, and 14.14 min are assigned to **2w'**, **2w**, and an unknown product (marked with an asterisk), respectively. A modified temperature program was used for the GC–MS analysis of this compound, in which samples were held at 50 °C for 7 min, heated from 50 to 100 °C at 30 °C/min and held for 3 min, then heated from 100 to 250 °C at 30 °C/min and held for 6 min. The inlet temperature was set constant at 250 °C. Compound **1w** was synthesized by following a previous procedure¹⁰. Both C=O and C=C bonds in **1w** were reduced after 12 h, and **Ir1** is more active than **Ir2**.

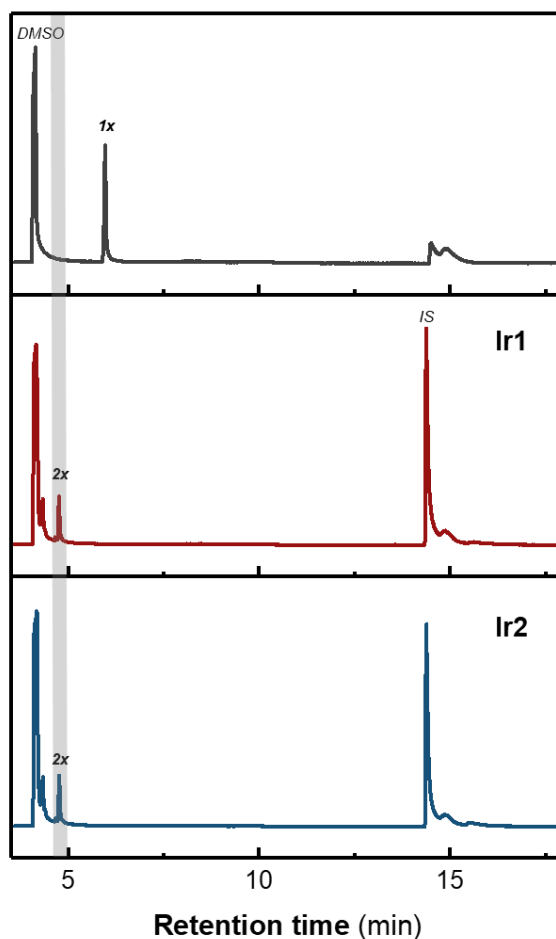
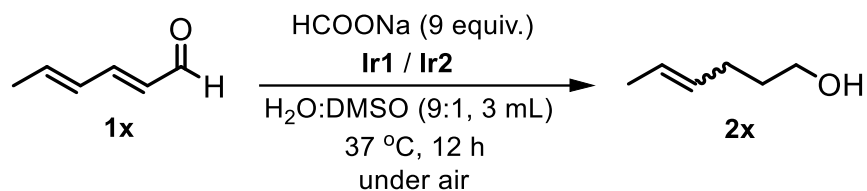


Figure S33. Representative GC traces showing the transfer hydrogenation between HCOONa and **1x** catalyzed by **Ir1** (middle trace) and **Ir2** (bottom trace) after 12 h. A GC standard of **1x** (~ 5.96 min) is showed as top trace. 1,3,5-Trimethoxybenzene (0.5 equiv. relative to the substrate) was added as an internal standard (IS), which showed a peak at ~ 14.38 min. A modified temperature program was used for GC–MS analysis of this compound, in which samples were held at 50 °C for 7 min, heated from 50 to 100 °C at 30 °C/min and held for 3 min, then heated from 100 to 250 °C at 30 °C/min and held for 6 min. The inlet temperature was set constant at 250 °C. A mixture of *E*- and *Z*- isomers of **2x** was observed.

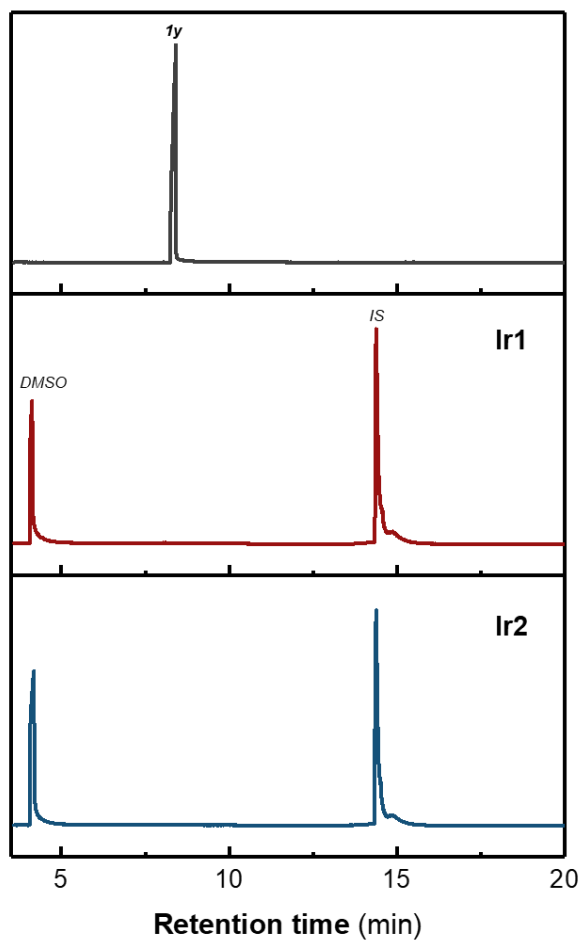
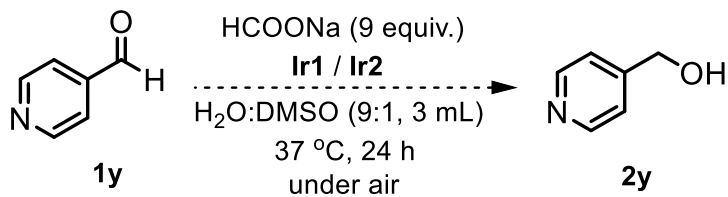
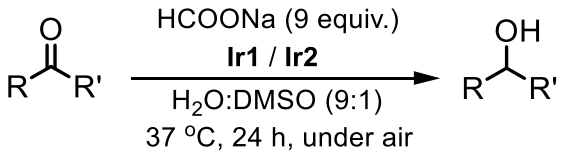
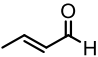
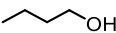
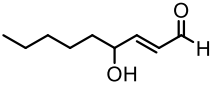
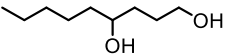
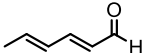
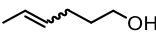
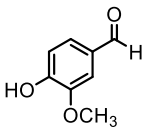
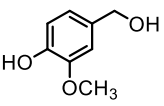
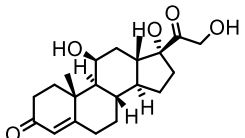
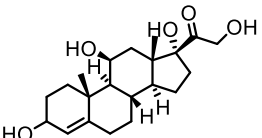


Figure S34. Representative GC traces showing the transfer hydrogenation between HCOONa and **1y** catalyzed by **Ir1** (*middle trace*) and **Ir2** (*bottom trace*) after 24 h. A GC standard of **1y** (~ 8.4 min) is shown in the top trace. 1,3,5-Trimethoxybenzene (0.5 equiv. relative to the substrate) was added as an internal standard (IS), which showed a peak at ~ 14.38 min. A modified temperature program was used for GC–MS analysis of this compound, in which samples were held at 50 °C for 7 min, heated from 50 to 100 °C at 30 °C/min and held for 3 min, then heated from 100 to 250 °C at 30 °C/min and held for 6 min. The inlet temperature was set constant at 250 °C. No products and starting material were detected after the reaction.

Table S11. Summary of Transfer Hydrogenation Between HCOONa and Various Biological Aldehydes and Ketones



Entry	Substrate	Product	Yield (%)	
			Ir1	Ir2
1 ^a			70 ^b	58 ^c
2			96 ^c	95
3			96 ^c	96 ^c
4			99	17
5 ^a			21	0

Standard conditions used: substrate (5 mM, 15 μ mol), HCOONa (135 μ mol), Ir complex (0.15 μ mol for **Ir1**, 0.075 μ mol for **Ir2**), H₂O: DMSO (9:1, 3 mL), 37 °C, 24 h. The reaction yields were determined by GC-MS using diphenyl ether, biphenyl, or 1,3,5-trimethoxybenzene as an internal standard. Yields are average of at least two independent runs. Substrates from entries 1, 4, and 5 were used for comparison, which were previously shown as compounds **1o** (crotonaldehyde), **1i** (vanillin), and **1v** (hydrocortisone), respectively.

^aFor substrates in entries 1 and 5, samples were prepared in D₂O: DMSO-*d*₆ (9:1, 1 mL) and yields were determined by ¹H NMR spectroscopy, using 1,3,5-trimethoxybenzene as an internal standard.

^bYields were determined after 6 h.

^cYields were determined after 12 h.

NMR Spectroscopic Data

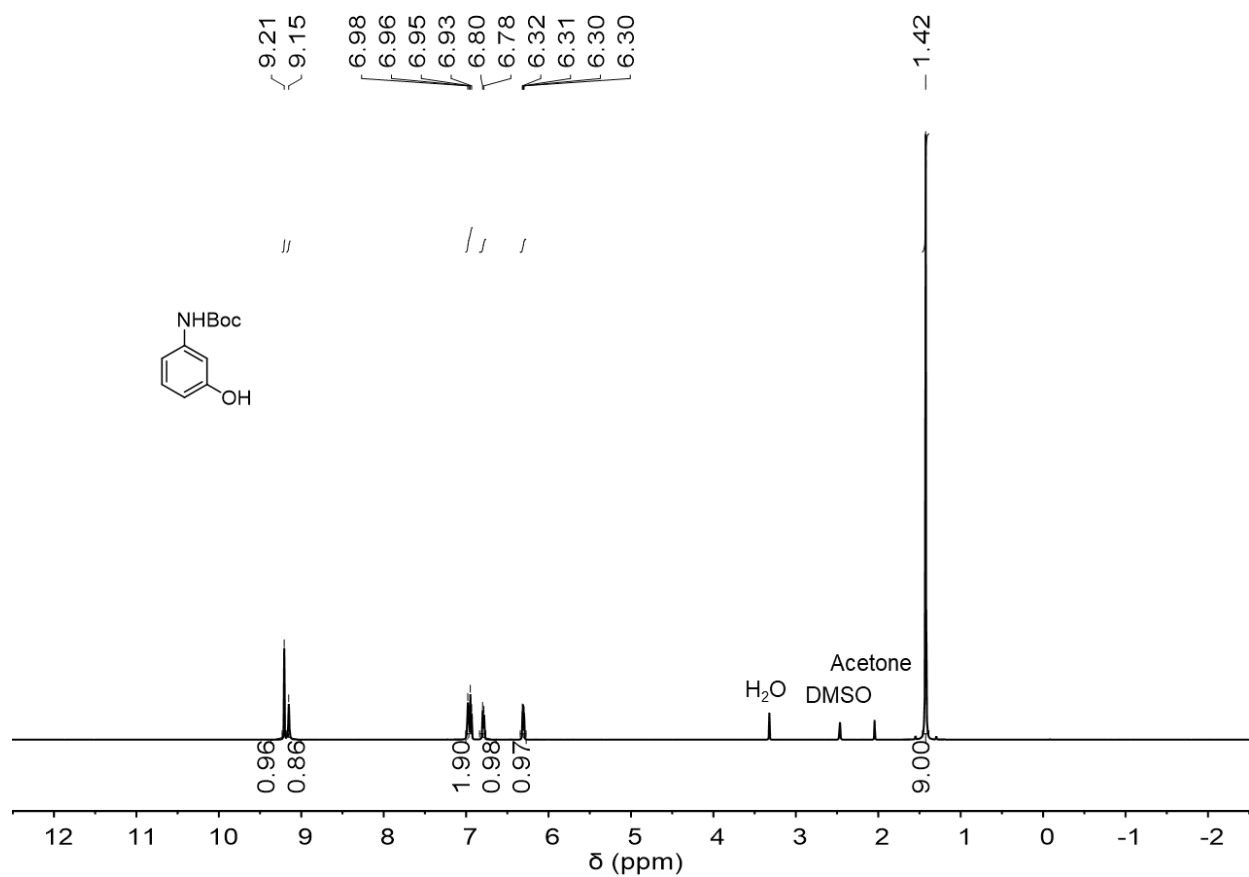


Figure S35. ¹H NMR spectrum (500 MHz, DMSO-*d*₆) of **L1**.

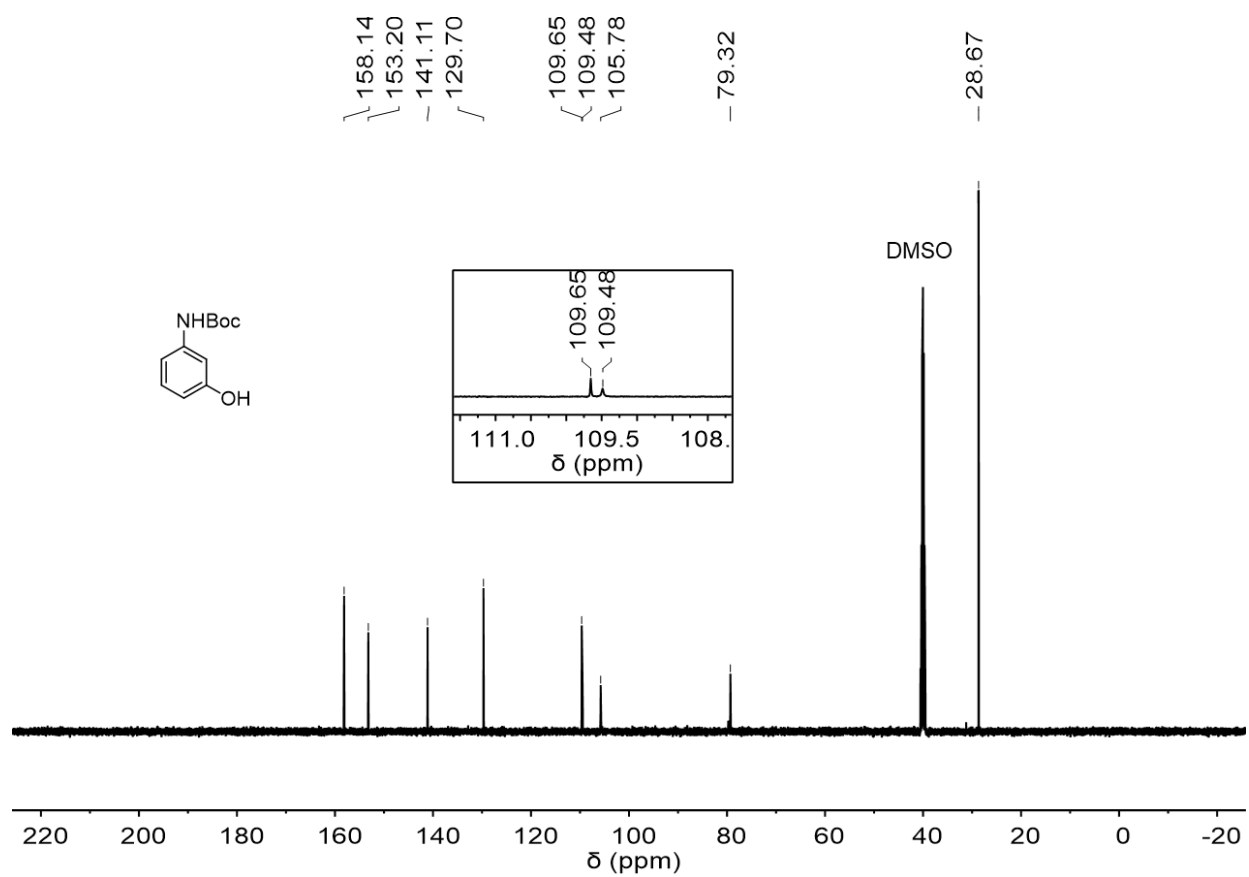


Figure S36. ^{13}C NMR spectrum (126 MHz, $\text{DMSO-}d_6$) of **L1**.

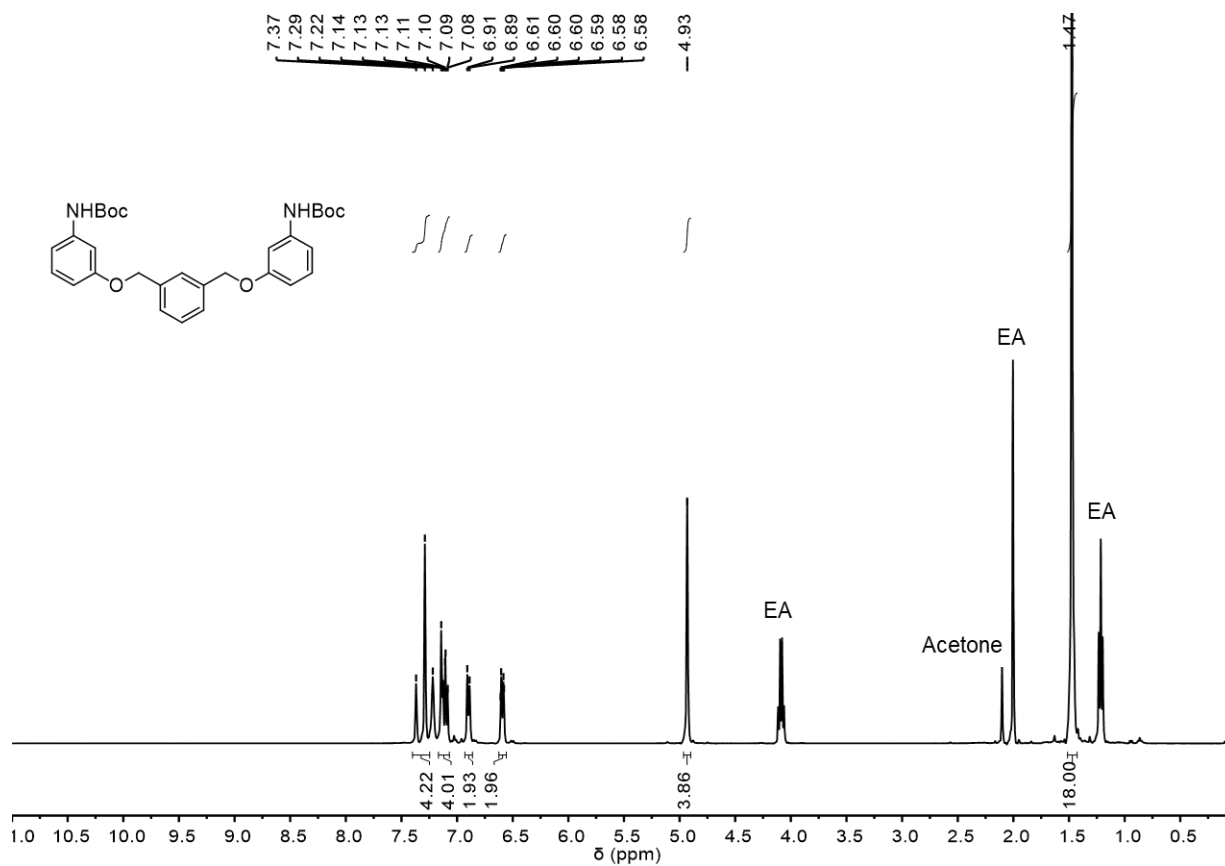


Figure S37. ¹H NMR spectrum (400 MHz, CDCl₃) of **L2**.

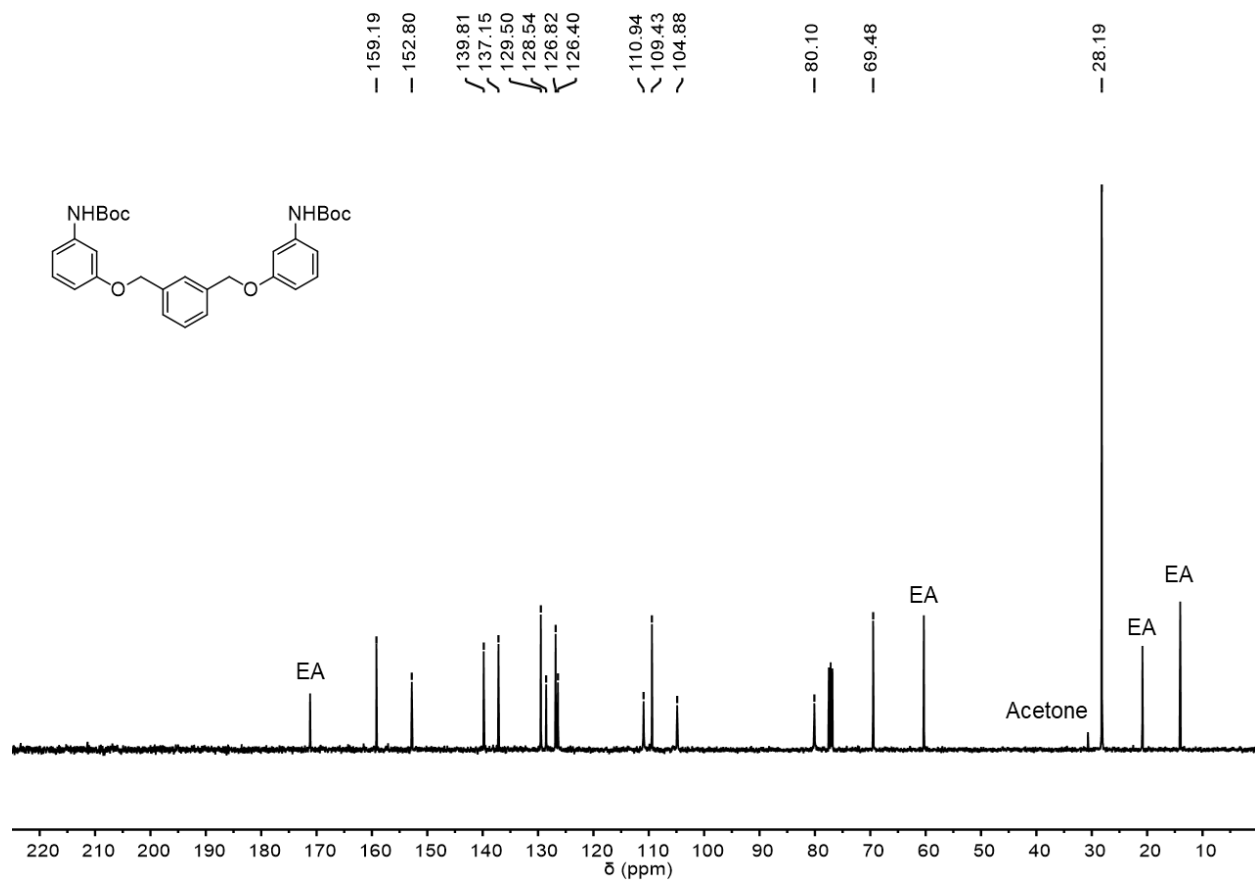


Figure S38. ¹³C NMR spectrum (400 MHz, CDCl₃) of **L2**.

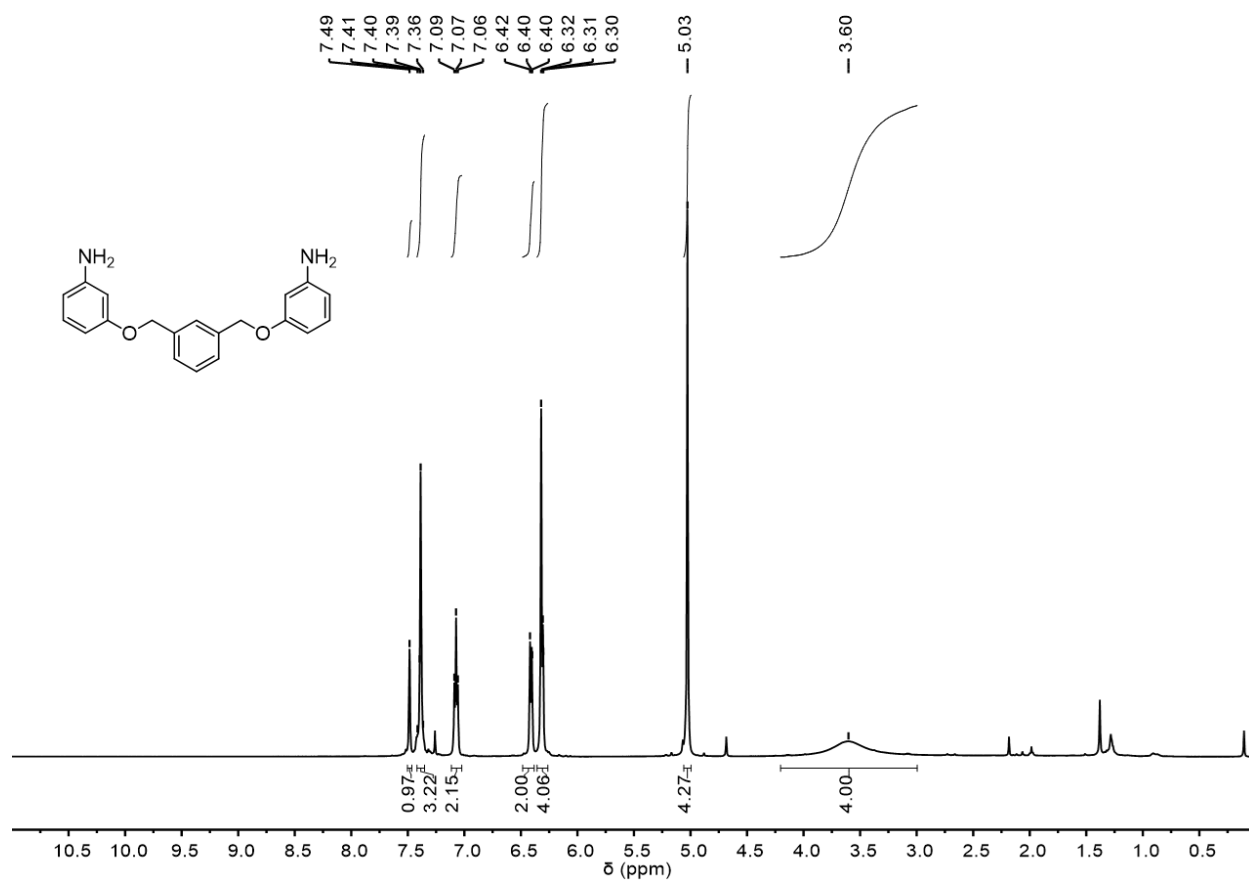


Figure S39. ¹H NMR spectrum (500 MHz, CDCl₃) of **L3**.

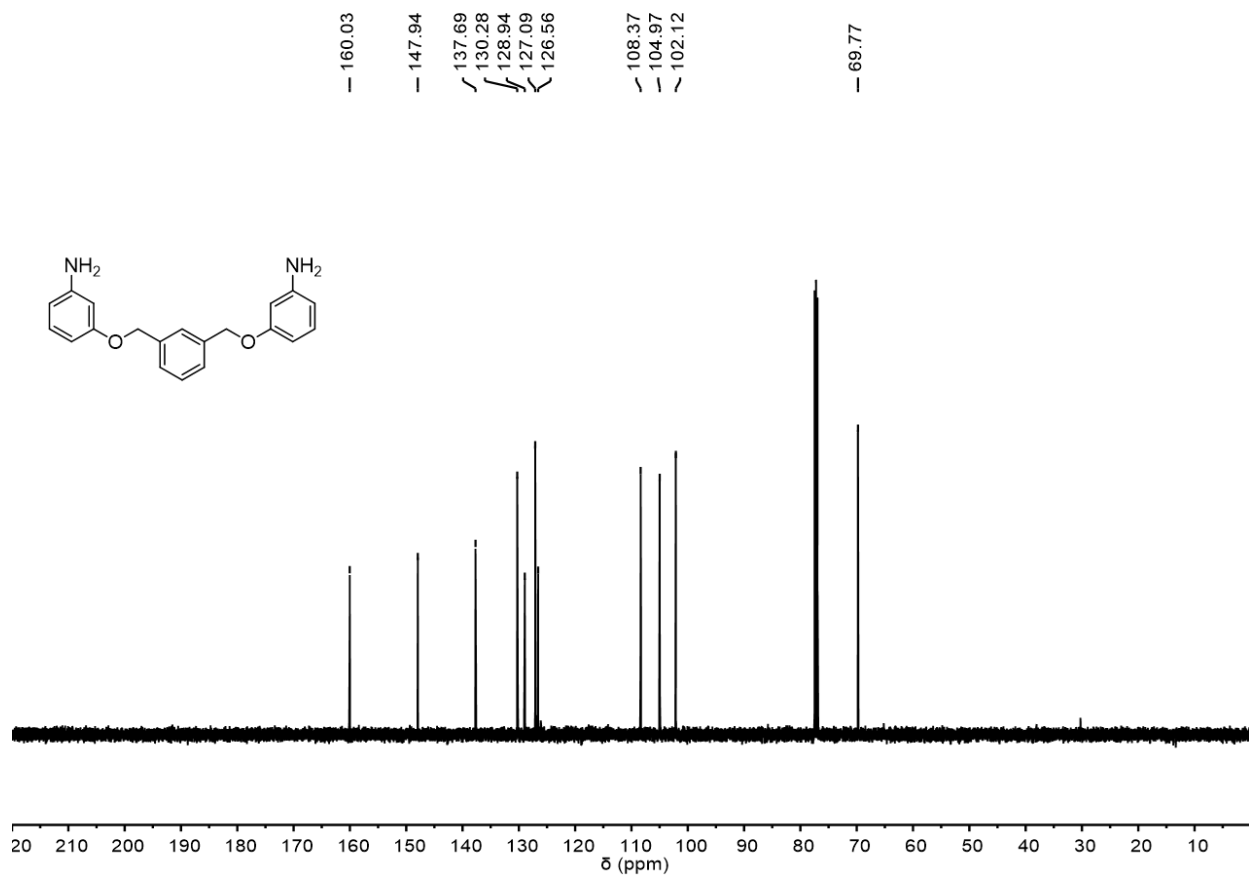


Figure S40. ¹³C NMR spectrum (126 MHz, CDCl₃) of **L3**.

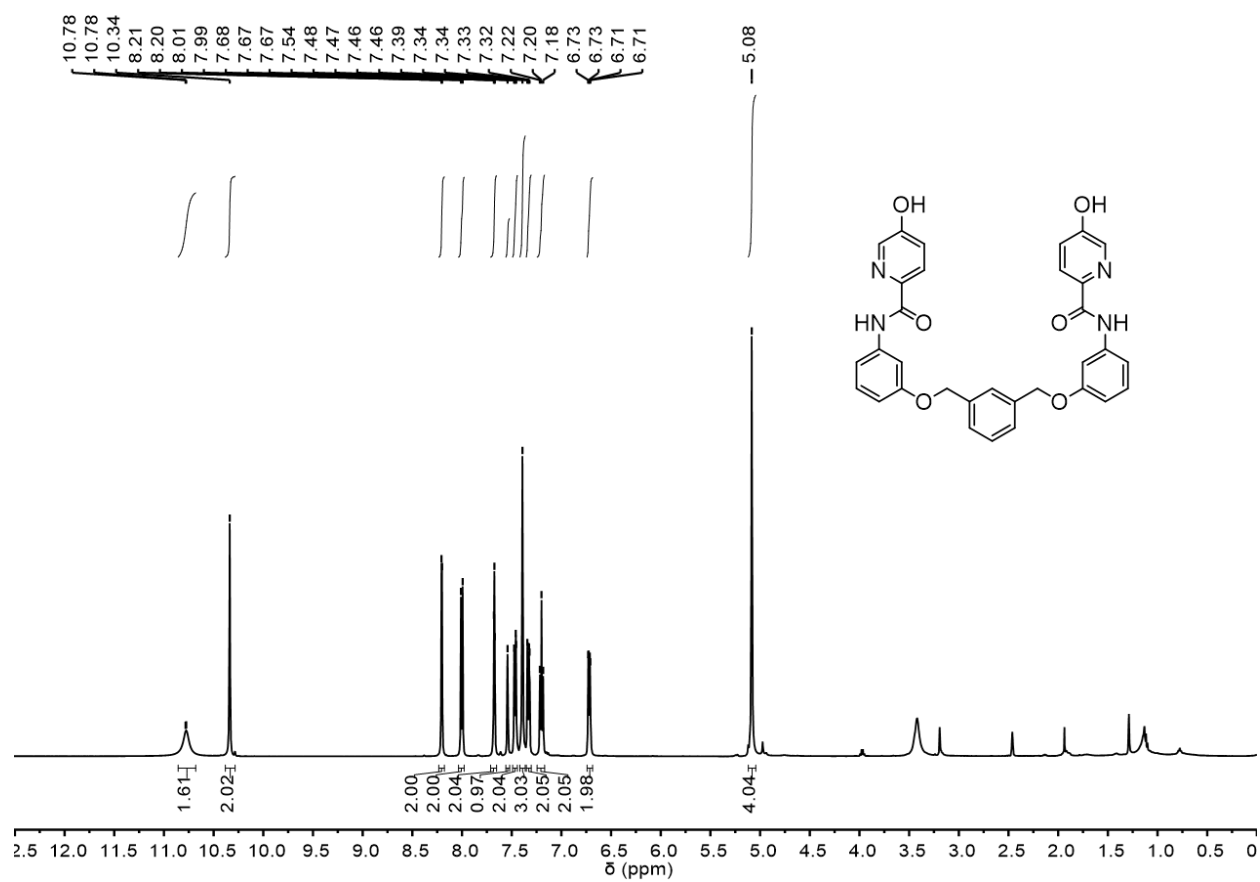


Figure S41. ^1H NMR spectrum (500 MHz, $\text{DMSO}-d_6$) of **L4**.

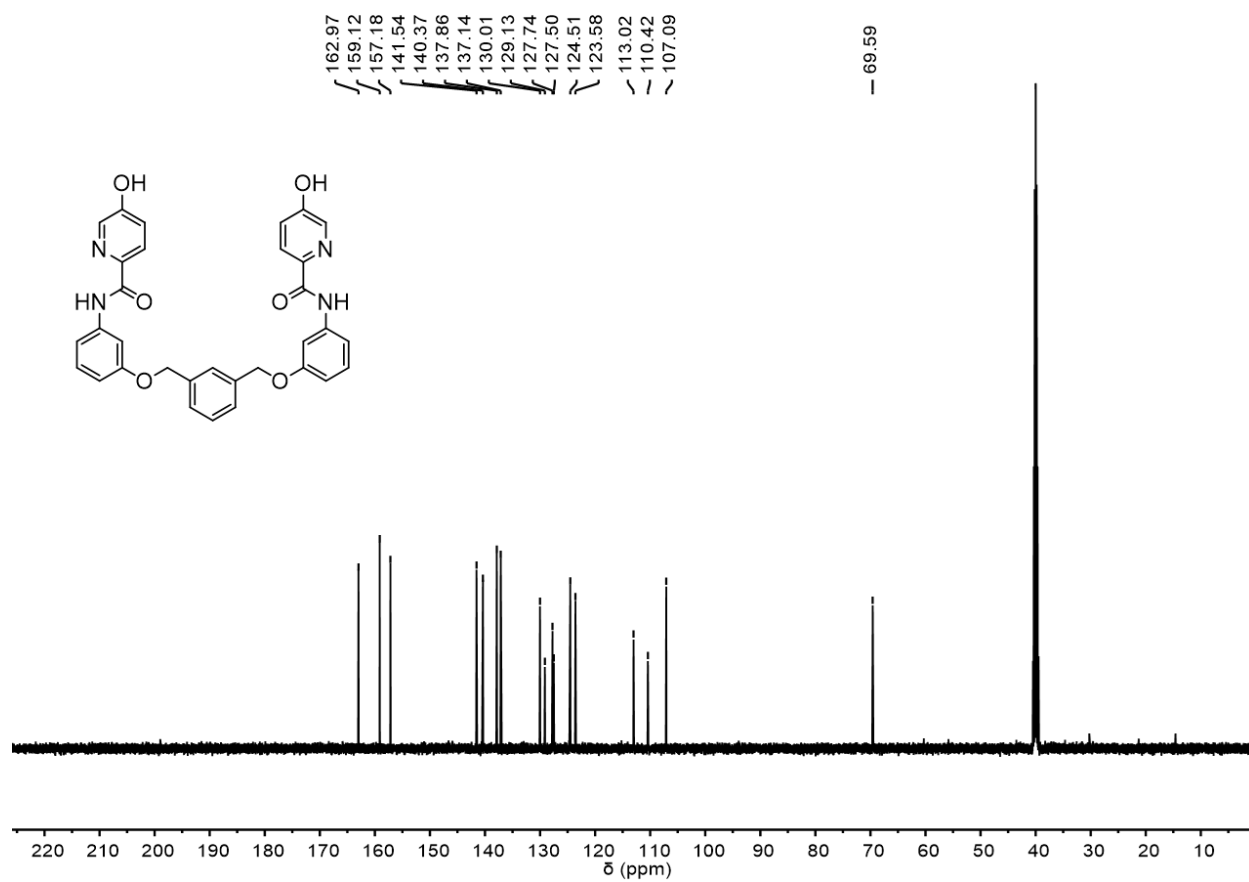


Figure S42. ¹³C NMR spectrum (126 MHz, DMSO-*d*₆) of L4.

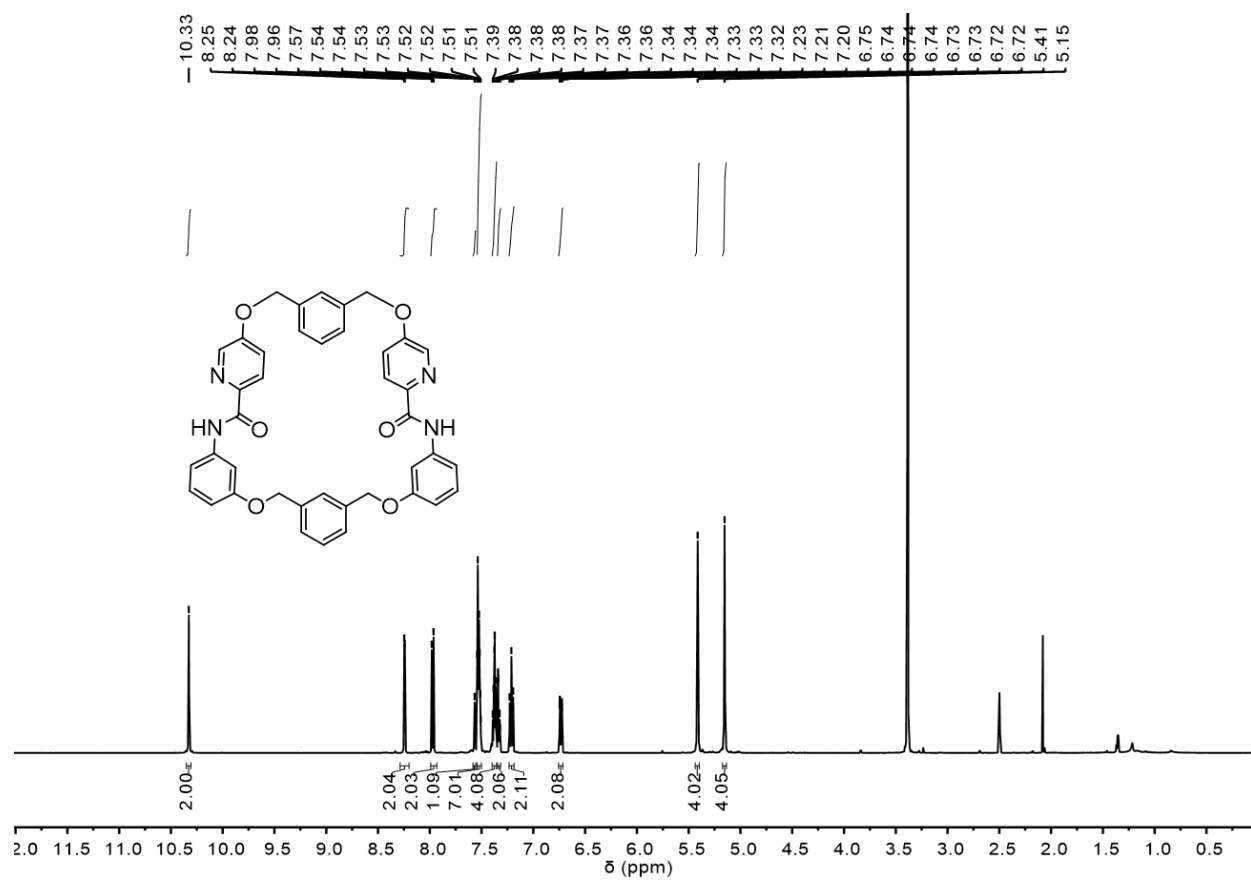


Figure S43. ¹H NMR spectrum (500 MHz, DMSO-*d*₆) of **L5**.

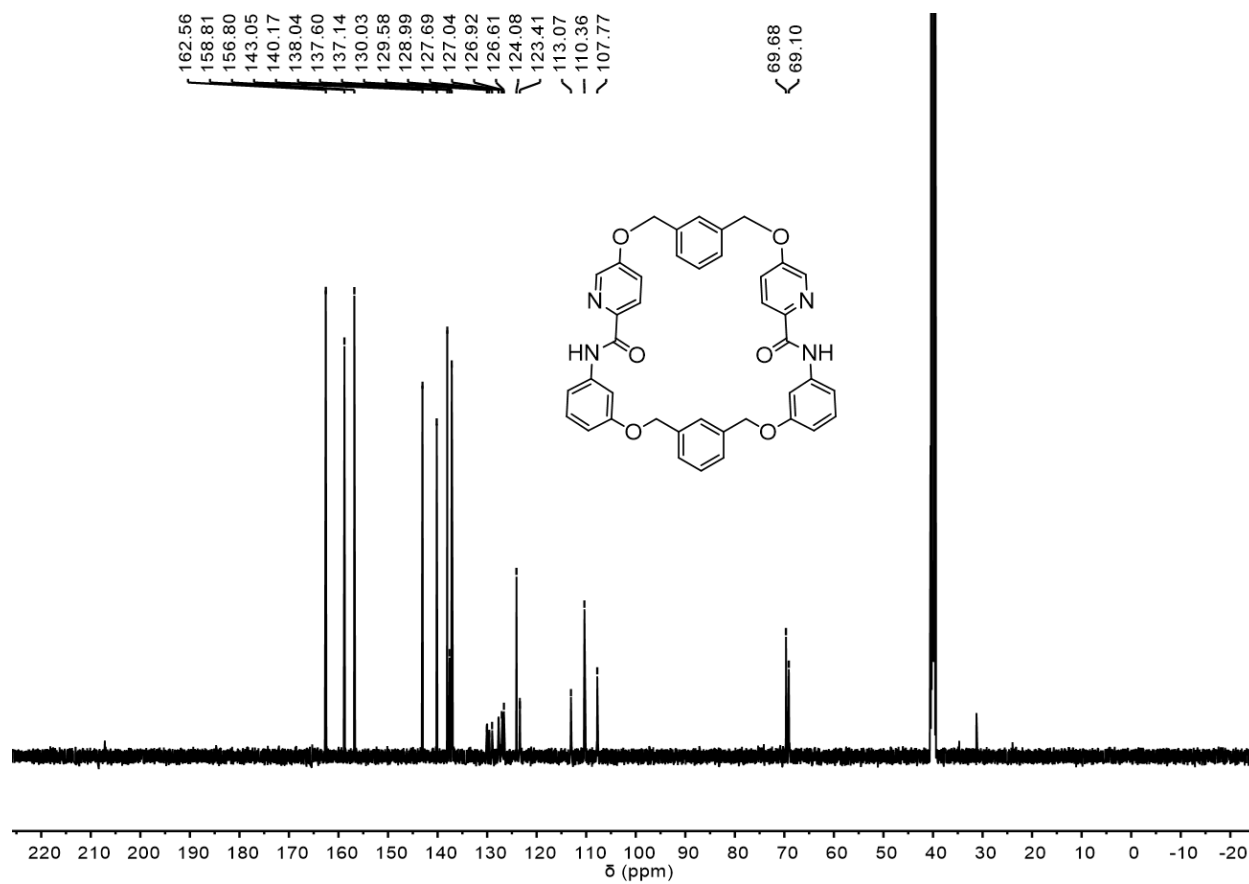


Figure S44. ^{13}C NMR spectrum (126 MHz, $\text{DMSO-}d_6$) of **L5**.

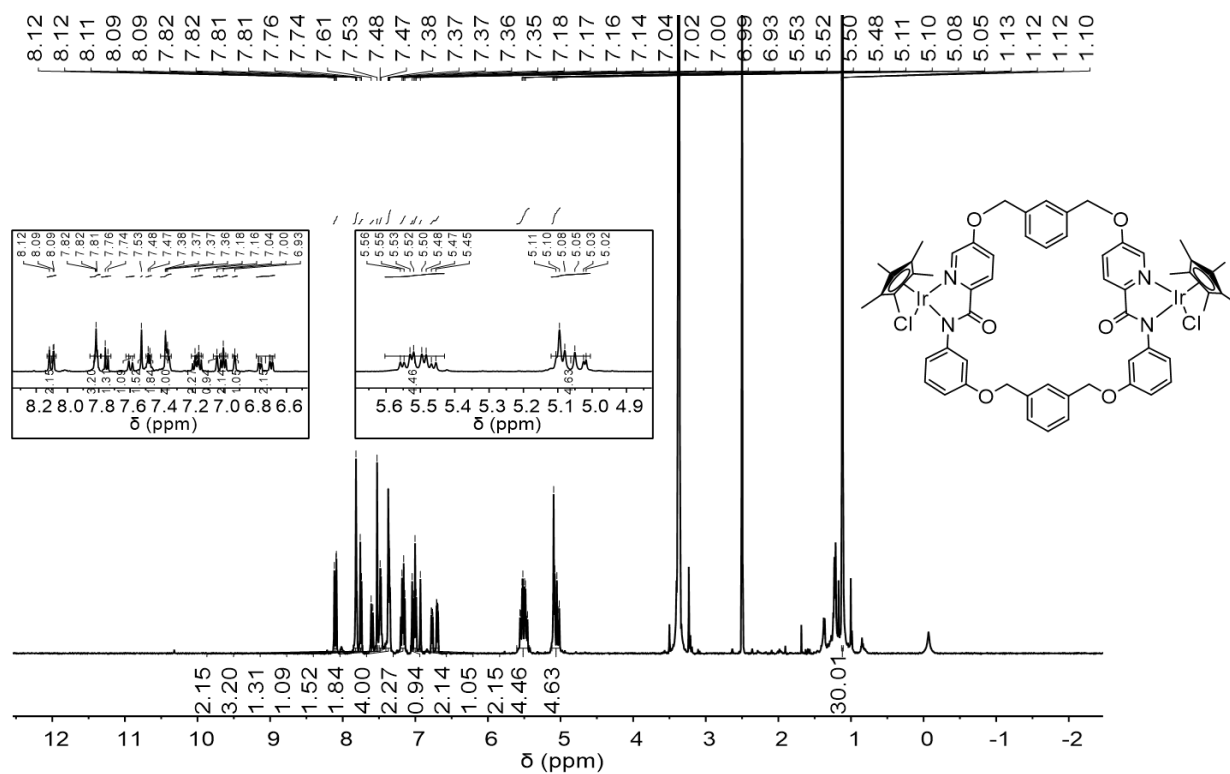


Figure S45. ^1H NMR spectrum (500 MHz, $\text{DMSO}-d_6$) of **Ir2**.

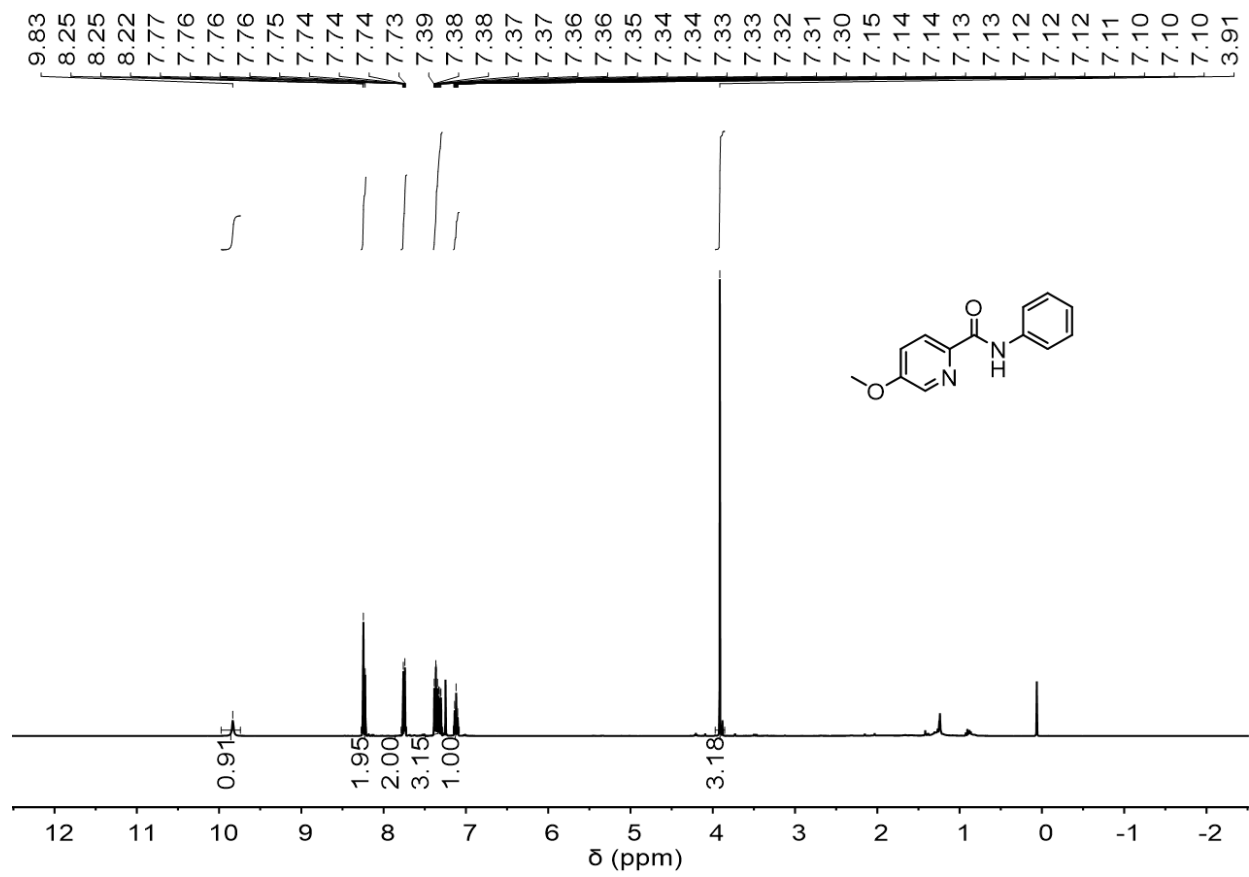


Figure S46. ^1H NMR spectrum (500 MHz, $\text{DMSO}-d_6$) of **L6**.

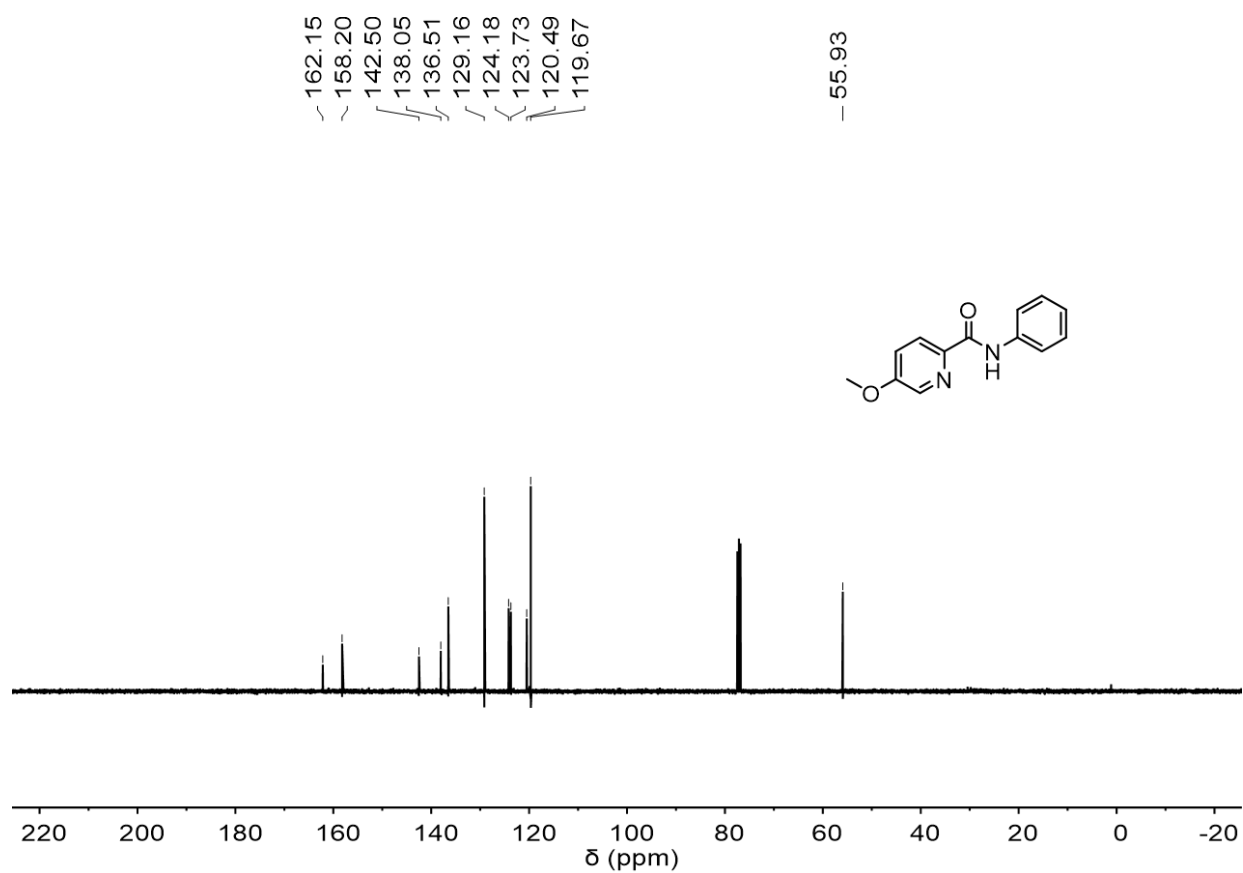


Figure S47. ¹³C NMR spectrum (126 MHz, DMSO-*d*₆) of **L6**.

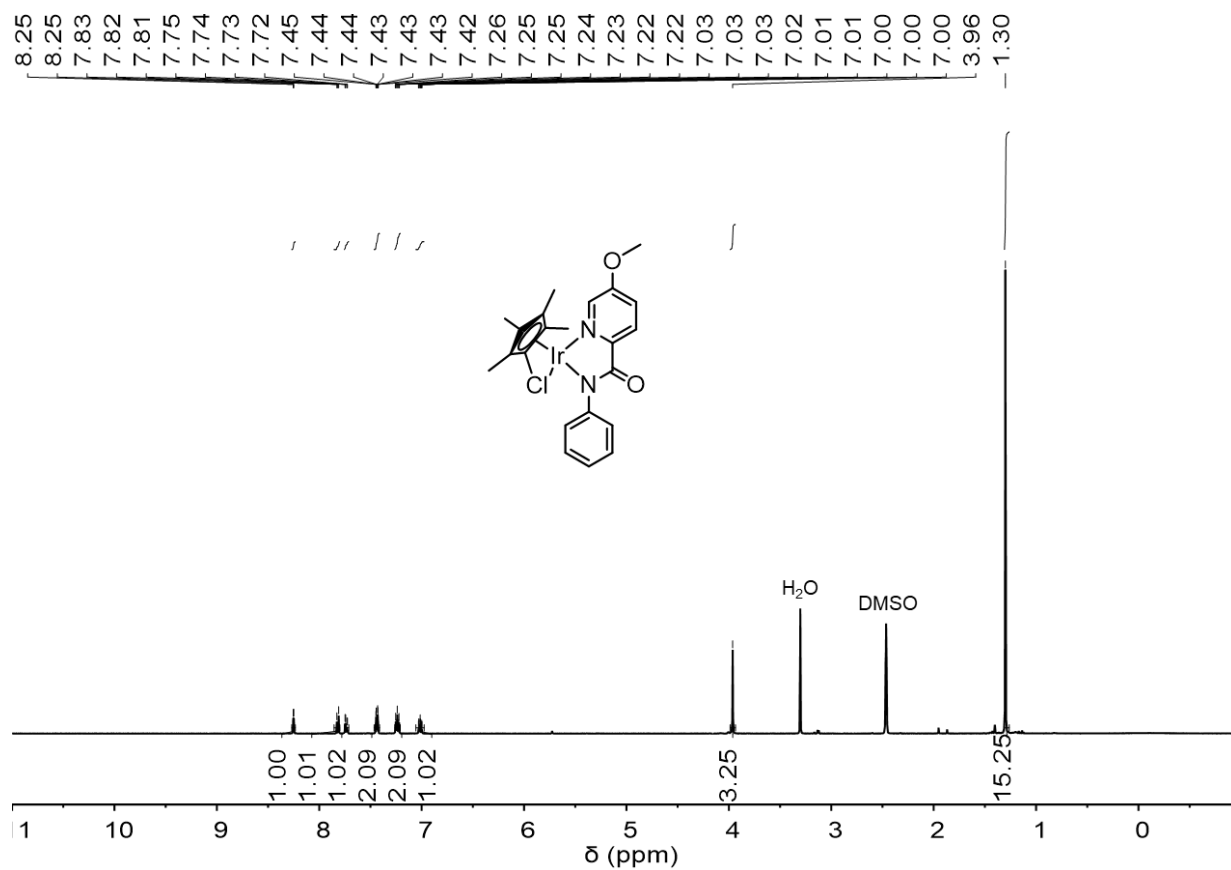


Figure S48. ^1H NMR spectrum (500 MHz, $\text{DMSO-}d_6$) of **Ir1'**.

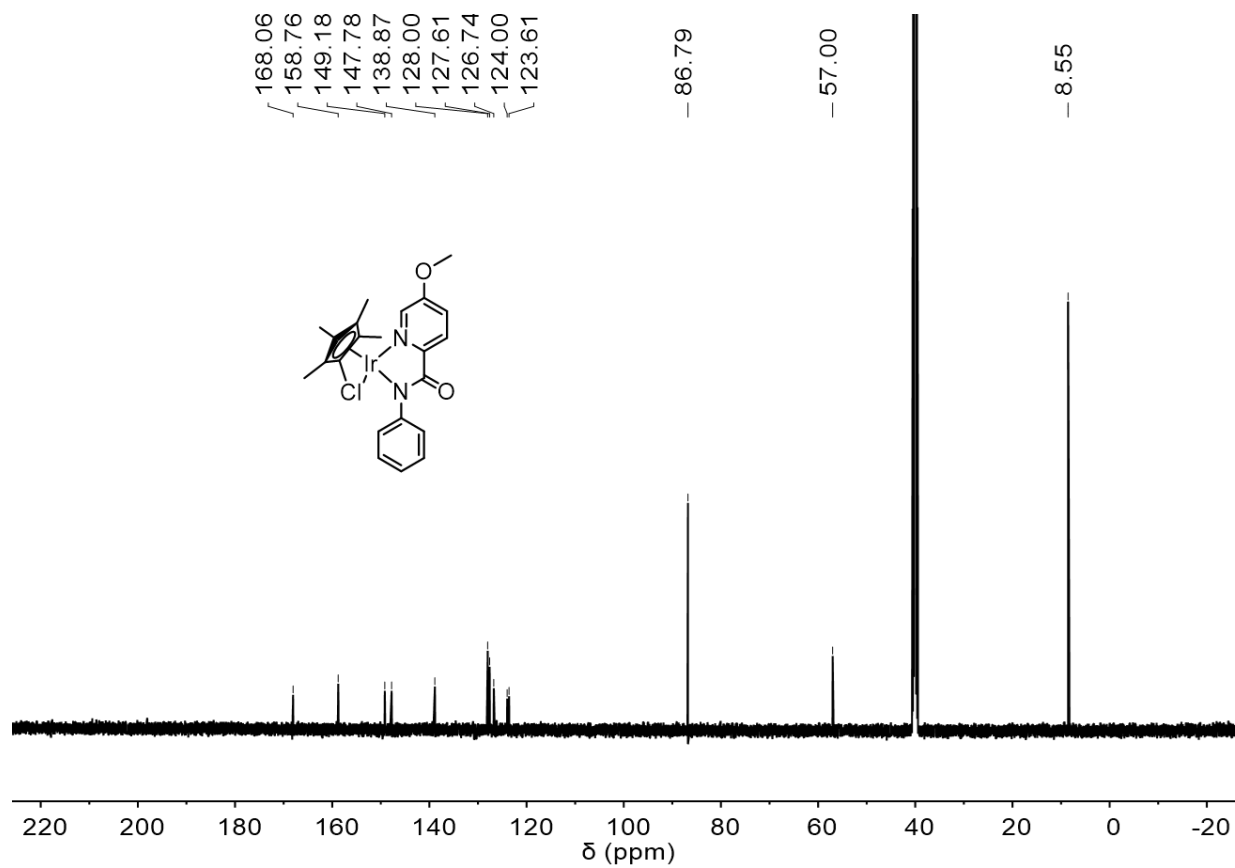


Figure S49. ¹³C NMR spectrum (126 MHz, DMSO-*d*₆) of Ir1'.

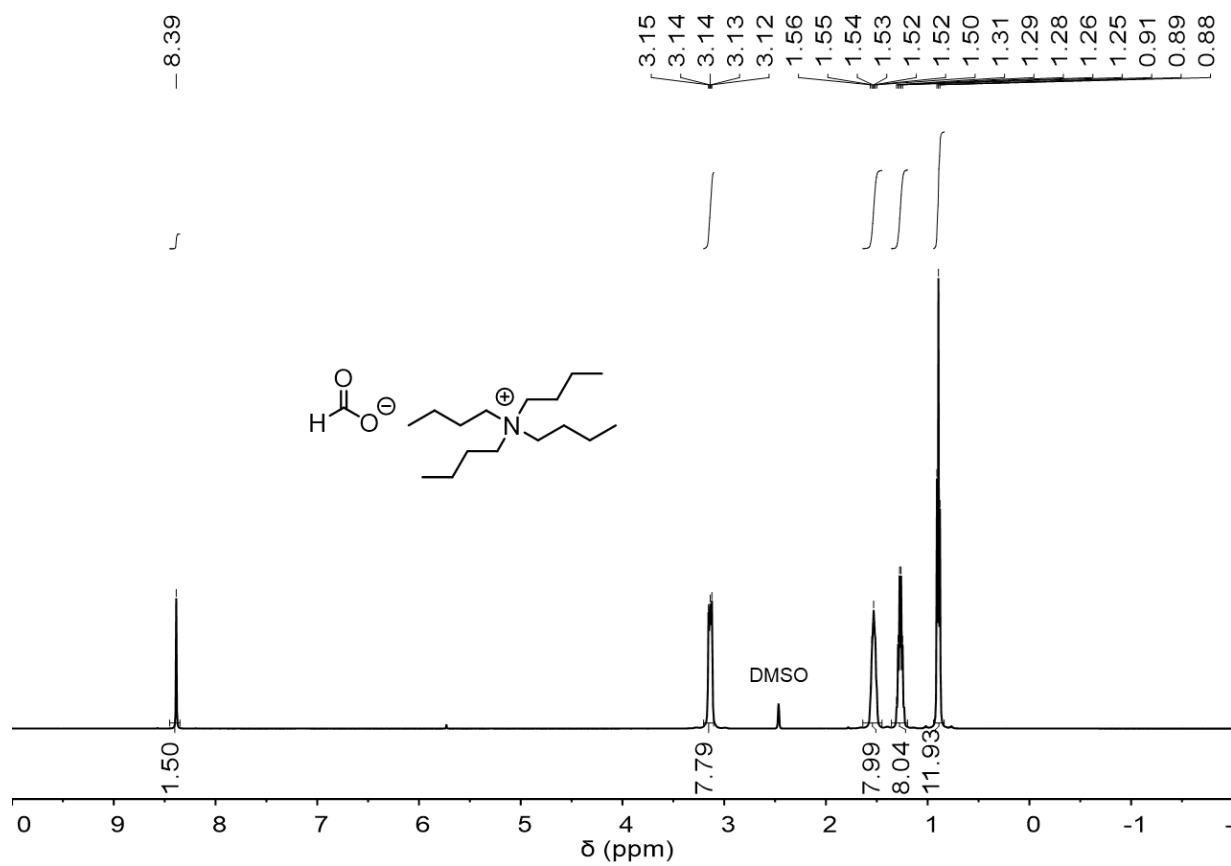


Figure S50. ¹H NMR spectrum (500 MHz, DMSO-*d*₆) of tetrabutylammonium formate.

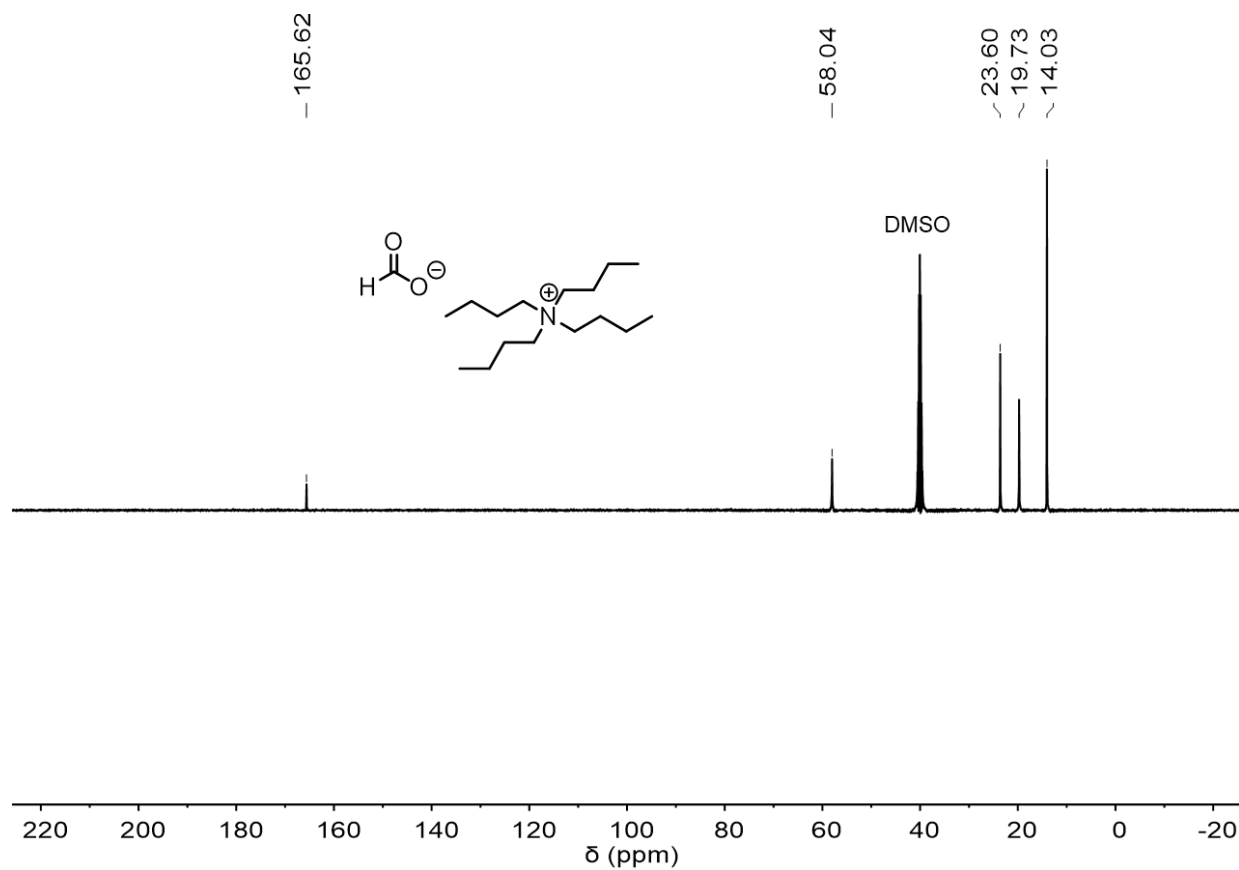


Figure S51. ^{13}C NMR spectrum (126 MHz, $\text{DMSO-}d_6$) of tetrabutylammonium formate.

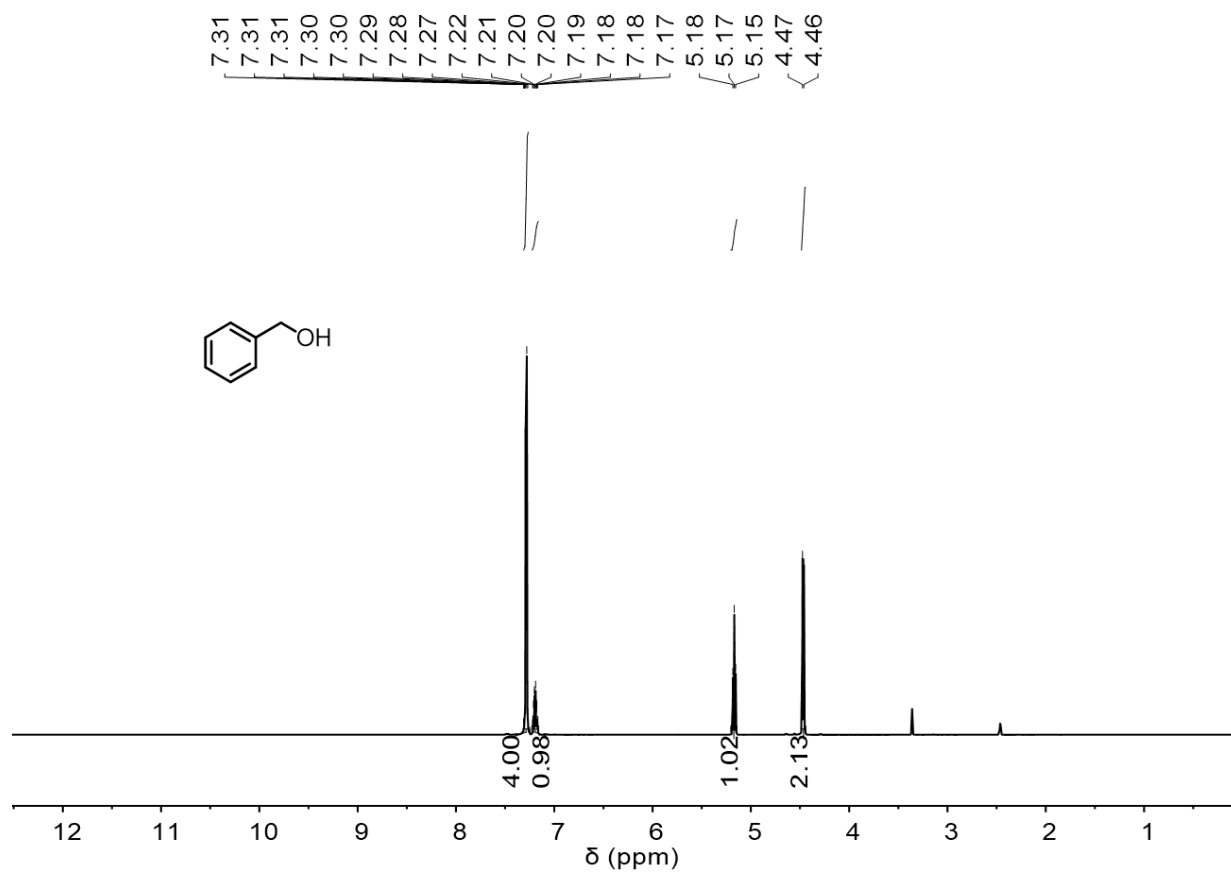


Figure S52. ¹H NMR spectrum (400 MHz, DMSO-*d*₆) of **2a**.

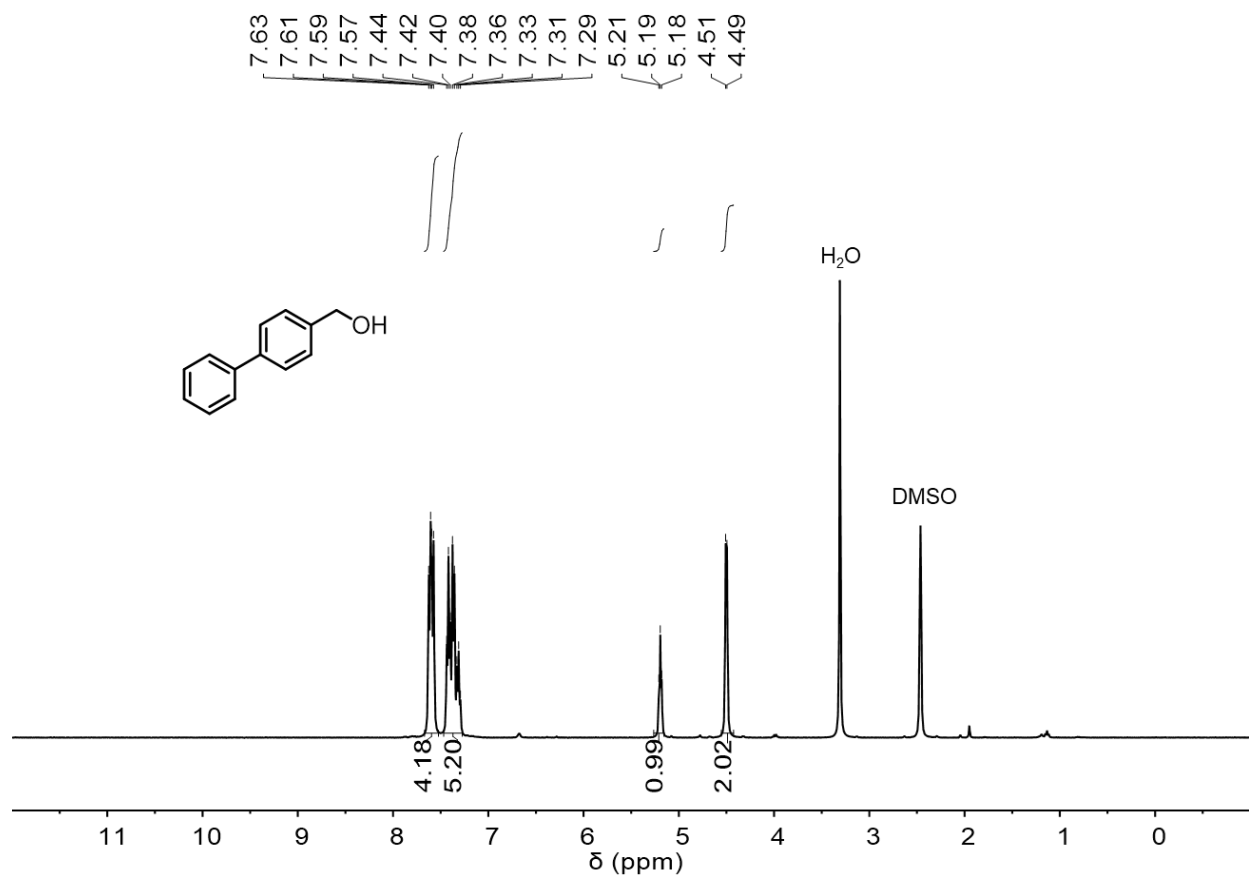


Figure S53. ¹H NMR spectrum (400 MHz, DMSO-*d*₆) of **2c**.

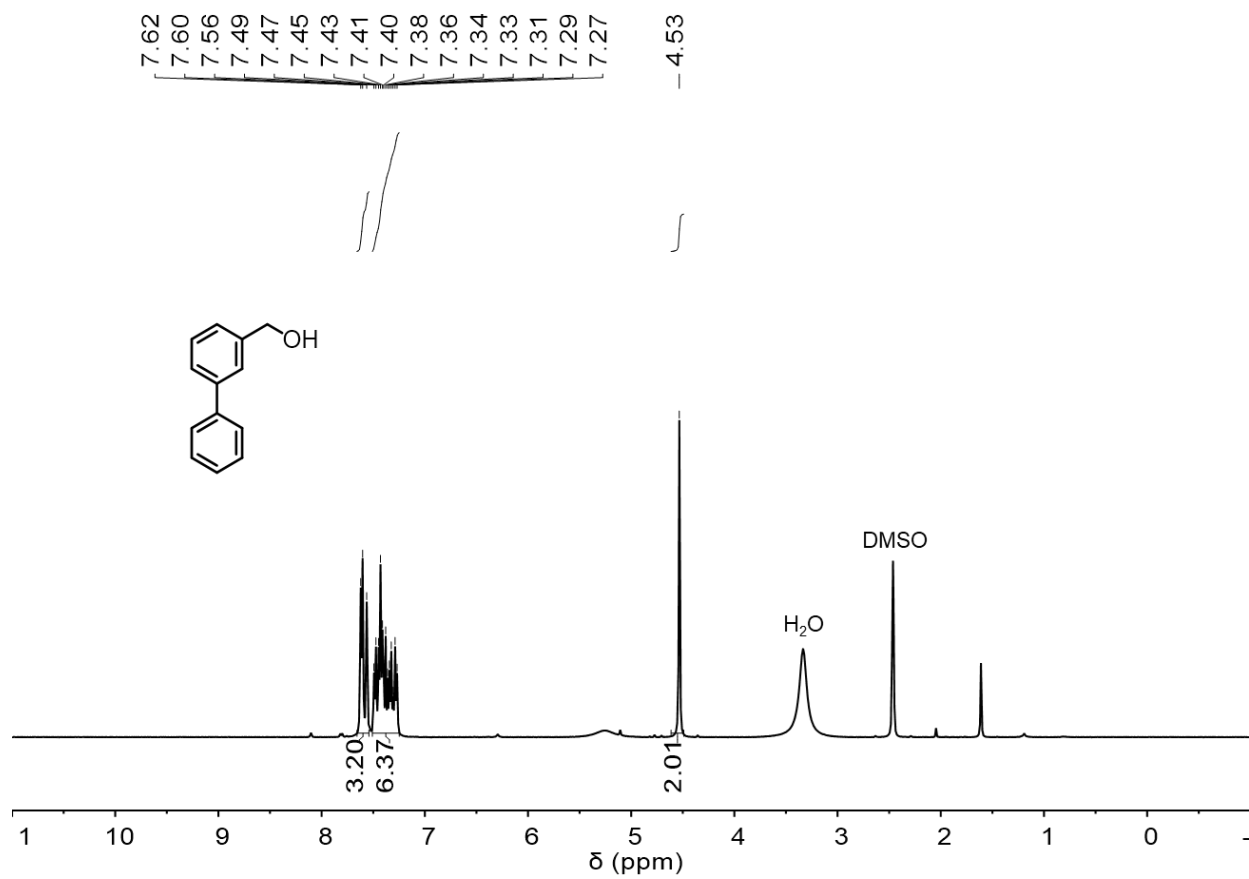


Figure S54. ¹H NMR spectrum (400 MHz, DMSO-*d*₆) of **2d**.

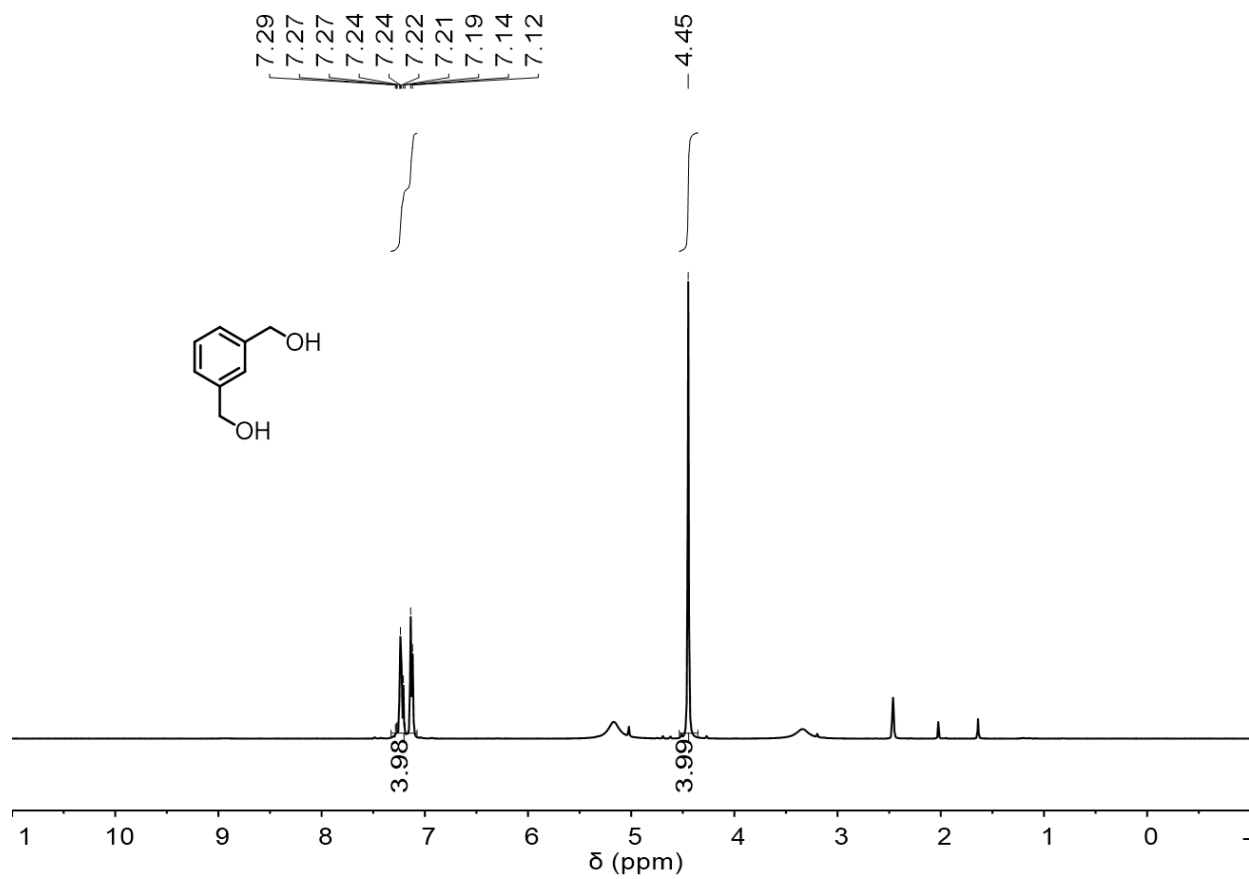


Figure S55. ¹H NMR spectrum (400 MHz, DMSO-*d*₆) of **2h**.

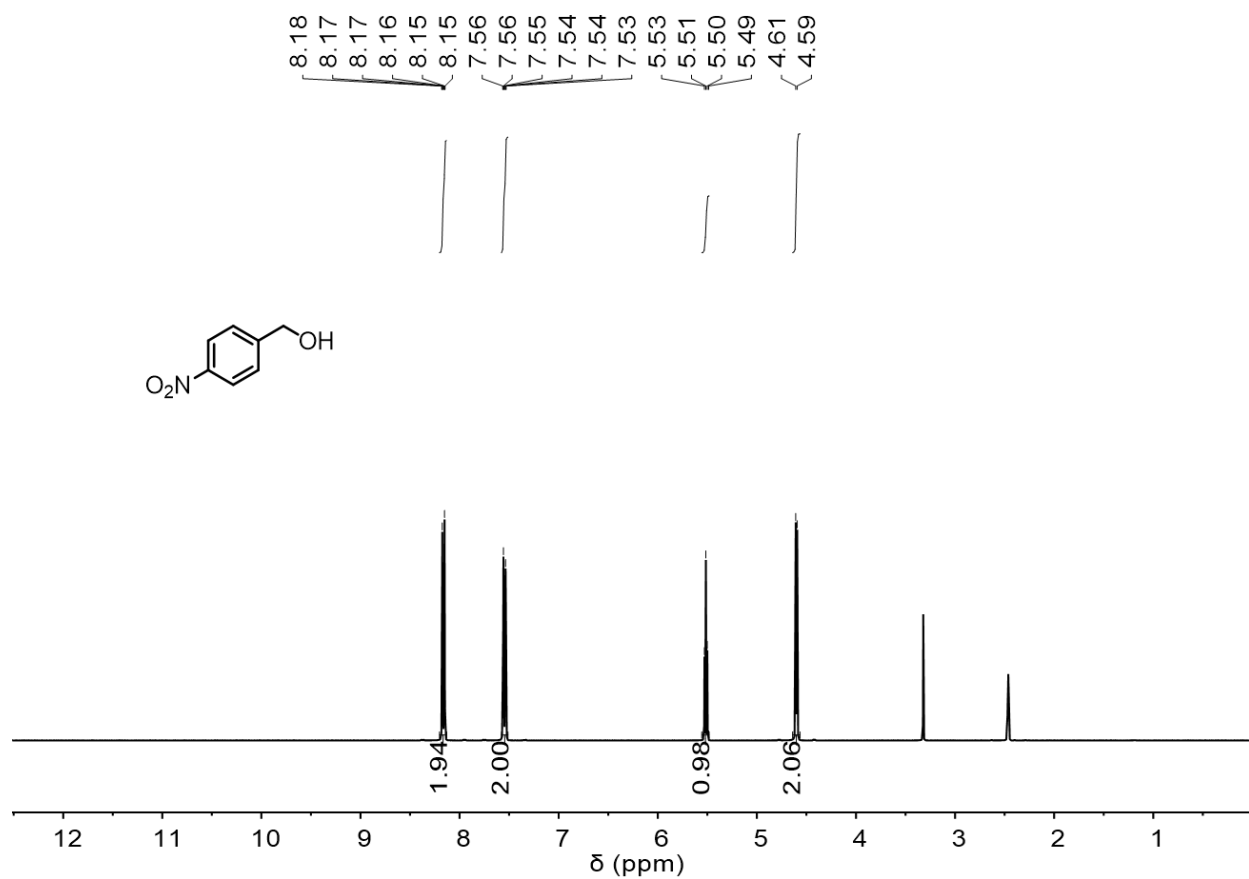


Figure S56. ¹H NMR spectrum (400 MHz, DMSO-*d*₆) of **2l**.

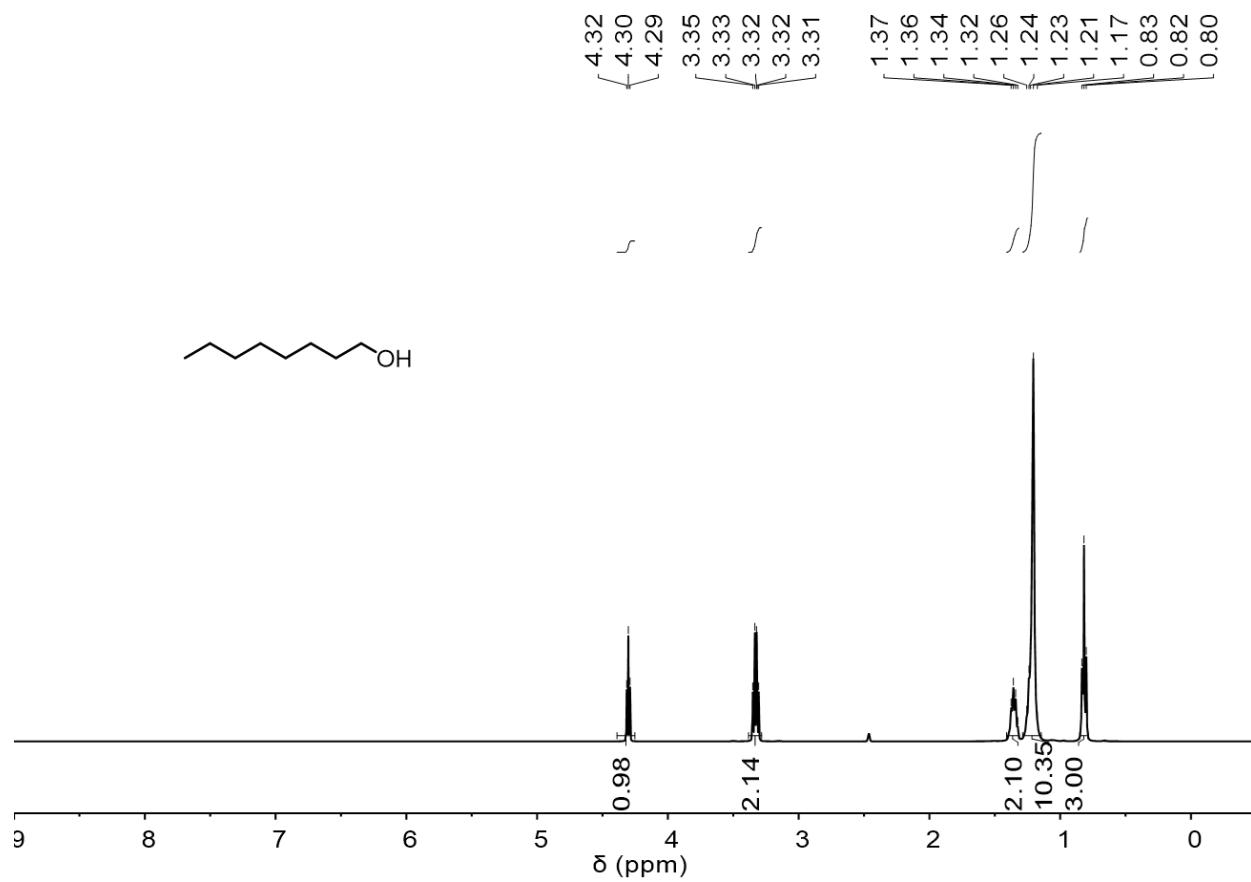


Figure S57. ^1H NMR spectrum (400 MHz, $\text{DMSO-}d_6$) of **2m**.

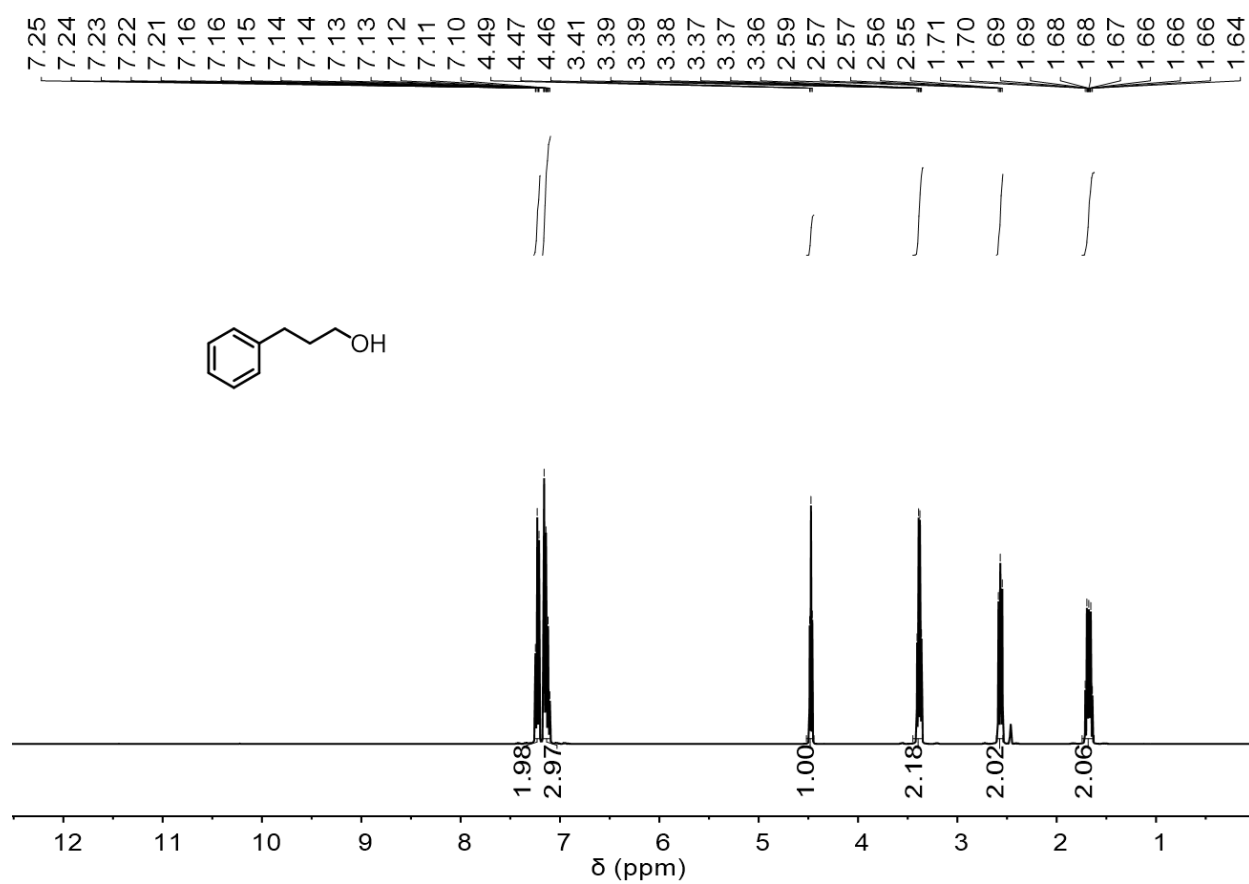


Figure S58. ¹H NMR spectrum (400 MHz, DMSO-*d*₆) of **2n**.

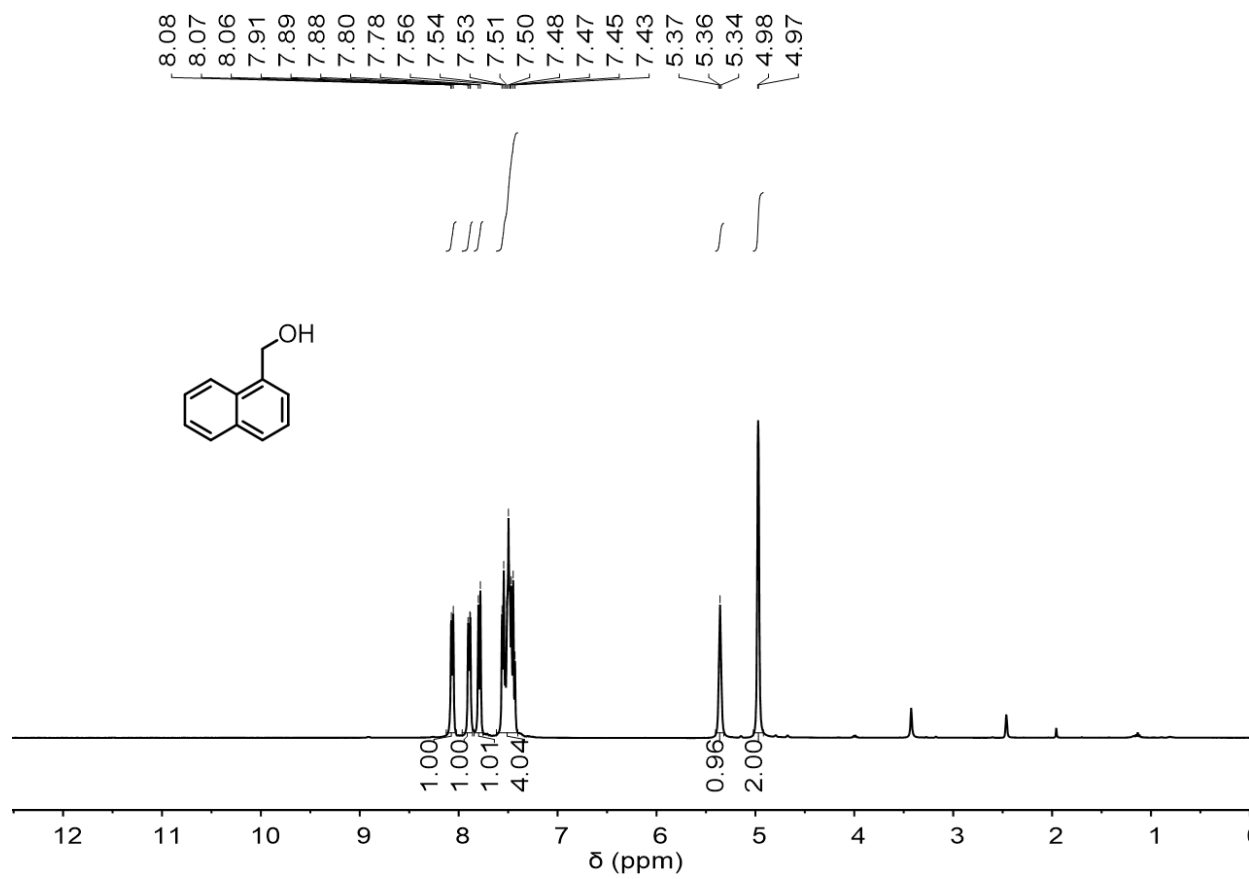


Figure S59. ¹H NMR spectrum (400 MHz, DMSO-*d*₆) of **2p**.

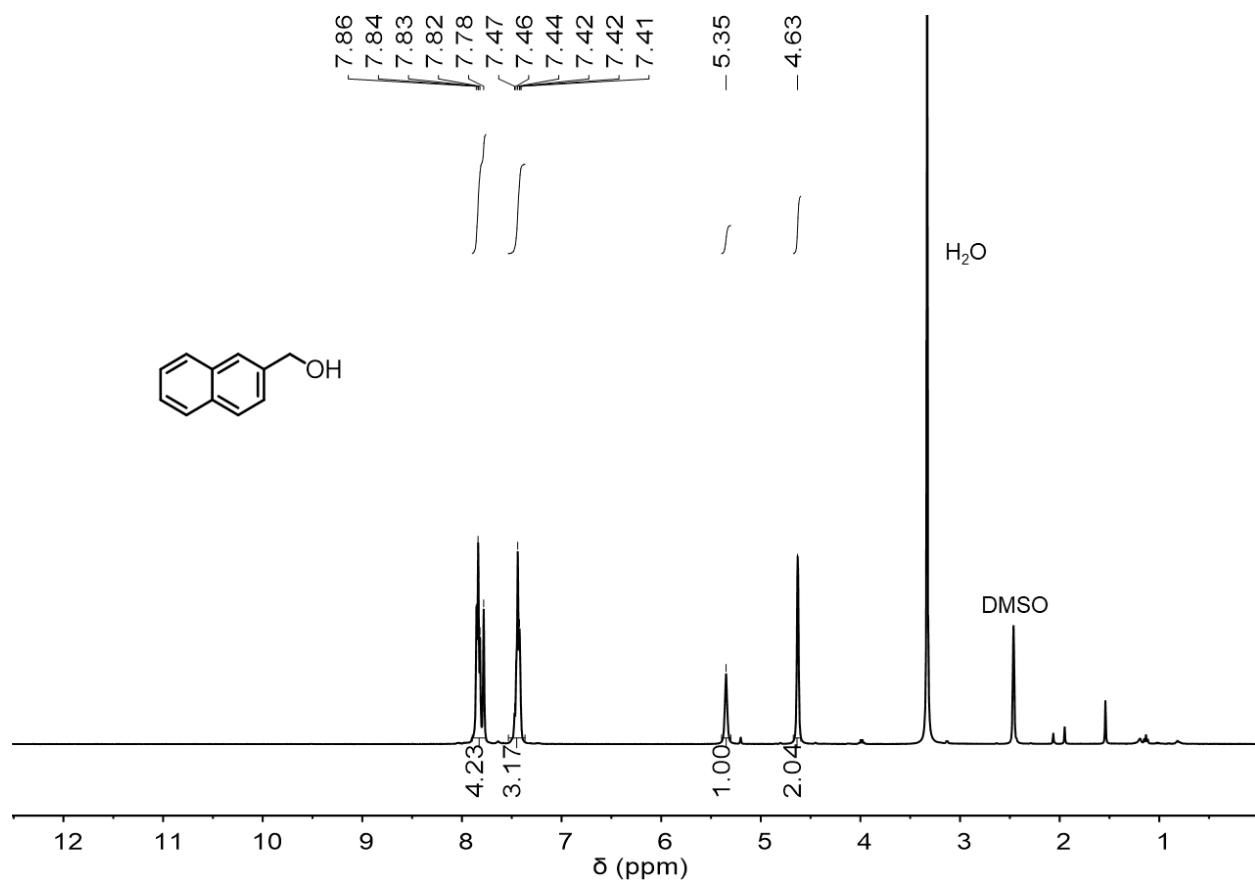


Figure S60. ¹H NMR spectrum (400 MHz, DMSO-*d*₆) of **2q**.

Mass Spectrometric Data

MS Zoomed Spectrum

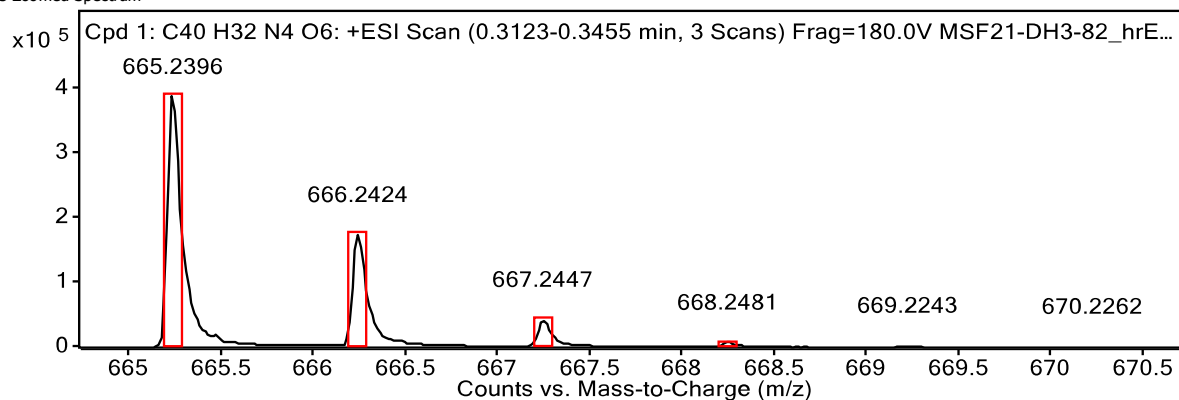


Figure S61. Mass spectrum of compound **L5** (ESI-MS, positive mode).

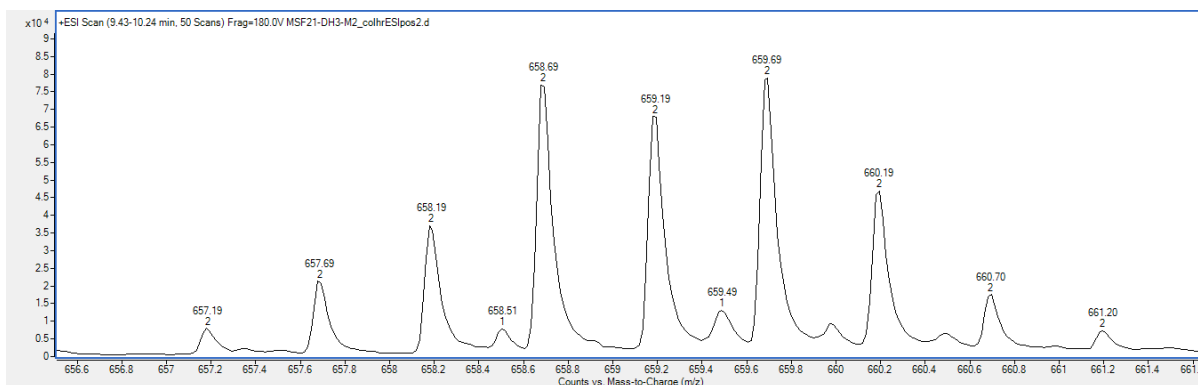


Figure S62. Mass spectrum of complex **Ir2** (ESI-MS, positive mode).

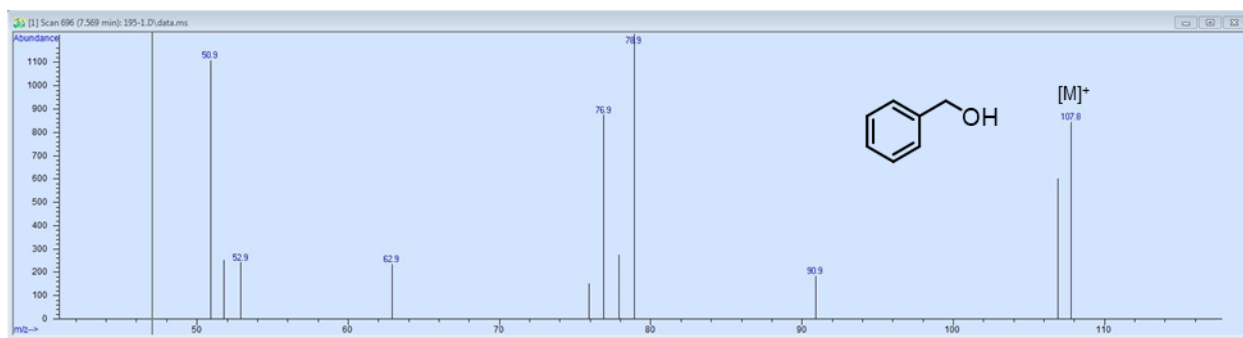


Figure S63. GC-MS spectrum of **2a**.

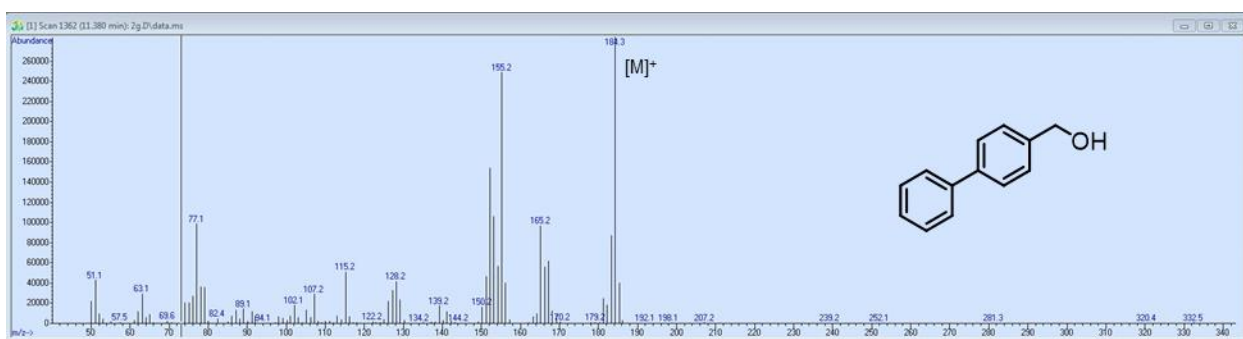


Figure S64. GC-MS spectrum of **2c**.

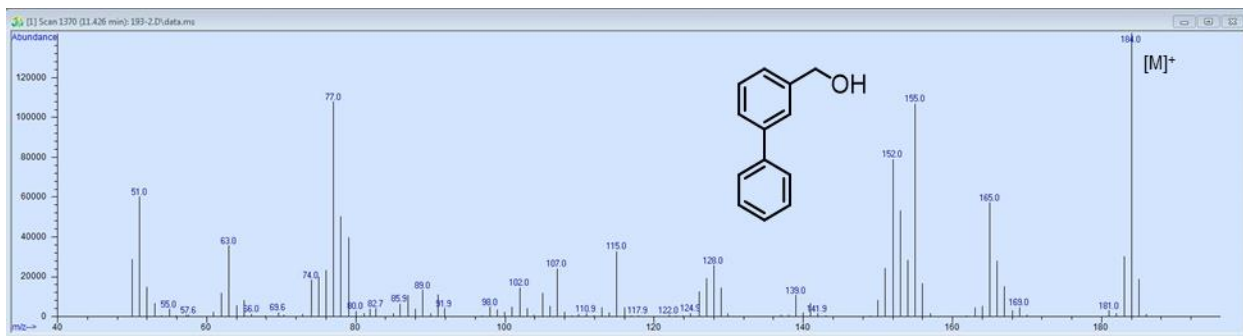


Figure S65. GC-MS spectrum of **2d**.

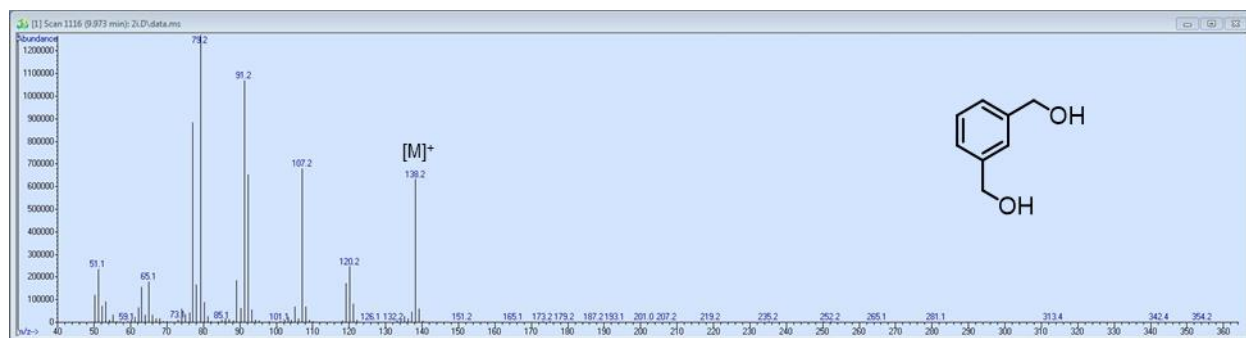


Figure S66. GC-MS spectrum of **2h**.

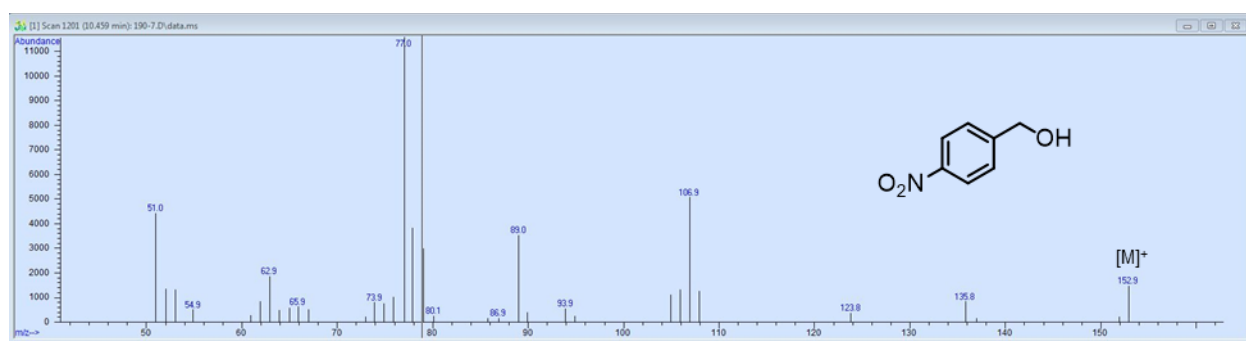


Figure S67. GC-MS spectrum of **2l**.

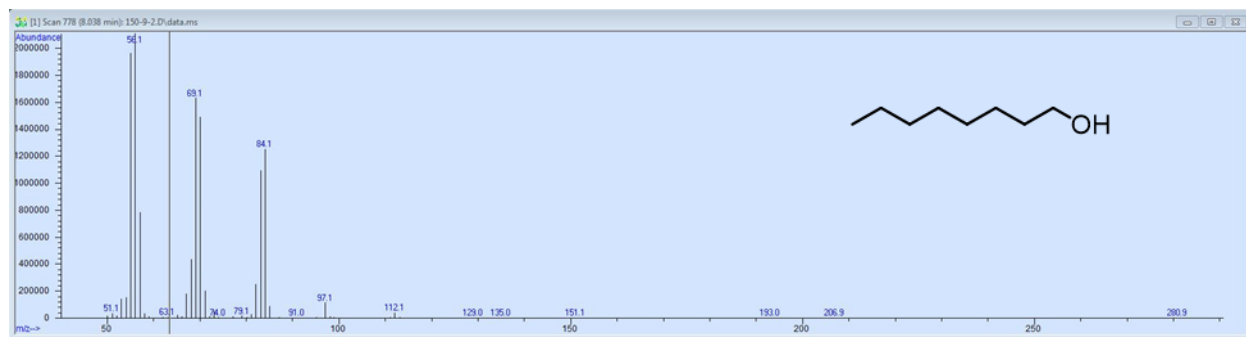


Figure S68. GC-MS spectrum of **2m**.

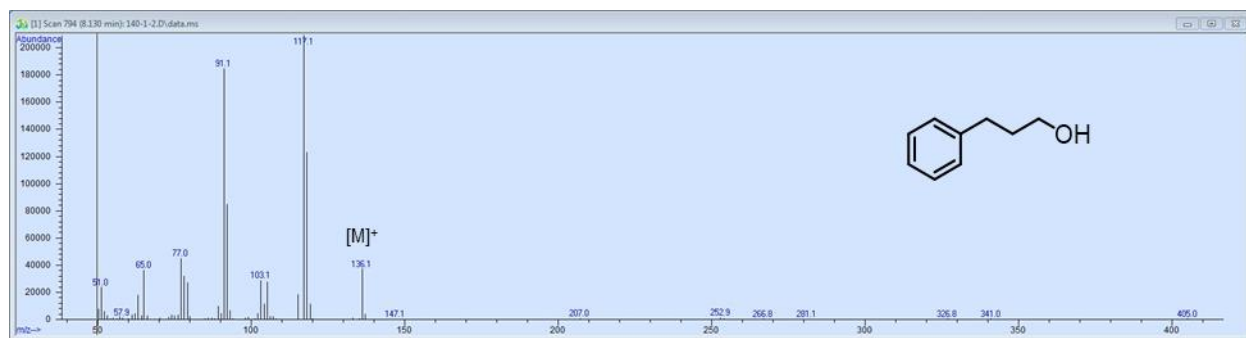


Figure S69. GC-MS spectrum of **2n**.

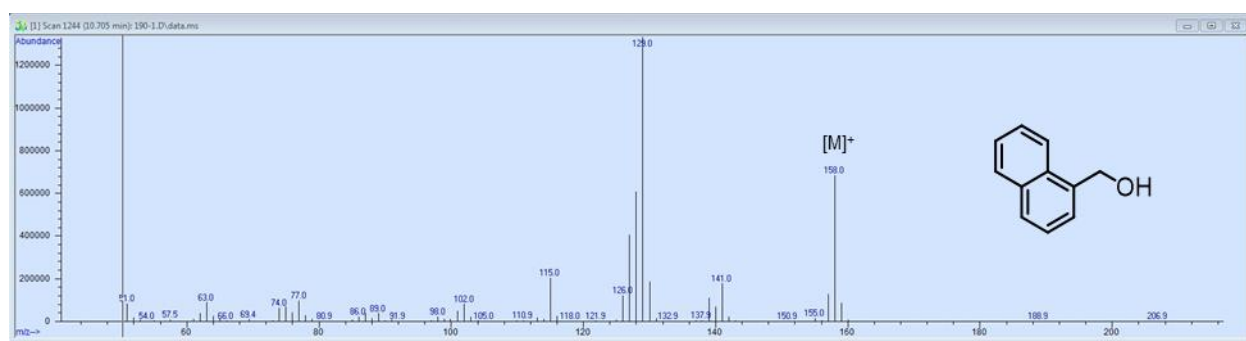


Figure S70. GC-MS spectrum of **2p**.

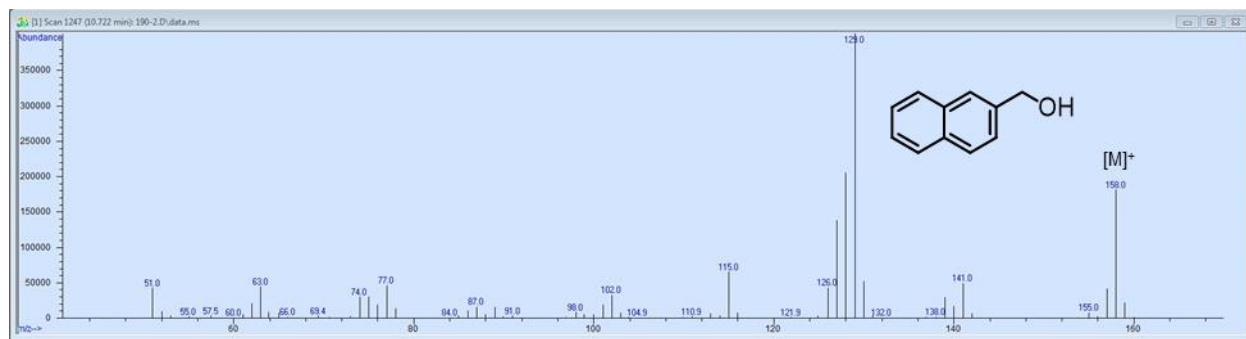


Figure S71. GC-MS spectrum of **2q**.

X-ray Data Collection and Refinement

Single crystals of **Ir2** were prepared by layering pentane over a CH₂Cl₂ solution of the complex containing trace amounts of NaCl at RT. Single crystals were picked out of the crystallization vials and mounted onto Mitogen loops using Paratone oil. The data were collected at -150°C using a Bruker Apex II diffractometer with Mo K α radiation ($\lambda = 0.71073$ Å) at a 6.0 cm detector distance. The diffraction data was collected to 0.8 Å, but was reduced to 1.1 Å during the refinement process because there were no signals at higher angles. Numerous attempts to grow larger and higher quality crystals were unsuccessful. The structure was solved by direct methods using the program SHELXT and refined by SHELXL.¹¹ The bridging cation was assigned as sodium (Na(1)) and the atom bound to it was assigned a water molecule (O(50)). The Cp* group was modeled using the program Disordered Structure Refinement (DSR),¹² which uses predefined molecular fragments taken from a database. A non-coordinating chloride anion was modeled with position disorder and refined with occupancies of 61 and 39%. The program Platon SQUEEZE¹³ was used to remove severely disordered solvent molecules, the presence of which is supported by NMR spectroscopic analysis of the crystal samples. Hydrogen atoms connected to carbon were placed at idealized positions using standard riding models and refined isotropically. All non-hydrogen atoms were refined anisotropically. The alert level A (THETM01_ALERT_3_A) and alert level B (RINTA01_ALERT_3_B and PLAT342_ALERT_3_B) in the checkCIF/PLATON report are due to the low resolution of the X-ray data. Although precise bond distances and angles cannot be obtained, our data provide useful information about atom connectivity.

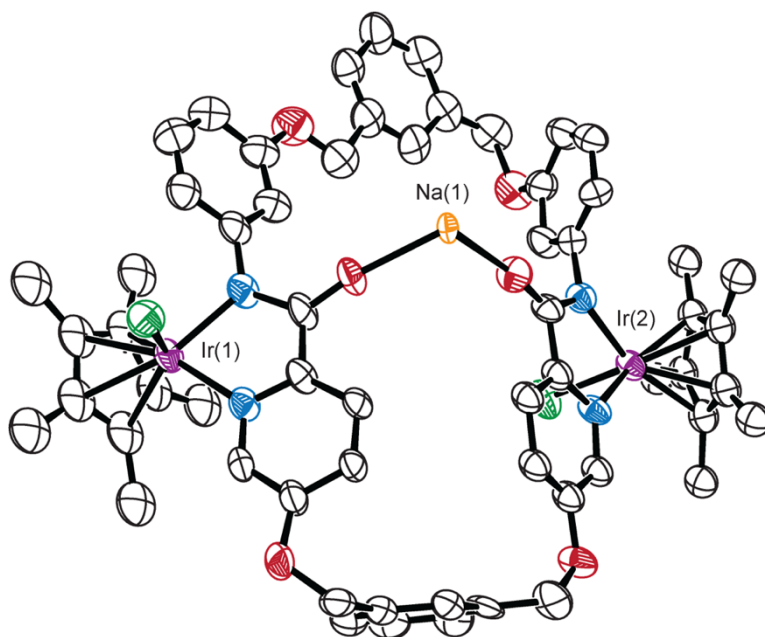
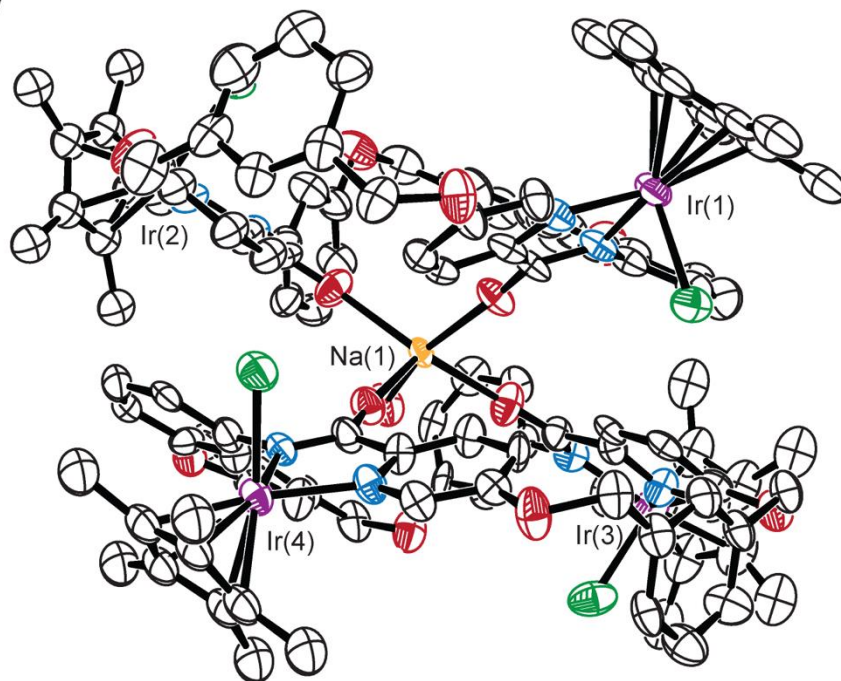


Figure S72. Molecular structure of [(**Ir2**)₂Na(H₂O)]Cl (**Ir2**-Na) showing only a single **Ir2** unit for clarity.

A) Side View



B) Top View

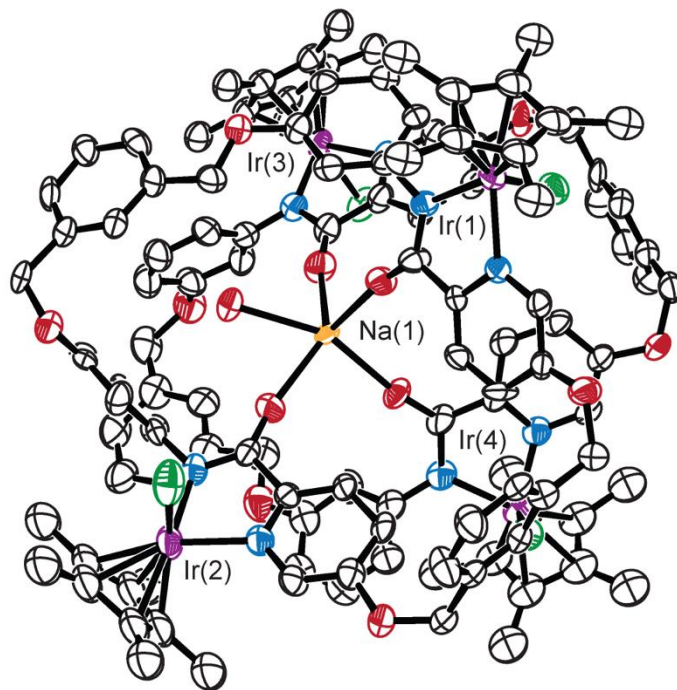


Figure S73. Molecular structure of complex $[(\text{Ir}2)_2\text{Na}(\text{H}_2\text{O})]\text{Cl}$ (**Ir2-Na**) shown in the side (A) and top (B) views.

Table S12. Crystal Data and Structure Refinement for **[(Ir2)₂Na(H₂O)]Cl**

	[(Ir2)₂Na(H₂O)]Cl
Empirical Formula	Ir ₄ NaC ₁₂₀ H ₁₂₀ Cl ₅ N ₈ O ₁₃
Temperature (°C)	-150
Wavelength (Å)	0.71073
Crystal System Space Group	Monoclinic, P2(1)/c
Unit Cell Dimensions	
<i>a</i> (Å)	27.7943(5)
<i>b</i> (Å)	16.0360(3)
<i>c</i> (Å)	12.7501(3)
<i>α</i> (°)	90
<i>β</i> (°)	110.6830(10)
<i>γ</i> (°)	90
Volume (Å³)	14201.1(5)
Z, Calculated Density (Mg/m³)	4, 1.334
Absorption Coefficient (mm⁻¹)	3.885
F(000)	5616
Theta Range for Data Collection (°)	1.241 to 27.643
Limiting Indices	-30 ≤ h ≤ 30 -17 ≤ k ≤ 17 -37 ≤ l ≤ 37
Reflections Collected/ Unique	302775/20395 [R(int) = 0.3161]
Data/ Restraints/ Parameters	20395/1592/1174
Goodness of Fit on F²	1.112
Final R Indices	R1 = 0.0979
[I > 2σ(I)]	wR2 = 0.2810
R Indices (All Data)	R1 = 0.2097
	wR2 = 0.3585
Largest Diff. Peak and Hole (e.Å⁻³)	4.579 and -1.476

Cell Cytotoxicity Studies

Cells were seeded in a 96-well plate (Corning 3595) and grown at 37 °C in an incubator with a humidified atmosphere containing 5% CO₂ (~15 h). Stock solutions of the test compounds were prepared in DMSO or DMEM, then diluted in cell culture media (DMEM: F12 (1:1) supplemented with 10% fetal bovine serum (FBS) and 1% penicillin-streptomycin 100× solution) to make a series of desired concentrations. The cell culture medium was then removed and replaced with fresh cell culture media containing the test compounds at different concentrations. The cells were then incubated for a desired amount of time. The solutions were removed by aspiration and the cells were washed with fresh DMEM before 100 µL of cell culture medium (with no FBS) was added to each well, followed by 50 µL of a fixative reagent (Cytoscan™ SRB Cytotoxicity Assay, G-Biosciences, catalog # 786-213). The 96-well plate was kept at 4 °C for 1 h, then the cells were washed 3 times with distilled water before drying for 2-3 h at 37 °C. A 100 µL solution containing sulforhodamine B (SRB) was then added to each well and the 96-well plate was kept in the dark at RT for 30 min. The cells were then rinsed 4 times with a 1× dye wash solution before drying for 2-3 h at 37 °C. A 200 µL solution of SRB solubilization buffer was added to each well and mixed by pipetting the mixture up and down to dissolve the dye completely. The absorbance of the 96-well plate was then measured at 510 and 565 nm on a Tecan Infinite M200 Pro microplate reader. The cell viability was considered to be proportional to the absorbance measured. The average absorbance value of wells containing only solubilization buffer (background) was subtracted from that of wells containing treated and untreated cells. The percent cell viability was calculated using the following equation: $(A_{\text{conc}}/A_{\text{control}}) \times 100\%$, where A_{conc} is the absorbance of wells containing cells treated with specific concentrations of the test compound and A_{control} is the absorbance of wells containing untreated cells. The IC₅₀ values were calculated from the sigmoidal curve fit of these data at 50% cell viability.

ICP-MS Analysis

Cells were grown in 100 mm tissue culture plates at 37°C under a 5% CO₂ atmosphere. When ~70% confluence was reached, the DMEM solution was removed by aspiration and replaced with fresh DMEM solution containing 20 µM of **Ir2** (0.2% DMSO was used to solubilize the **Ir2** complex). After 24 h of incubation, the cells were washed twice with phosphate-buffered saline (PBS), detached by treatment with trypsin, and 10 µL of the cell suspension was taken for cell counting. The trypsinized samples were then centrifuged and the supernatant was discarded. The cell pellet was washed with fresh DMEM and PBS through vortexing, centrifuging, and removing the supernatant. The cell pellets were digested using 0.2 mL of 65 -70% metal-free distilled HNO₃ at room temperature overnight. To each sample, 5.8 mL of HPLC-grade water was added to obtain a 2% HNO₃ solution. The resulting cloudy solutions were centrifuged to obtain clear samples for ICP-MS analysis.

An iridium standard solution (10 µg/mL) was diluted in 2% HNO₃ solution to make a series of concentrations from 0 to 20 ppb. The iridium content of each sample was measured in order to establish a calibration curve. By using this calibration curve, the iridium concentrations in the lysate samples were determined. The final concentration of iridium was calculated using the following equation: [Ir] (ng/10⁶ cells) = (total Ir)/(total cells), and total Ir (ng) = [Ir] (in ppb) × 10³ × 0.006 (L).

Table S13. Accumulation of **Ir2** in NIH-3T3 cells

Complex (conc.)	[Ir] (ppb)	Total Ir (ng)	Total Cells (× 10 ⁶)	[Ir] (ng/10 ⁶ cells)	Average [Ir] (ng/10 ⁶ cells)	Std. Dev.
Control	0.3097	1.990	1.645	1.209		
Ir2 (20 µM)	306.3	1968.3	1.327	1482.9		
	342.2	2199.0	1.523	1444.1	1487.7	46.2
	322.7	2073.7	1.350	1536.0		

^a Cells were incubated with 20 µM of the **Ir2** for 24 h.

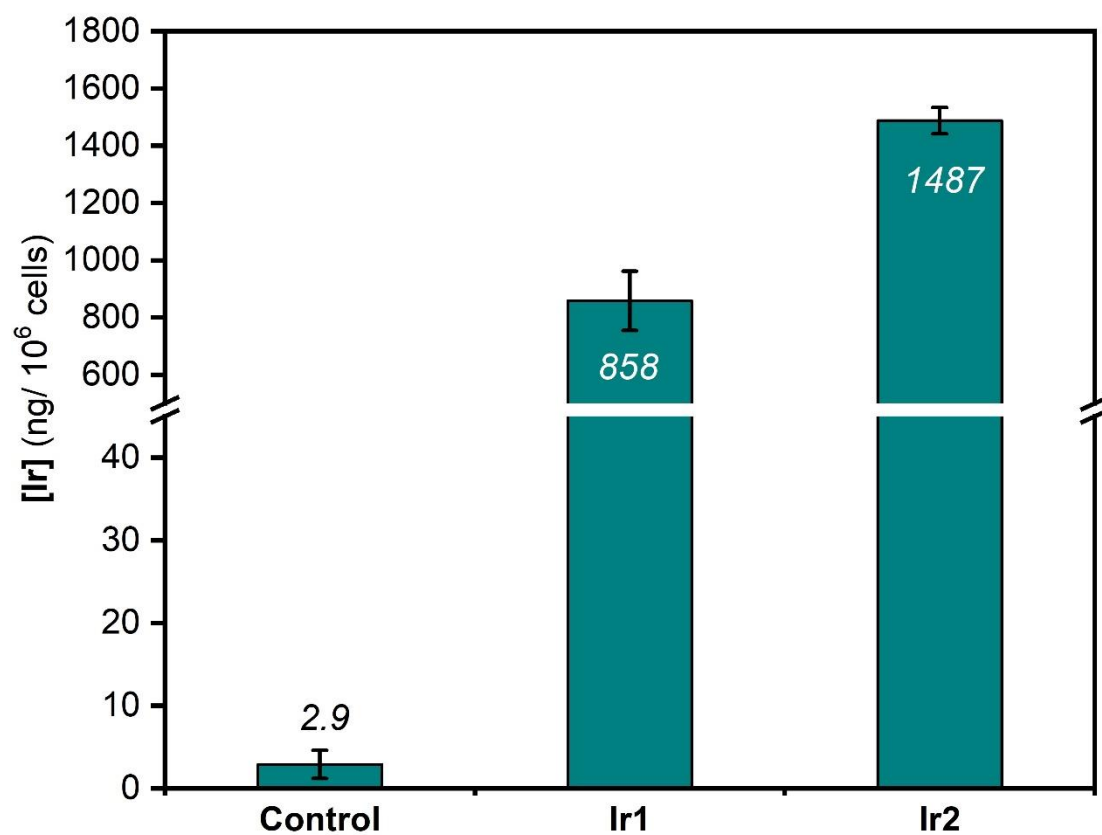


Figure S74. Comparing the accumulation of iridium complexes in NIH-3T3 cells after treatment for 24 h (concentration of **Ir** = 20 μ M). The ICP-MS data for Ir1 was reported previously.¹⁰

References

- (1). Kang, J. W., Moseley, K., Maitlis, P. M., *J. Am. Chem. Soc.*, **1969**, *91*, 5970–5977.
- (2). Almodares, Z., Lucas, S. J., Crossley, B. D., Basri, A. M., Pask, C. M., Hebden, A. J., Phillips, R. M., McGowan, P. C., *Inorg. Chem.*, **2014**, *53*, 727–736.
- (3). Zamora, A., Pérez, S. A., Rothmund, M., Rodríguez, V., Schobert, R., Janiak, C., Ruiz, J., *Chem. Eur. J.*, **2017**, *23*, 5614–5625.
- (4). Pastine, S. J., Youn, S. W., Sames, D., *Org. Lett.*, **2003**, *5*, 1055–1058.
- (5). Martin, K., Nöges, J., Haav, K., Kadam, S. A., Pung, A., Leito, I., *Eur. J. Org. Chem.*, **2017**, *35*, 5231 – 5237.
- (6). Jolley, K. E., Zanotti-Gerosa, A., Hancock, F., Dyke, A., Grainger, D. M., Medlock, J. A., Wills, M., *Adv. Synth. Catal.*, **2012**, *354*, 2545–2555.
- (7). Hamasaka, G., Tsuji, H., Uozumi, Y., *Synlett*, **2015**, *26*, 2037–2041.
- (8). Filosa, R., Peduto, A., De Caprariis, P., Saturnino, C., Festa, M., Petrella, A., Loddo, R., *Eur. J. Med. Chem.*, **2007**, *42*, 293–306.
- (9). Li, W., Xie, J. H., Yuan, M. L., Zhou, Q. L., *Green Chem.*, **2014**, *16*, 4081–4085.
- (10). Jana, R. D., Ngo, A. H., Bose, S., Do, L. H., *Chem. Eur. J.*, **2023**, *29*, e202300842.
- (11). Hübschle, C. B., Sheldrick, G. M., Dittrich, B., *J. Appl. Crystallogr.*, **2011**, *44*, 1281–1284.
- (12). Kratzert, D., Krossing, I., *J. Appl. Crystallogr.*, **2018**, *51*, 928–934.
- (13). Spek, A. L., *Acta Crystallogr. C Struct. Chem.*, **2015**, *71*, 9–18.